THE JOURNAL OF COMPARATIVE NEUROLOGY 365:173–216 (1996)

Retinal Neurons of the California Ground Squirrel, *Spermophilus beecheyi*: A Golgi Study

KENNETH A. LINBERG, SETSUKO SUEMUNE, AND STEVEN K. FISHER
Neuroscience Research Institute (K.A.L., S.S., S.K.F.) and the Department of Biological Sciences (S.K.F.), University of California, Santa Barbara, Santa Barbara, California, 93106-5060, and the Department of Oral Anatomy, Hiroshima University School of Dentistry, Hiroshima, Japan (S.S.)

ABSTRACT

Although the optic nerve fibers of the cone-dominant ground squirrel retina have been well studied physiologically, the morphological details of the retinal neurons have not. To that end, retinal neurons of the California ground squirrel have been studied in Golgi-impregnated wholemounts.

Two types of horizontal cell have been identified: H1 has an axon and axon terminal, whereas H2 is axonless. The dendritic field of H1 cells enlarges in a nonuniform manner with increasing displacement from the central retina. The smallest examples lie centrally in the visual streak, and the largest occur in the superior periphery.

Eight types of bipolar cell are distinguished by morphological differences in dendritic branching pattern and field size in the outer plexiform layer, cell body size, and layering within the inner nuclear layer and by the morphology and stratification of axon terminals in the inner plexiform layer. A large bistratified bipolar cell (B8) is introduced here; the other 7 types closely resemble those in the retinas of other sciurid species described by R.W. West (1976, J. Comp. Neurol. 168:355–378; 1978, Vision Res. 18:129–136). The B1 type is proposed as a blue cone bipolar cell.

Amacrine cells are classified into 27 cell types. Six of these occur as mirror-image pairs across the inner plexiform layer, the soma of one of each pair being "displaced" to the ganglion cell layer. The best described of these pairs is the very elaborate starburst amacrine cell, A5, which stains regularly in these wholemounted retinas. Changes in dendritic field size of both A5 subtypes with retinal location are quantified. The morphology of three amacrine cell types identified in *Spermophilus beecheyi* suggests that their possible counterparts in *S. mexicanus* (West, 1976) were, as displaced amacrine cells, misidentified as ganglion cells. Amacrine cell types that may play roles in the rod pathway, the blue cone pathway, and ganglion cell directional selectivity are discussed.

No type of interplexiform cell was observed.

Ganglion cells are classified into 19 cell types, 9 of which probably correspond to the ganglion cells described by West (1976) in the Mexican ground squirrel. The bistratified G11 cell is proposed as an ON–OFF directionally selective type.

Indexing terms: light microscopy, horizontal cell, bipolar cell, amacrine cell, ganglion cell

Although ground squirrels were once thought to have an all-cone retina, several studies have identified a small, yet structurally and physiologically distinct, population of rod photoreceptors in a variety of species (Green and Dowling, 1975; West and Dowling, 1975; Fisher et al., 1976; Jacobs et al., 1976; Ahnelt, 1985; von Schantz et al., 1994). In the California ground squirrel, *Spermophilus beecheyi*, the frequency of rods in the photoreceptor mosaic is known to increase from 5–7% in the central retina to 15–20% in the periphery (Long and Fisher, 1983). This population of rods subserves the weak scotopic vision observed in this species (Jacobs et al., 1976). The remaining photoreceptors are cones, about 10% of which have been morphologically

Accepted July 7, 1995.

Address reprint requests to Dr. Steven K. Fisher, Neuroscience Research Institute, University of California, Santa Barbara, Santa Barbara, CA 93106-5060.

classified as blue cones (Long and Fisher, 1983). Their contribution to the dichromatic vision of California ground squirrels has been well characterized physiologically by Jacobs and co-workers (Jacobs and Tootell, 1980, 1981; Jacobs et al., 1981, 1985). Electrophysiological studies of optic nerve fibers in ground squirrels (Michael, 1968a–c; Jacobs and Tootel, 1980, 1981; Jacobs et al., 1981; McCourt and Jacobs, 1984a,b) have also clearly shown ganglion cell coding of contrast and directional selectivity, yet the morphology of the neurons that might underlie these various physiological pathways in squirrel retina has not been well characterized.

The multitiered retina is the site of this neuronal processing and, as in all vertebrate retinas, interneuronal contacts are made primarily, although not exclusively (see Hughes, 1985), in the 2 main plexiform layers: the outer plexiform layer (OPL) and the inner plexiform layer (IPL; see Dowling, 1987; Rodieck, 1988; Wässle and Boycott, 1991). How extensively and in what form each retinal cell type arborizes in these synaptic layers determines the unique set of synaptic contacts central to its particular physiology. Ground squirrel IPL is known to be thicker than that of many species, suggesting that an especially large number and variety of interneuronal contacts may occur in this layer. However, the IPL is not of uniform thickness as Long and Fisher (1983, their Fig. 1A,C) have shown, being 65-μm thick in the central visual streak and only 25-μm thick in the retinal periphery.

In several mammalian species, highly specific circuits have been described for retinal neurons of the rod pathway (Kolb and Nelson, 1983; Dacheux and Raviola, 1986; Daw et al., 1990; Vaney et al., 1991) and the blue cone pathway (Mariani, 1984; Kouyama and Marshak, 1992; Dacey and Lee, 1994). To that end, we were curious as to whether any of the well-studied neurons of these 2 mammalian pathways might exist in a retina where cones so vastly outnumber rods and green cones similarly predominate over blue cones. Indeed, because blue cones can be recognized morphologically and their distribution is known, the ground squirrel retina might ultimately prove to be a good mammalian model for understanding the synaptic circuitry underlying color opponent receptive fields at the ganglion cell level.

This is not the first study of Golgi-stained neurons in squirrel retina. West and Dowling (1972, 1975) focused on several types of Golgi-impregnated neurons in a variety of sciurid retinas. Mariani (1985) described 2 types of horizontal cell in the red squirrel's retina. West (1976) catalogued numerous cell types in vertically sectioned, Golgi-impregnated retinas of the Mexican ground squirrel (formerly *Citellus mexicanus*, now *Spermophilus mexicanus*) and gave additional descriptions of horizontal and bipolar cells in the retina of the gray tree squirrel, *Sciurus carolinensis* (1978). In this study, we use retinal wholemounts of *S. beecheyi* to describe more fully the overall morphology of each cell and better assess the size of its axon terminal and/or dendritic fields. As a result, the catalog of cell types in the ground squirrel retina is expanded greatly because we show not only examples of cells similar to almost all the sciurid types described by West (1976, 1978) but also introduce several new ones, particularly among the amacrine and ganglion cells.

Some of these data have appeared in abstract form (Linberg et al., 1988).

METHODS

California ground squirrels (*Spermophilus beecheyi*) were killed by lethal doses of sodium pentobarbitol injected intraperitoneally. Once dead, their eyes were enucleated and the anterior structures removed. The eyes of 17 squirrels of both sexes and varying ages were studied. Retinas were carefully peeled from the eyecup while in isotonic phosphate buffer and each was processed for Golgi impregnation as described elsewhere (Kolb et al., 1992).

Cells that seemed well impregnated were studied with a Zeiss Universal Research microscope using a 40× Zeiss planapo oil immersion lens and drawn with the aid of a camera lucida usually at a magnification just under 1,400×.

Because certain cell types in mammalian retinas increase in size with increasing eccentricity (Boycott and Kolb, 1973; Boycott and Wässle, 1974), particular care was taken to pinpoint each cell's location relative to the center of the retina. For primate and cat retina that have a fovea or area centralis respectively, a single measurement of a cell's displacement suffices. This is not true for the ground squirrel's retina because it has an elongated visual streak around which certain cell types form elliptical, not concentric, isotropic contours (Long and Fisher, 1983). As the exact position of the center of the visual streak region is indistinct, all cells described herein are positioned relative to the linear optic nerve head (ONH) and are standardized in such a way as to eliminate differences between right and left eyes. We first ascribe the Cartesian coordinate of (0,0) to the ONH midpoint with the right eye as the standard. Then, an ocular graticule is used to note each cell's location by measuring its horizontal displacement in millimeters along the ONH (x-axis) and ascribing a positive value (+) if located in the nasal hemisphere or a negative value (−) if located temporally. Then each cell's vertical distance from the linear optic nerve head is measured in millimeters (y-axis), ascribing a positive value (+) to cells lying in the superior hemiretina or a negative value (−) if located in the inferior hemiretina. Four quadrants result: 2 small superior quadrants and 2 larger inferior quadrants. A cell located in the superior nasal quadrant (SN) would have a position indicated by 2 positive values and that of a cell in the inferior temporal quadrant (IT) would be indicated by 2 negative values. Those cells lying in the superior temporal quadrant (ST) have negative x and positive y coordinates and those in the inferior nasal quadrant (IN) have the opposite sign designations. Tables 1–3 list such coordinates for all cell types drawn by camera lucida except for those in Figures 1–3 and 11. Table 4 lists coordinates for cells depicted in these figures and those in the photographs of Figures 5, 8, 21, and 28. Although exact cell positions are given, such measurements necessarily represent approximations of each cell's true position in any given eye as there is always some variation in the size of the eyes.

In Tables 1–3, we list an approximate sample size for each cell type representing the number of examples either drawn, photographed, or studied. By "few" we mean 2–4, by "several" we mean 5–10, and by "many," a dozen or more.

Perhaps the main drawback in gathering data from wholemounted retinas is obtaining precise stratification of cell perikarya and their processes (Kolb et al., 1981). Here we estimate the stratification of cell dendrites or axon terminals in the IPL by measuring the thickness of the IPL

at each site and dividing it equally into 5 strata (S1–S5; Ramón y Cajal, 1893).

Dendritic and axon terminal field dimensions and areas were measured using a Zeiss Mop digital analyzer by drawing a line around each cell extending through the tips of its dendrites or axon terminal branches. Diameters of each cell type given in the text are always its maximum diameter D_{max}. When describing the finer morphology of dendrites and axon terminals, we often use the terminology of Cameron et al. (1983) in describing dendritic spines as pedunculated (lollipop-shaped) or sessile (straight, unadorned) and appendages as single- or multilobed.

A Zeiss Photomicroscope III was used for photomicrography.

RESULTS

As in the rabbit eye, the ground squirrel retina has a horizontally elongated ONH that separates the retina into superior and inferior regions. In the eye of one specimen, the ONH measured 9.1 mm long and 125 μm wide. The ONH lies above the retinal equator such that it divides the retina into unequal portions, the lower portion being larger than the upper. For convenience, we refer to these superior and inferior regions as "hemiretinas." The prominent ONH served as our primary landmark for determining a cell's position in each retina, thereby allowing examples of the same type of cell to be compared between eyes of the same or different individuals. Two millimeters inferior to the ONH lies the visual streak (Long and Fisher, 1983), a region usually associated with maximal visual acuity in the retina of certain lower mammals (see Wässle and Boycott, 1991). In general, the smallest size classes of most cell types are found in this region.

As documented for certain cell types in rabbit (Famiglietti, 1985) and tree shrew (Müller and Peichl, 1993) retina, certain cell types in the California ground squirrel retina display a nonuniform increase in size with increasing distance from the visual streak. Examples of such types not only increase in size with distance from this central region but do so more rapidly in a preferred direction. In the retina of *S. beecheyi*, a generalized central-to-peripheral increase in cell size is combined with a dorsal-versus-ventral size gradient. This results in cells, at equivalent distances from the visual streak, being larger in the superior retina than their counterparts in the inferior retina. We have illustrated and described this dual trend in populations of axon-bearing horizontal cells (Fig. 3) and starburst amacrine cells (Fig. 11). We could not determine whether or not the many other cell types described in this study also exhibit a similar pattern of increasing size with distance from the retinal center. This was due principally to insufficient numbers of impregnated examples.

Horizontal cells (Figs. 1–5; Table 4)

We have identified two types of horizontal cell in the retina of *S. beecheyi* with the most commonly impregnated being an axon-bearing type (H1; Figs. 1, 2a, 3, 5a) similar to that described by West and Dowling (1975) in *S. mexicanus* and by Mariani (1985) in *Tamiasciurus hudsonicus*, the red squirrel. An axonless type was also found (H2; Figs. 2b, 5b,g), although it failed to stain in many of the specimens.

Figures 1 and 2a show entire examples of the H1 type. The cell in Figure 1 lies 4 mm inferior to the linear ONH (2 mm inferior to the visual streak) and has a total length of

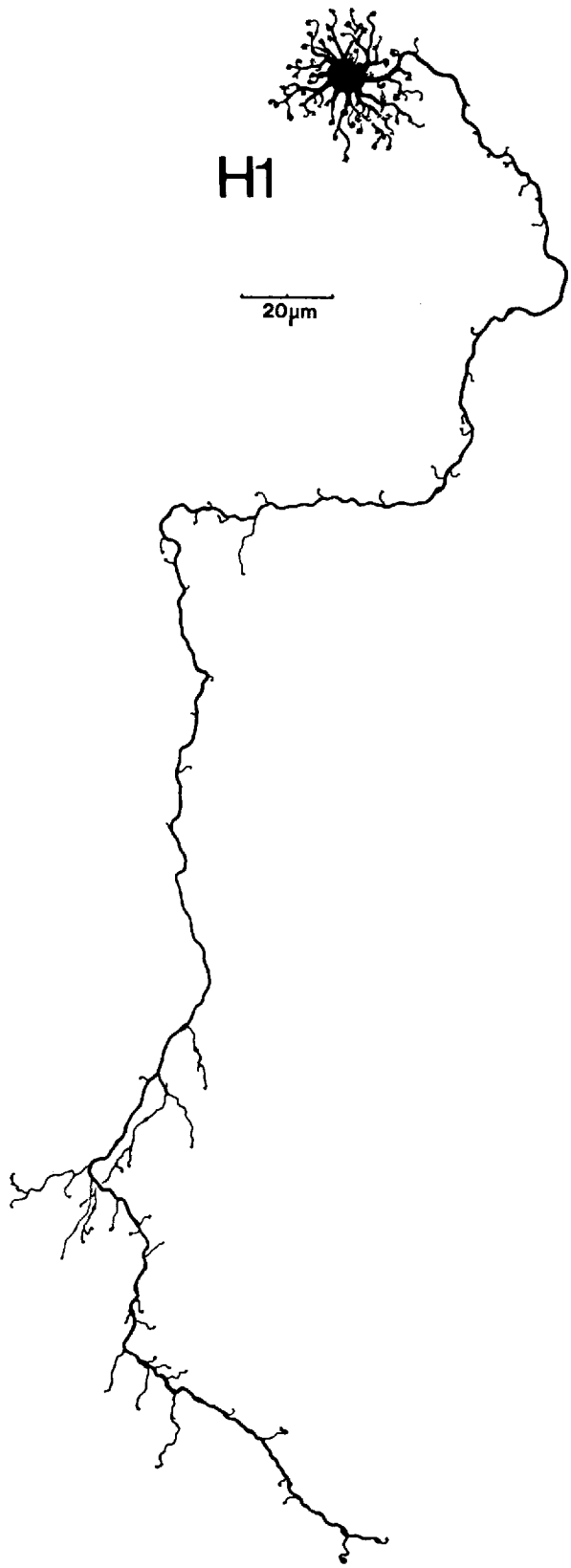

Fig. 1. An axon-bearing horizontal cell (H1), lying 4 mm inferior to the optic nerve head (ONH), has a 500-μm long axon that arborizes distally.

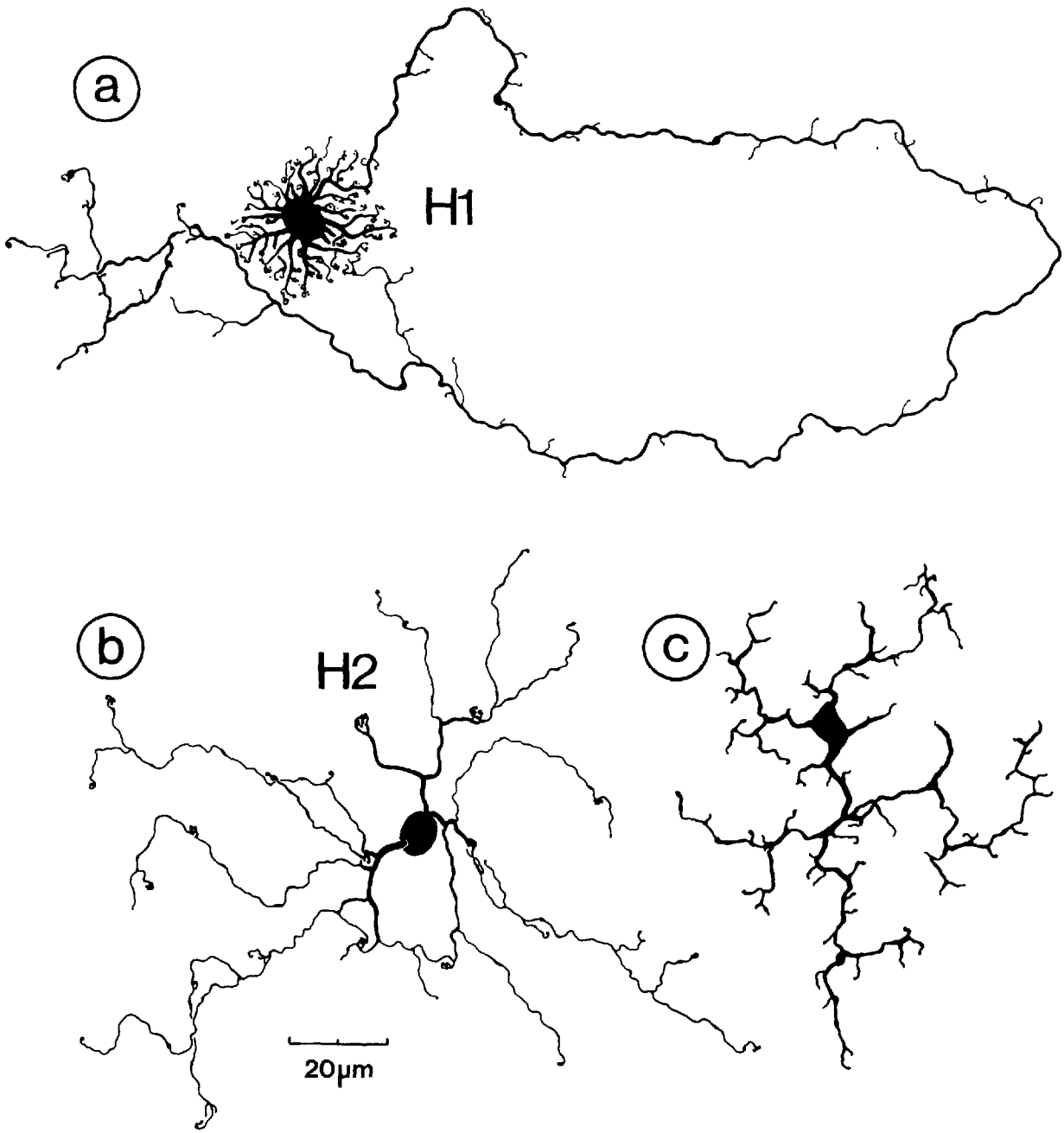

Fig. 2. **a:** An axon-bearing horizontal cell (H1) folds such that its axon terminal adjoins its dendrites. Located 4.1 mm below the ONH, its axon is about 525 μm long. **b:** An axonless horizontal cell (H2) lies 3 mm inferior to the ONH. A photograph of this cell is shown in Figure 5b. **c:** For comparison, a microglial cell located 4.7 mm beneath the ONH is shown. Note the angularity of both its cell body and processes.

just over 500 μm. Numerous tapered dendritic trunks radiate away from the H1 cell perikaryon and branch 1–3 times before terminating as fine fibers tipped with tiny, clustered, and rounded dendritic terminals (Figs. 3, 5e,f). Spines, small terminal branchlets of varying lengths, and varicosities occur sporadically all along the meandering axon (Figs. 1, 2a). The axon terminal is sparsely branched and loosely organized (Figs. 1, 2a, 5c). In areas where many cells were impregnated, both the dendrites and axonal arborizations of neighboring H1 cells extensively overlap.

Figure 3 illustrates H1 cell dendrites at varying positions across the ground squirrel retina. Each cell's position is given in millimeters of displacement above or below the ONH. The corresponding horizontal displacement of each from the midpoint of the ONH is given in Table 4. The H1 cell with the smallest dendritic field shown here (Fig. 3b, D_{max} = 33 μm) lies in the inferior hemiretina 1.7 mm below the ONH and the largest (Fig. 3g, D_{max} = 127 μm), almost 4 times as wide, lies in the periphery of the upper hemiretina, 4.4 mm above the ONH. Although H1 dendritic field size

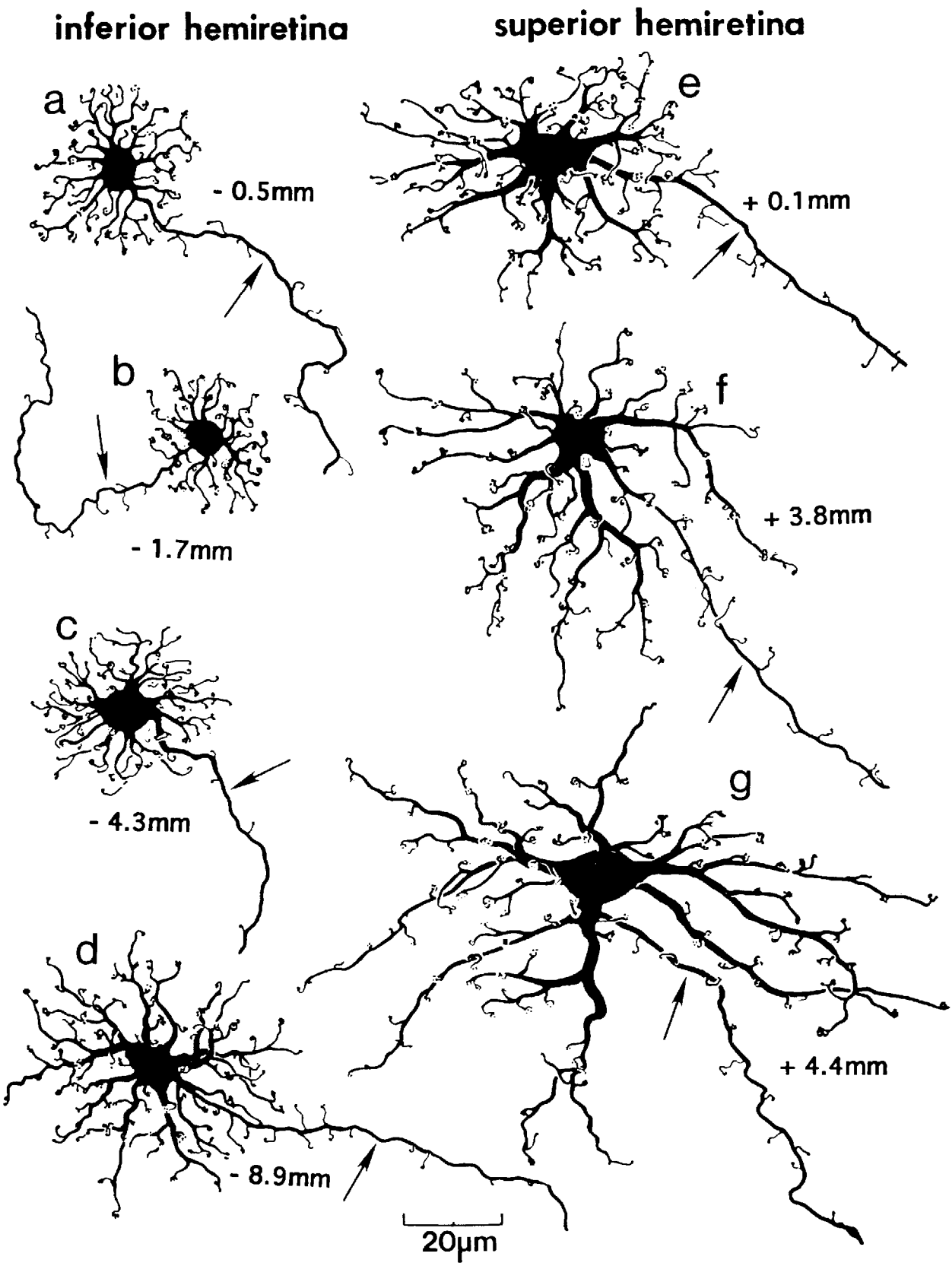

Fig. 3. **a–g:** A comparison of the size and dendritic morphology of H1 cells from inferior and superior hemiretinas. The displacement of each cell from the midpoint of the ONH is given in millimeters. Note that the cells in the inferior hemiretina are more circular than those of the superior. Arrows indicate axons.

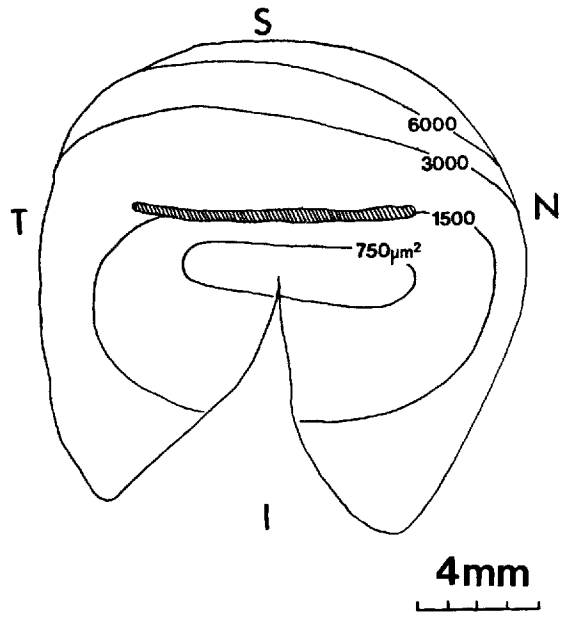

Fig. 4. The dendritic field area of 760 H1 cells from the retinas of 2 ground squirrels were measured and plotted relative to the linear ONH (shaded area). The smallest cells are restricted to a nasally displaced, central region that includes the visual streak.

increases in both hemiretinas with distance from the visual streak, cells above the streak enlarge at roughly twice the rate as those cells lying below it. The dendritic field of a H1 cell about 2 mm below the visual streak (Fig. 3c, 4.3 mm below the ONH) has a D_{max} of nearly 40 μm, whereas another at a similar distance above the visual streak (Fig. 3e, 0.1 mm above the ONH) measures 70 μm across. Peripherally, at 6.9 mm below the visual streak (Fig. 3d, 8.9 mm below the ONH), the dendritic tree of a H1 cell has a D_{max} of 60 μm, whereas that of its counterpart in the superior retina (Fig. 3g, 4.4 mm above the ONH) measures 127 μm. The dendritic trees of H1 cells in the inferior hemiretina appear to be more circular in profile, whereas those in the superior hemiretina are more elliptical. Figure 3 also shows that H1 cell somata tend to increase in size from the center (D_{max} = 8 μm) to the periphery (D_{max} = 15 μm), as do the caliber and prominence of their tapered primary dendrites. Conversely, the density of dendritic clusters apparently decreases along this same gradient.

We observed fewer than a dozen entire H1 cells in 30 ground squirrel retinas, too few to establish any trend in axonal length vis-à-vis retinal location. The shortest axon we measured was located just below the visual streak and had a length of 300 μm. The longest we observed was located deep (9+ mm) in the inferior retina, and although it was not completely stained, it extended 850 μm. The remaining cells had an axon 450–600 μm in length. H1 axons originate either directly off the perikaryon or from a dendritic trunk (see Fig. 3) and stream away from their respective perikarya in apparently random directions. Impregnated axons were seen to cross each other at all angles. Some had kinks, right-angle turns, major collaterals, or small loops along their lengths. Figure 2a shows an H1 cell whose axon folds such that its dendrites lie adjacent to its telondendria.

Figure 4 shows the change in H1 dendritic field area with retinal location based on measurements of 760 H1 cells from 2 retinas. Cells with field areas less than 750 μm² were confined to a nasally displaced central region that includes the visual streak. H1 cells with dendritic field areas of 3,000 μm² or more were found only in the superior periphery.

The axonless H2 cell (Fig. 2b) differs greatly from the axon-bearing type. At any retinal location, its dendritic tree is far larger and more loosely organized than that of the H1 cell (Figs. 2, 5b). H2 cells were often hard to discern due in part to the fine and spidery nature of their dendrites; in part because they seem to be very planar and narrowly stratified and also because they simply appear to stain less intensely. Their description was further complicated by having to discern these cells through the many overlying layers of cells when viewed from the ganglion cell side. H2 cells have 3, or occasionally 4, sturdy dendritic trunks that abruptly arise from the perikaryon and taper slightly while bifurcating and giving rise to the secondary and tertiary dendrites that occasionally branch dichotomously off them. Many of these fine and somewhat wavy processes end singly, but an almost equal number of them form tight clusters of 3–6 dendritic tips. These clusters appear to lie in a fairly regular array, each being about 20–30 μm from any other. The H2 cell shown in Figures 2b and 5b lies 3 mm inferior to the ONH (1 mm below the visual streak). The dendritic field of the H2 cell is often assymmetric and in outline ranges from almost circular to elongated. In fact, neighboring H2 cells can be quite different, both in overall shape and in size. In contrast to H1 cells, we have not seen extensive overlap between the dendrites of neighboring H2 cells, although their peripheral dendrites can overlap (Fig. 5g).

A total of 51 H2 cells were studied, and all but 2 lay in the inferior hemiretina. These cells did not seem to increase in dimension with distance from the visual streak. Rather, at any point in the inferior retina including the visual streak, their dendritic field area ranged from 8,300 to 32,000 μm². The 2 examples in the midperiphery of the upper hemiretina were, however, the largest observed, measuring 46,000 and 55,000 μm² in dendritic field area.

H2 cell somata tend to be round or ovoid and are much better defined in the ground squirrel than those of the axonless horizontal cells in rabbit (Bloomfield and Miller, 1982; Dacheux and Raviola, 1982), cat (Gallego, 1971; Fisher and Boycott, 1974), or guinea pig (Peichl and González-Soriano, 1994) retina, where the demarcation between perikaryon and dendritic trunks can be hard to identify. For the 49 H2 cells lying in the inferior hemiretina, the diameter of the somata ranged from 8.5 to 11 μm. In contrast to H1 cell perikarya, H2 cell somata in *S. beecheyi* do not show much variation in size with respect to retinal location; somal diameter seems not to correlate with dendritic field size. The largest somal dimensions (D_{max} of 11–13 μm) belong at once to the smallest H2 cells of the inferior retina and to the largest of the superior retina, the same two mentioned earlier.

Microglial cells (see Gallego, 1986) also can be found among the neurons of the outer inner nuclear layer (INL) and have been mistaken for horizontal cells in the past (Gallego, 1976; West, 1978; Boycott and Hopkins, 1981). Figures 2c and 5d show microglial cells of *S. beecheyi*. Their lack of characteristic terminals, their jagged and irregularly thick branches, and the angularity of their cell bodies are all features at odds with those typical of the H2 cells.

Bipolar cells (Figs. 6–8; Tables 1, 4)

Eight types of bipolar cell are distinguished chiefly by differences in the morphology of their dendrites and axon

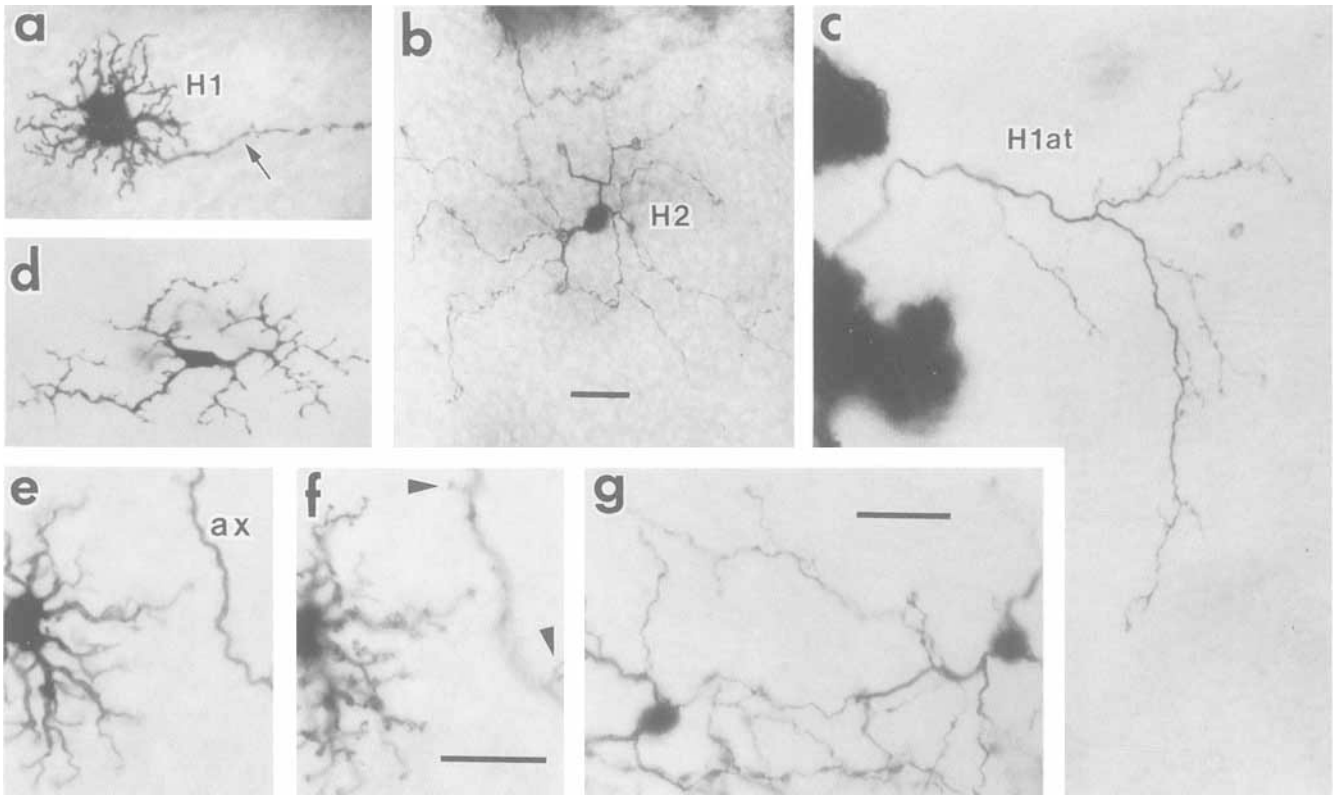

Fig. 5. Light micrographs of horizontal cells and microglia photographed from the ganglion cell side of the retina. Table 4 gives the dimensions and retinal positions of the cells shown here. **a:** An H1 cell body gives rise to a radial array of dendrites and a beaded axon (arrow). Photographed from below, central dendrites are obscured by the interposed perikaryon. This cell lies in the inferior periphery, 7.5 mm below the ONH. **b:** Shown at the same scale, the axonless H2 cell pictured here is the same one drawn in Figure 2b. It lies centrally, 2.9 mm below the ONH. Its very narrowly stratified dendritic field is far larger than adjacent H1 cells. **c:** An H1 cell axon terminal (H1at), shown at the same magnification, located centrally just under the ONH. **d:** Also at the same scale is a microglial cell, 2.4 mm above the ONH. Although processes at the level of the outer plexiform layer (OPL) are planar, 2 descend into the inner nuclear layer (INL) and appear here as shadows. **e:** At higher magnification, part of an H1 perikaryon lies next to an axon (ax) of a different H1 cell. At this level of focus, the axon and the branching of the primary dendrites can be seen. These cells lie 2.5 mm above the ONH. **f:** At a slightly more sclerad level of focus, H1 dendritic tips can be seen, as can the tips of the branchlets (arrowheads) that arise along the axon. **g:** The dendrites of 2 adjacent H2 cells overlap. These cells lay 3.7 mm below the ONH. Scale bars = 20 μm.

terminals. As each of the 7 bipolar cell types in *S. mexicanus* described by West (1976) has a close counterpart in the retina of *S. beecheyi*, we have adopted his nomenclature for these types. In addition, a large bistratified bipolar cell is described for the first time in squirrel retina. Figure 6 shows examples of all 8 bipolar cell types lying 2 mm below the visual streak in the eye of 1 specimen (4 mm inferior to the ONH). The upper row of drawings shows the cells' dendrites in the OPL and the lower shows their axon terminals in the IPL. For B3, B6, and B8, the 3 types of bistratified bipolar cells, each of their distinct terminal layers is drawn independently. Beneath the drawings of these cells, each cell type is schematically portrayed in vertical section to show its respective levels of perikaryl and telodendritic stratification as well as the relative dimension of its processes in both plexiform layers. Figure 7 presents different examples of the same cell types (seen oblique to the horizontal plane, axon terminals in the foreground), all of which lie in the superior retina 3 mm above the visual streak (1 mm superior to the ONH). Dimensions and locations of the cells shown in Figures 6 and 7 are listed in Table 1. Inasmuch as the illustrated examples of each cell type were located at roughly equivalent distances below (Fig. 6) and above (Fig. 7) the visual streak, data in Table 1 show that, for most bipolar cell types, cell dimensions are greater in the superior retina. We did not attempt, however, any systematic study of bipolar cell size with displacement from the visual streak. Figure 8 shows examples of Golgi impregnated bipolar cells photographed from the vitread surface of the retina; their locations are given in Table 4. All types are depicted at the same magnification.

In the central, inferior retina, the B1 cell has a small, round cell body (D_{max} = 6 μm) that issues a stout, ascending dendrite that branches only once, if at all. These nontapering dendrites and branches seem to converge onto a single cone pedicle (Figs. 6, 8a,d), in which case the B1 cell has a dendritic field that is the smallest of all 8 bipolar cell types (Fig. 6). In the periphery of the inferior hemiretina and across the entire superior hemiretina, however, B1 cells often have 2, sometimes 3, ascending dendrites that appear to stretch out to innervate 2 or more widely separated photoreceptors (Figs. 7, 8b). The 2 tiny dendritic clusters of the B1 cell in Figure 7 are 28 μm apart. This cell is located just above the ONH in the SN quadrant. Lying in the far periphery of the superior hemiretina above the ONH midpoint, the B1 cell shown in Figure 8b has 3 clusters of dendritic tips that are all roughly 38 μm equidistant from each other. As in *S. mexicanus* (West, 1976), the B1 cell

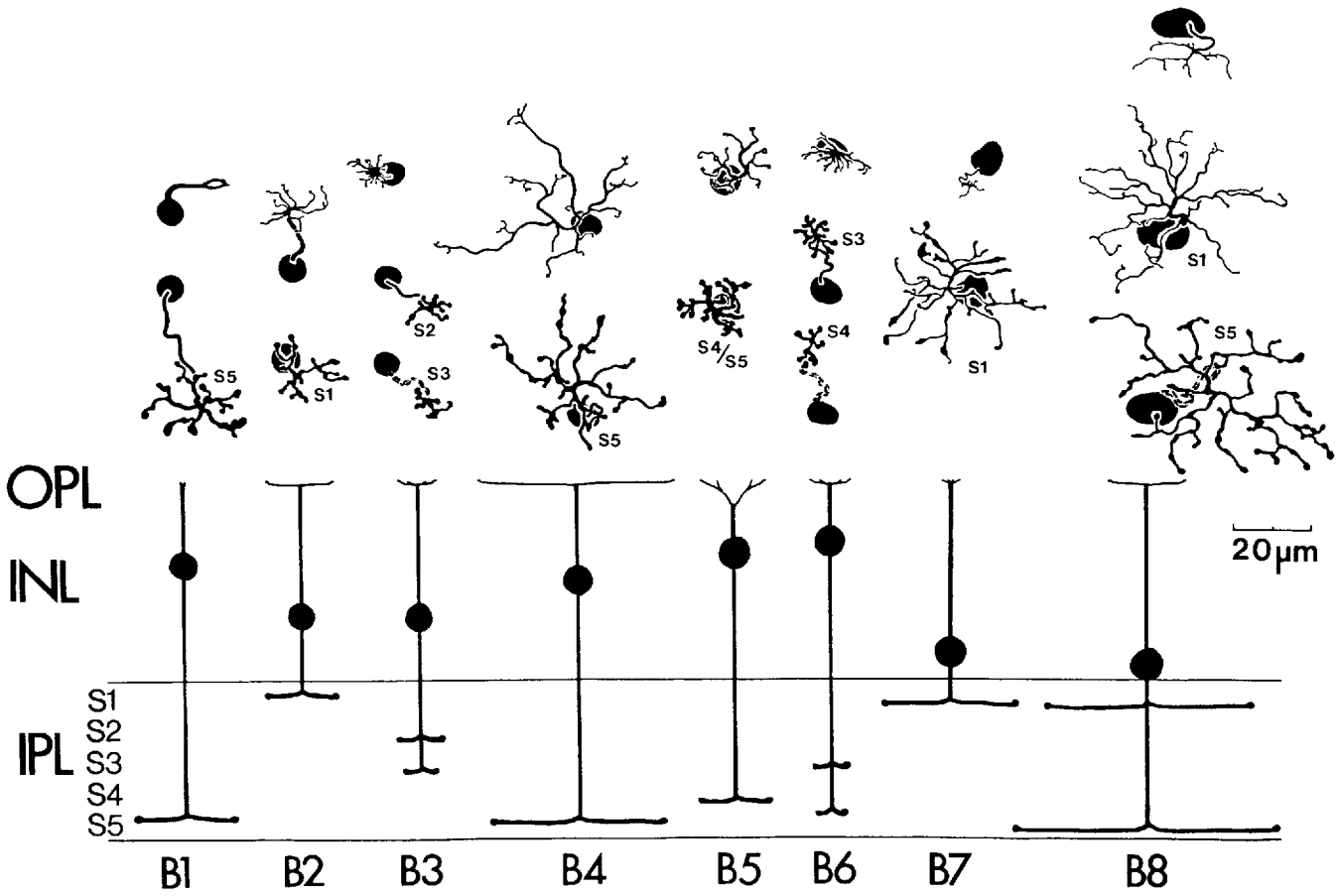

Fig. 6. Drawings and a schematic summary illustrate the 8 bipolar cell types of *Spermophilus beecheyi* by showing their relative breadth of dendritic and terminal fields and the depth of their axon terminal stratification in the IPL. All depicted examples lay roughly 4mm inferior to the ONH in a single retina.

body of *S. beecheyi* typically lies high in the INL (Figs. 6, 8d). A long and relatively thick axon descends through the INL and most of the IPL to terminate as a sparsely branched, heavily varicose axon terminal narrowly stratified to IPL stratum S5 (Fig. 8c,d). The B1 cells are readily distinguishable when focusing through wholemounts because their terminals lie deeper in the IPL than any of the other bipolar cell types. As we viewed these cells axon terminal end up, one might expect that the diminutive dendritic cluster of a "single-headed" B1 cell would be obscured by its much larger cell body looming over it nearby in the distal INL. Rarely do we see this. Instead, the single array of dendritic tips generally lies off to one side of the perikaryon (Fig. 8a). Such an impression is confirmed when the B1 cell is seen in radial section, where the ascending dendritic trunk rises obliquely in the OPL (Fig. 8d). West (1976) showed that the dendrites of the B1 cell in *S. mexicanus* are ribbon related and as such he termed the cell an "invaginating midget bipolar."

The B2 cell perikaryon usually lies in the lower INL just above the amacrine cells. A single ascending dendrite gives rise to a radial but loosely organized array of simple, fine branches with beaded tips (Figs. 6, 8e). These branches often bear a few pedunculated spines. Typically, the dendrites of B2 cells in the superior retina spread more widely and are more arborized (Fig. 7). The B2 axon terminal is restricted to IPL stratum S1, where it spreads narrowly (Fig. 8f). It is less varicose than that of the B1 cell. In the superior retina, the B2 cell axon terminal has thinner and less varicose branches, although the terminals are larger and more highly branched (Fig. 7). The B2 cell axon terminal field is somewhat broader than its dendritic field. Insofar as the B2 dendrites of the California ground squirrel are of the size and shape to innervate several photoreceptors, their gross morphology more closely resembles that of similar cells in the tree squirrel *Sciurus carolinensis* (West, 1978) than in *S. mexicanus*, where West (1976) stated that the B2 dendritic field sometimes can be so small as to innervate a single cone. In both sciurid species, West (1976, 1978) showed by Golgi–electron microscopy that B2 cells are flat bipolars contacting cones exclusively.

The B3 cell body generally lies in the lower one-half of the INL. A single ascending dendrite gives rise to a tuft of many short, fine dendritic processes beaded at their tips (Figs. 6, 8e), creating an array not only much smaller but also much denser than that of the B2 cell. In the inferior hemiretina, both its dendritic field and its varicose, bistratified axon terminal are quite small. B3 cells lying in the superior hemiretina prove to have larger and more complex processes in both plexiform layers (Fig. 7). Here the B3 dendrites are more arborized. Still, compared with the B2

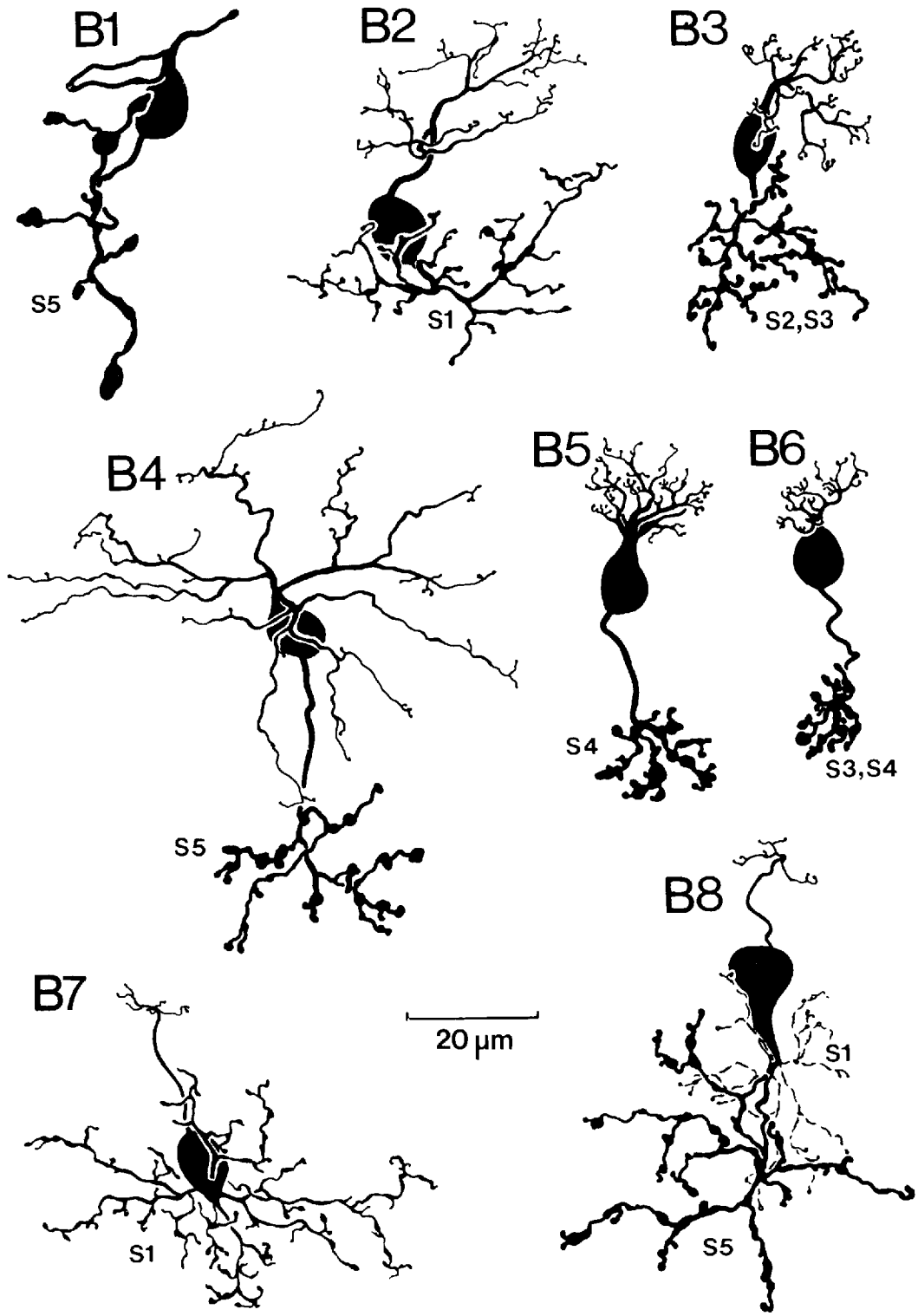

Fig. 7. Examples of the 8 bipolar cell types, all about 1 mm superior to the ONH in a single retina, are seen in an oblique plane of section, with axon terminals in the foreground, such that whole cells can be seen. Three simple branches ascend from the B1 cell body and appear to contact 2 photoreceptors. Its long axon ends in S5, with a broad, varicose terminal. The soma of B2 lies low in the INL. Its fine, branching dendrites in the OPL and axon terminals in S1 are both widely spread. B3 has its cell body in the lower one-half of the INL. Its fine and branching dendrites have beaded tips. The varicose terminal is bistratified in S2 and S3 (not evident in this oblique plane of section). The B4 cell body lies in the upper one-half of the INL. Its dendrites in the OPL spread somewhat wider than its terminal in S5. The B5 cell body lies in the outer INL. The ascending dendrite branches low in the OPL and ends as clustered dendritic terminals. Its narrow axon terminal arborizes in S4. The B6 cell is similar to B3 except that its cell body lies higher in the INL and its terminals arborize deeper in the IPL (bistratified to S3 and S4). The B7 cell soma lies in the amacrine cell sublayer of the INL. A fine, ascending process gives rise to simple, fine, and short dendrites in the OPL. Its narrowly stratified axon terminal radiates widely in S1. The B8 cell is bistratified with a large cell body in the amacrine cell layer. The small dendritic field of simple, fine processes contrasts with the wide-field terminal arborizing in S1 and S5.

TABLE 1. Bipolar Cells of *Spermophilus beecheyi*

Cell type (sample size)	Figure	Stratification in IPL S1	S2	S3	S4	S5	Displacement (mm) from ONH midpoint* (x, y)	Soma size (μm)	D_{max} (μm) Dendritic field	Axon terminal field	Probable equivalent in *S. mexicanus*[1]	Possible equivalent in rabbit[2]	Possible equivalent in human[4]
B1	7					■	+3.7, +0.4	8 × 8	2	44	B1	wb	BBb
(many)	6					■	+5.2, −3.8	6 × 6	2	25			
B2	7	■					+3.0, +1.3	11 × 8	37	53	B2	ma	DBa
(many)	6	■					+5.0, −4.2	7 × 7	18	17			
B3	7		■				+3.2, +0.6	6 × 6	24	29	B3	nab	—
(many)	6		■				+4.9, −4.3	7 × 6	11	12			
B4	7					■	+3.6, +0.6	7 × 7	79	32	B4	rb[3]	RBb
(many)	6					■	+4.1, −4.0	8 × 6	51	44			
B5	7				■		+3.5, +0.6	7 × 7	19	19	B5	nb2	DBb
(several)	6				■		+3.9, −4.0	7 × 7	17	19			
B6	7			■			+2.9, +0.7	7 × 7	16	15	B6	nb1	—
(many)	6			■			+3.6, −4.3	8 × 6	14	11			
B7	7	■					+3.5, +1.3	7 × 7	12	60	B7	wa	BBa?
(many)	6	■					+4.2, −4.0	8 × 7	6	35			
B8	7	■				■	+1.9, +0.6	9 × 9	14	36/53**	—	—	GBa,b
(several)	6	■				■	+3.5, −4.3	13 × 7	24	50/66**			

*Superior nasal quadrant (SN) = +, +; superior temporal quadrant (ST) = −, +; inferior nasal quadrant (IN) = +, −; inferior temporal quadrant (IT) = −, −.
**Upper tier (S1)/lower tier (S5).
[1]West, 1976.
[2]Famiglietti, 1981.
[3]Dacheux and Raviola, 1986.
[4]Kolb et al., 1992.

cell of the upper hemiretina, the B3 dendritic tree is smaller and more compact (Fig. 7). Restricted to the middle of the IPL, the B3 cell axon terminal ramifies independently in both S2 and S3 (Figs. 6, 8f,g). The upper group has slightly thinner processes and smaller varicosities than those of the lower group in S3. In the superior retina, processes of both groups are longer and more highly branched. West showed that B3 cells made only flat contacts in *S. mexicanus* (1976) and in *Sciurus carolinensis* (1978). In the latter species, he pointed out that, although most of the flat contacts were onto cones, B3 cells can make flat contacts onto rods as well, earning their nickname as "mixed" flat bipolar cells.

The cell body of the B4 cell lies in the outer one-half of the INL. A single ascending dendrite gives rise to 4 or 5 long, simple, and tapering dendritic trunks along which short branches or spines occasionally arise, each beaded at its tip. The B4 cell has the widest dendritic field of all 8 bipolar cell types seen in *S. beecheyi*, often spreading 50 μm in the inferior retina (Figs. 6, 8e) and up to 80 μm in the superior retina (Fig. 7). These dendrites are rather cone bipolarlike and appear to almost stretch in seeking out the few rods available in the OPL. A stout axon descends directly through the INL and IPL before its branched axon terminal spreads widely and narrowly in S5 (Fig. 8h). Generally, the B4 cell's axon terminal field is slightly smaller than its dendritic field; its thick axon terminal branches are loosely organized (Fig. 8h). West (1978) reported that the B4 cells in both *S. mexicanus* and *Sciurus* contact rods only. Although he showed that these contacts with the rods were "ribbon related" in both species, the B4 cell of *Sciurus* made flat contacts onto the rods as well. The B4 cell of *S. beecheyi* differs from its counterparts in these 2 species in that its axon terminal is larger relative to its dendrites and more elaborate.

The B5 cell perikaryon lies in the outer INL. Its ascending dendrite branches more proximally in the OPL than the

Fig. 8. Light micrographs of Golgi-impregnated bipolar cells photographed from the ganglion cell side of the retina. Table 4 presents the dimensions and retinal position of the cells shown here. **a:** Two B1 cells, whose dendritic terminals are 60 μm apart, lie at the inferior periphery (6.5 mm below the ONH). Each has 2 or 3 ascending dendritic trunks that apparently converge into a single cluster located off to the side of their respective somata (seen here as shadows). **b:** A B1 cell of the superior periphery (4.5 mm above the ONH) appears to innervate 3 nonadjacent photoreceptor terminals. A fourth branch (arrowhead) ends with a small beaded tip out of this plane of focus, perhaps due to a fold in the wholemount. Its soma, lying at the outer edge of the INL, is quite evident. **c:** The varicose axon terminal of the B1 cell shown in b is narrowly stratified to IPL stratum S5. **d:** A B1 cell is seen in radial aspect in a retinal fold near the ONH. Its single dendritic trunk rises obliquely through the OPL apparently to contact a single photoreceptor base. Its perikaryon lies in the outermost INL while its planar terminal spreads along the inner edge of the IPL. **e:** The dendrites of 5 different types of bipolar cell from the inferior periphery, 7.6 mm below the ONH. The highly arborized dendrites of 2 B4 cells are much larger than those of the other types. Among the narrow-field types, B2 dendrites are the most loosely organized and least branched; B3 dendrites the most densely arborized; and B5 and B6 are intermediate in form. Lying in the outer INL, the cell bodies of the B4, B5, and B6 cells appear as dense shadows. **f:** This same field at the border of S2 and S3 separates sublamina a from b. The B2 cell axon terminal is evident as is the smaller, more densely organized outer tier of B3 terminal processes. The descending axons of the B5 and B6 cells are shown at the arrowheads. The perikarya of the B2 and B3 cells, located in the inner one-half of the INL, are evident as shadows. **g:** At the border of S3 and S4, the dense inner tier of the B3 terminal and the outer tier of the B6 cell axon terminal can be seen. **h:** At the border of S4 and S5 lie the broad terminals of the B4 cells as well as those of the B5 cell and the inner tier of B6 processes. **i:** The tiny, thin, and finely beaded dendrites of the B7 cell seem to spread widely enough to contact several adjacent photoreceptor terminals. **j:** The B7 cell axon terminal is much broader than its dendrites, and its processes are less varicose than those of the cell types described above. The B7 cell lies in the superior periphery, 4.4 mm above the ONH, and its soma at the inner edge of the INL is evident. **k:** The same B8 bistratified bipolar cell that is depicted in Figure 6 has fine dendrites that here lie beneath the small, dense dendrites of 2 B6 cells. This group of cells is located 4 mm below the ONH. **l:** At the S1/S2 border, the outer layer of the B8 cell axon terminal consists of relatively thin processes free of varicosities or beads. The oval shadow of the B8 cell soma is seen at the left. Arrowheads point to descending B6 axons. **m:** At the inner edge of S3, the upper tier of B6 cell dendrites is smaller and denser than those at the periphery (g). An arrowhead points to the B8 axon linking the two terminal layers. **n:** The B8 axon terminal in S5 is sturdy and varicose. The lower tier of both B6 terminals is also seen.

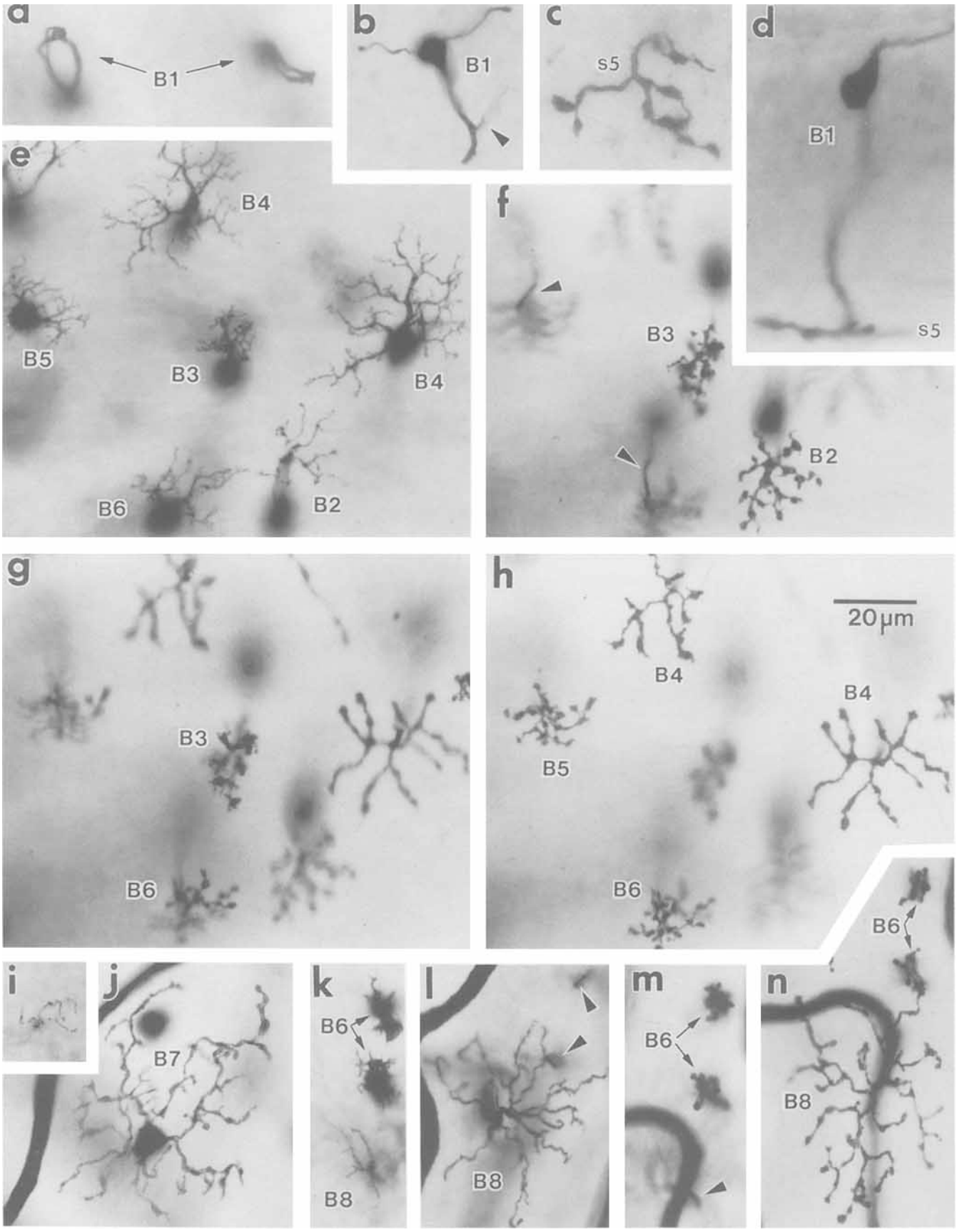
a
B1
b
B1
c
S5
d
B1
S5
e
B4
B5
B3
B4
B6
B2
f
B3
B2
g
B3
B6
h
20μm
B4
B4
B5
B6
i
j
B7
k
B6
B8
l
B8
m
B6
n
B6
B8

Figure 8

other bipolar cell types (Fig. 7) and forms a rather narrow dendritic tree that ends in clustered terminals with beaded tips. The B5 axon terminal also is small and arborizes in S4 (Figs. 6, 8h). Its relatively few branches are varicose and knobbed (Figs. 6, 7). B5 cells located in the superior hemiretina (Fig. 7) have dendritic and axon terminal processes that are longer and more arborized than those in the inferior hemiretina (Fig. 6). Although the B5 cell is the least-characterized bipolar cell type in squirrel retina, West (1976, 1978) showed that it makes numerous invaginating contacts with cones.

The B6 cell is similar to B3, except that its soma is more sclerad in the INL (Figs. 6, 8e), and its bistratified axon terminal arborizes deeper in the IPL, to sublayers S3 and S4. Its dendritic and axon terminal fields are usually smaller and more compact than those of the B5 cell (Figs. 6, 7). The upper group of processes in S3 are somewhat more complex than the group in S4 (Figs. 6, 8m,n). West (1976, 1978) reported that the B6 cell was the only mammalian bipolar cell then known whose axon terminal lay in IPL sublamina b yet made flat contacts with photoreceptor terminals, in that case, only with cones. Note that B6 cells lying in the central retina (Fig. 8k,m,n) are smaller than those in the inferior periphery (Figs. 8e,g,h).

The soma of the B7 cell lies in the amacrine cell sublayer slightly above the INL/IPL border (Figs. 6, 8j). A very thin apical dendrite ascends into the OPL, giving rise to a few short, simple, fine processes that together comprise a very small dendritic field (Fig. 8i). In contrast, the stout B7 axon terminal radiates widely but narrowly in S1, with varicosities and swellings occuring mostly at the end of its branches (Figs. 6, 7, 8j). Some of these branches cross each other. Lacking in *Sciurus* (West, 1978), B7 cells in *S. mexicanus* were termed midget flat bipolars by West (1976) because each made flat contacts onto a single cone pedicle. In *S. beecheyi*, the dendritic field of the B7 cell seems larger and much less compact than that of the B1 cell—broad enough to contact more than a single cone pedicle.

The previously undescribed B8 cell type is a large bistratified bipolar cell whose axon terminal, but not its dendrites, seem similar to the giant bistratified bipolar cells seen in monkey (Mariani, 1983) and in human (Kolb et al., 1992). Its large cell body, 9–11 μm in diameter, lies in the amacrine cell sublayer bordering on the IPL. A thin ascending process only slightly thicker than that of the B7 cell, gives rise to a small, wispy array of fine, simple secondary dendrites. Its loosely organized dendritic field seems like a larger version of B7's field (Figs. 6, 7, 8k). Some, but not all, of the sparse B8 cell dendrites are beaded at their tips. The B8 cell dendritic field clearly seems large enough to innervate several photoreceptors, yet its relatively small size contrasts with the cell's wide, globally bistratified axon terminal arborizing in both S1 and S5. The axon terminal processes in S1 consist of tapering and branching processes that bear few beads or spines and sometimes cross one another (Figs. 6, 8l). The sturdy axon terminal processes spreading in S5 are varicose, less arborized, and slightly wider in extent (Figs. 6, 7, 8n).

Amacrine cells (Figs. 9–21; Tables 2, 4)

When using radial sections, West (1976) identified only 5 types of amacrine cell in the retina of *S. mexicanus*. Using retinal wholemounts let us identify these 5 as well as 22 additional amacrine cell types in *S. beecheyi*, 3 of which, being displaced to the ganglion cell layer (GCL), West perhaps misidentified as ganglion cells.

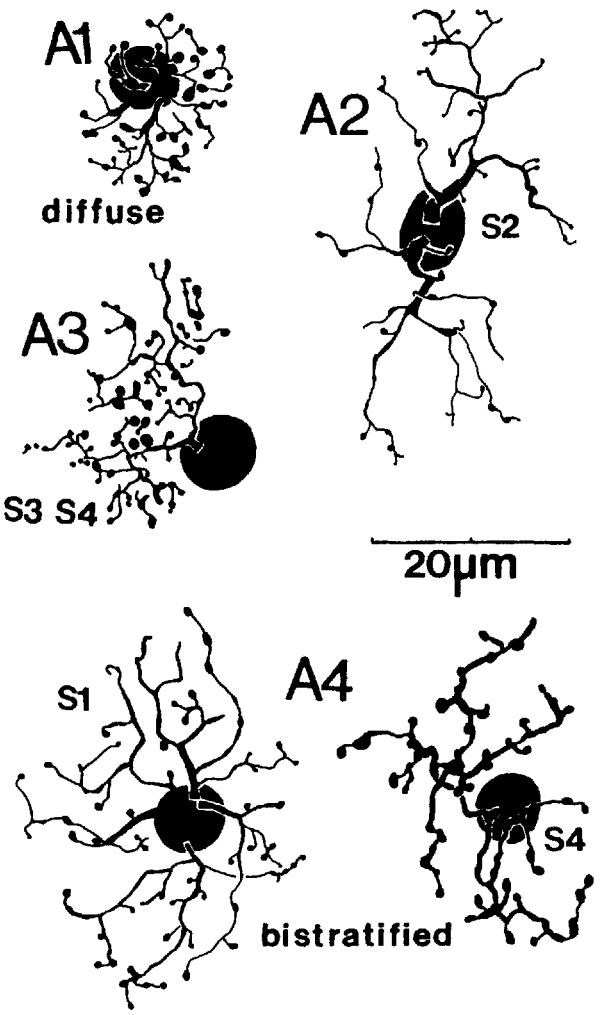

Fig. 9. Examples of the smallest amacrine cell types. The diffuse amacrine cell, A1, is the smallest of them all. Its beaded and lobular appendages descend through the IPL. A2 has an elongate dendritic tree narrowly stratified to S2. The single dendritic trunk of the A3 cell gives rise to beaded dendrites broadly stratified to S3 and S4 of IPL sublamina b. The A4 cell is bistratified with dendritic tiers of differing morphologies arborizing in S1 and S4.

Table 2 lists all the amacrine cell types that we have observed in *S. beecheyi*. It presents the somal and dendritic dimensions of all the amacrine cell examples shown, as well as the dendritic stratification of each and its position, in millimeters, relative to the ONH midpoint. Table 2 lists a number of amacrine cell types termed "mirror-image pairs" whose subtypes are marked "a" and "b." In each case, the a subtype has its cell body in the amacrine cell sublayer of the INL, and the b subtype has its soma in the GCL. Although it is certain in the case of the starburst amacrine cell, A5, that its two subtypes tile the entire retina, it is not yet clear that this is true of the other mirror-symmetric pairs, largely due to insufficient numbers of impregnated examples. We have seen, however, multiple examples of all such subtypes. Typically, the dendrites of these subtypes occupy different IPL sublaminae, usually whichever sublamina is nearest its cell body (sublamina a consists of Ramón y Cajal's S1 and S2; sublamina b, his S3, S4, and S5; Famiglietti and Kolb,

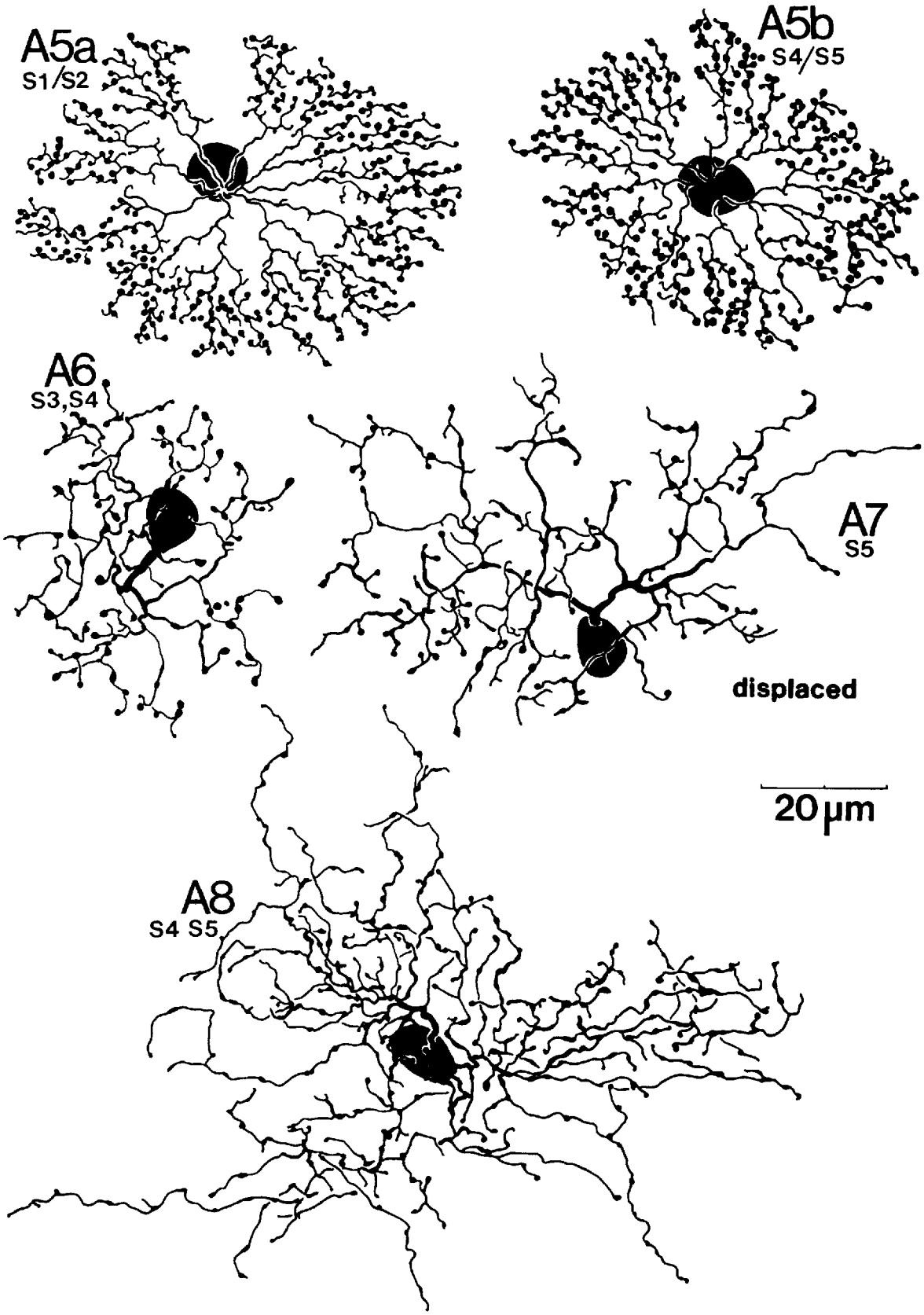

Fig. 10. Examples of 4 other types of small amacrine cells. A5a and A5b are examples of the 2 subtypes of starburst amacrine cells. A5a has its soma in the INL and its dendrites narrowly stratified to the border of S1 and S2. A5b has its soma displaced to the GCL, with its dendrites confined to the border of S4 and S5. The A6 cell has a thick dendritic trunk that branches in both S3 and S4. The displaced A7 amacrine cell is narrowly stratified to S5. The A8 cell ramifies broadly in S4 and S5.

1976). Here, only the A19 pair defies this convention (see below). We argue that, because the subtypes of these pairs ramify in different IPL sublaminae, they are in fact distinctive subtypes and not accidental or atypical "displacements."

The diffuse amacrine cell, A1 (Figs. 9, 21a), is the smallest of all 25 types. It has a small, round cell body and a dendritic tree that ramifies across the IPL (S1–S5), although only the tips of 1 or 2 of its branches reach into S5. A1 cell dendrites bear varicosities of varying size. This cell type seems directly analogous to the "narrow-field diffuse" A1 cell described in *S. mexicanus* (West, 1976).

The loosely organized and elongated dendritic tree of the monostratified A2 cell (Fig. 9) spreads only in S2. Its simple, rarely overlapping, and tapered dendrites bear occasional beads, pedunculated spines, and branchlets. It has not been described previously in squirrel retina.

The single dendritic stalk of the A3 cell (Figs. 9, 21a) gives rise to a beaded dendritic tree that is quite a bit larger than that of the A1 type and ramifies only in S3 and S4 of IPL sublamina b. This cell has no known sciurid counterpart.

The commonly impregnated, bistratified A4 amacrine cell (Fig. 9) has beaded dendrites spreading to equal extent in both S1 and S4. Those in S1 are thin and more arborized (Figs. 9, 21f), and those in S4 are thick and varicose (Figs. 9, 21g). The dendrites of both tiers bear pedunculated spines. This cell type seems homologous to the narrow-field bistratified A4 cell described in *S. mexicanus* (West, 1976) and even to the narrow-field bistratified A8 amacrine cell described in cat retina (Kolb et al., 1981). The bistratification pattern of the A4 cell is global (see Amthor et al., 1983).

The amacrine cell type that we studied most is the A5 or "starburst" amacrine cell (Famiglietti, 1983a). Starburst amacrine cells have been identified in a wide variety of vertebrate retinas, and thus the A5 cell is the most familiar of the 6 types of mirror-image amacrine cell that we describe here. The A5a cell perikaryon lies in the INL with dendrites spreading in OFF sublamina a of the IPL. The A5b subtype has its cell body in the GCL and its dendrites arborizing in IPL ON-sublamina b. Other than the location of their cell bodies and the depth of their dendritic arbors in the IPL, the morphology and dendritic field size of the 2 subtypes differ only in subtle ways (see below). Thus, the A5 cell subtypes are the best examples of mirror-symmetric pairs in *S. beecheyi* retina.

Both subtypes of starburst amacrines have relatively large cell bodies. By measuring the D_{max} of A5 somata from all regions of the retina (210 A5a and 212 A5b cells), we determined that the D_{max} of both subtypes ranged from 8 to 13 μm, most being 9–11 μm across. On average, the A5b cells have slightly larger perikarya (10.3 vs. 9.6 μm). We also noted that there was no uniform change in size of these cell bodies with displacement from the visual streak. Thus, although adjacent cells of both subtypes have roughly equivalent dendritic field sizes (see below), their somata might be quite different in size.

Typically, 4–6 primary dendrites leave the cell bodies of both subtypes and enter the IPL. However, about 10% of the A5b cells issue a single, thick dendritic stalk up to 11 μm long that ascends vertically into the IPL before giving rise to these radiating dendrites. For both subtypes, these primary dendrites taper abruptly before bifurcating within the inner one-half of the dendritic field and then branching more profusely in the outer one-half. The highly branched perimeter of both A5 cell subtypes is conspicuously invested with uniformly sized beads, whereas the fine, inner, spokelike array of wavy primary and secondary branches are only sparsely adorned with thin, sessile spines. This structural dichotomy creates the annular, starburst appearance of these cells (Figs. 10, 11, 21d,h). The dendrites of the A5a subtype typically spread along the border of S1 and S2 (Fig. 21d). The A5b dendritic arbors stratify to the border of S4 and S5 (Fig. 21h). This latter subtype most likely is the equivalent of the G12 ganglion cell described in *S. mexicanus* (West, 1976). West himself wondered if this "easily recognized cell" with its "doughnutlike" dendritic tree might be an amacrine cell because he never saw axons emanating from cell bodies and because he observed that some of these cells had somata in the INL. He additionally noted that the dendrites of these "displaced" cells ramified in the outer rather than inner layers of the IPL, so he was also seeing the A5a variety on occasion.

Compare the A5a cell with the A5b cell in Figure 10, both of which are located 2.8 mm below the ONH in the same retina; photographs of both are also shown in Figures 21d and 21h, respectively. Several subtle morphological differences in the 2 subtypes can be seen. The dendritic field area of the A5b cell is smaller than that of the A5a, and its perikaryon is the larger of the two. As a consequence, the diameter of the beadless central field around the A5b nucleus seems foreshortened. The peripheral beads on the A5b cell dendrites are slightly larger than those on the A5a cell. By focusing up and down through the retinal wholemounts (see Fig. 21d,h), we studied 326 mirror pairs of A5a and A5b cells in all retinal locations (most from the same retina). Every pair measured had dendrites that either overlapped or were within 100 μm of each other. From this data, we determined that the dendritic field area of the A5a subtype typically averages 1.2 times that of the A5b subtype.

This analysis also demonstrated that A5 cells in the same retinal locus are very similar in size and that examples of both subtypes increase in dendritic field area with increasing distance from the visual streak. This is illustrated for the A5a subtype in Figure 11. As with the H1 horizontal cells, this rate of increase in dendritic field size with displacement from the visual streak is greater for cells above it than for those below. From this same figure, it appears that the outer beaded portion of the A5 dendritic tree is less arborized in peripheral retina (Figs. 11d,f) than centrally (Fig. 11a–c). Figure 12 shows the dendritic field size distribution for both A5 subtypes and results from the measurement of 1,235 A5 cells in 2 retinas; 435 were subtype a, 800 were subtype b. It also shows that the A5b cells are consistently smaller than adjacent A5a cells at all locations (e.g., the region containing cells whose dendritic areas are less than 2,500 μm^2 is larger for the A5b cells than for the A5a cells).

As reported in a number of other species, the dendrites of neighboring A5 cells (both subtypes) extensively overlap, forming a dense plexus when a patch of adjacent cells stain. One unexpected finding was that, despite eccentricity, the number of dendritic beads per cell remains relatively constant, typically about 400. Of course, this data should be appraised in light of the known risks of assuming any cell's complete impregnation by the Golgi method.

The A6 cell (Fig. 10) has a single, sturdy dendritic trunk that descends into the IPL before arborizing broadly in S3 and S4. Its dendrites bear many rather large beads and small, sometimes overlapping, appendages that appear to

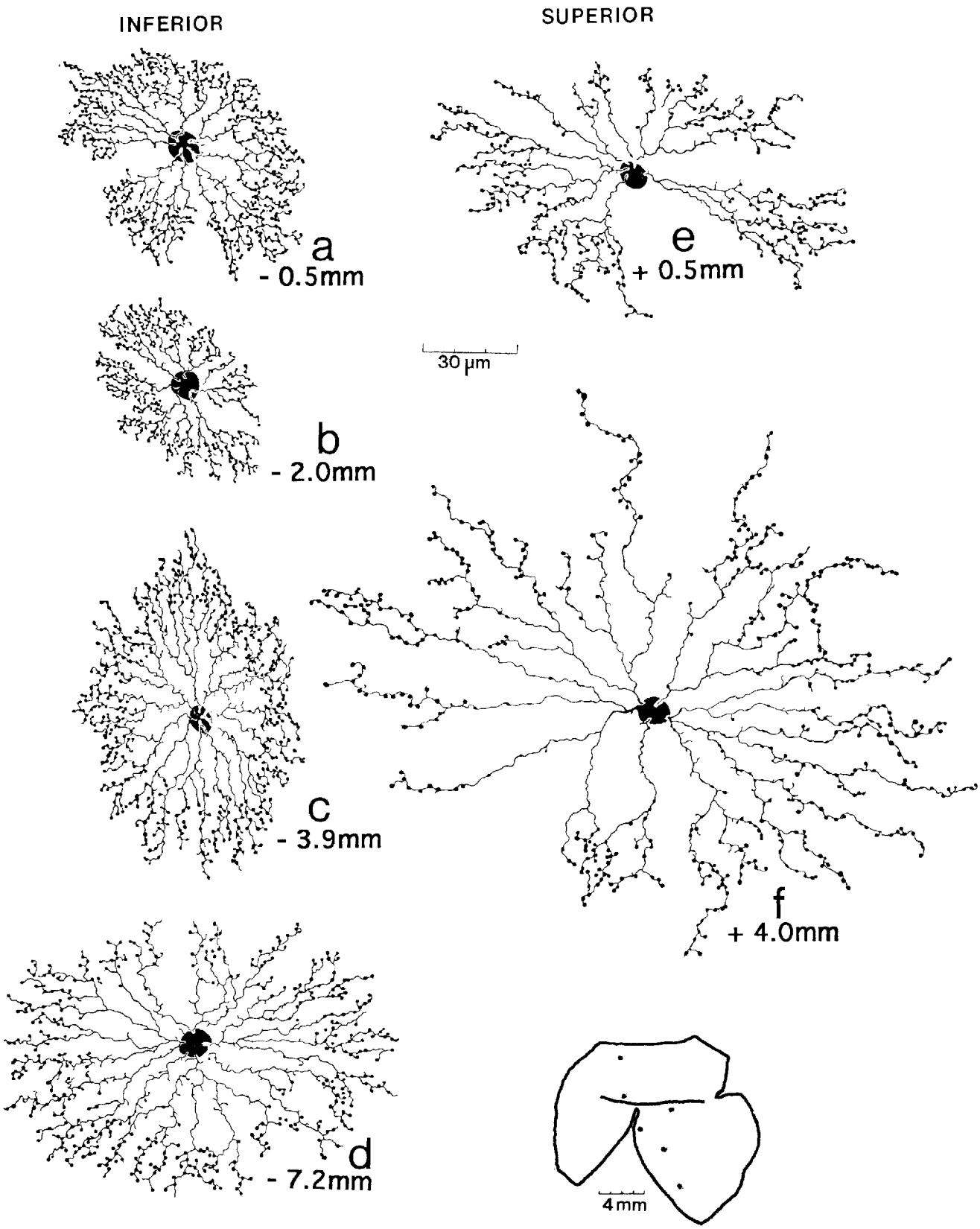

Fig. 11. **a–f:** The dendritic field size of the A5a amacrine cell changes with retinal location. The dimension given beneath each cell is the vertical distance from the ONH. Cell dimensions and locations are given in Table 4. **Inset:** The location of each of the examples shown in this figure is shown in this drawing of a wholemount.

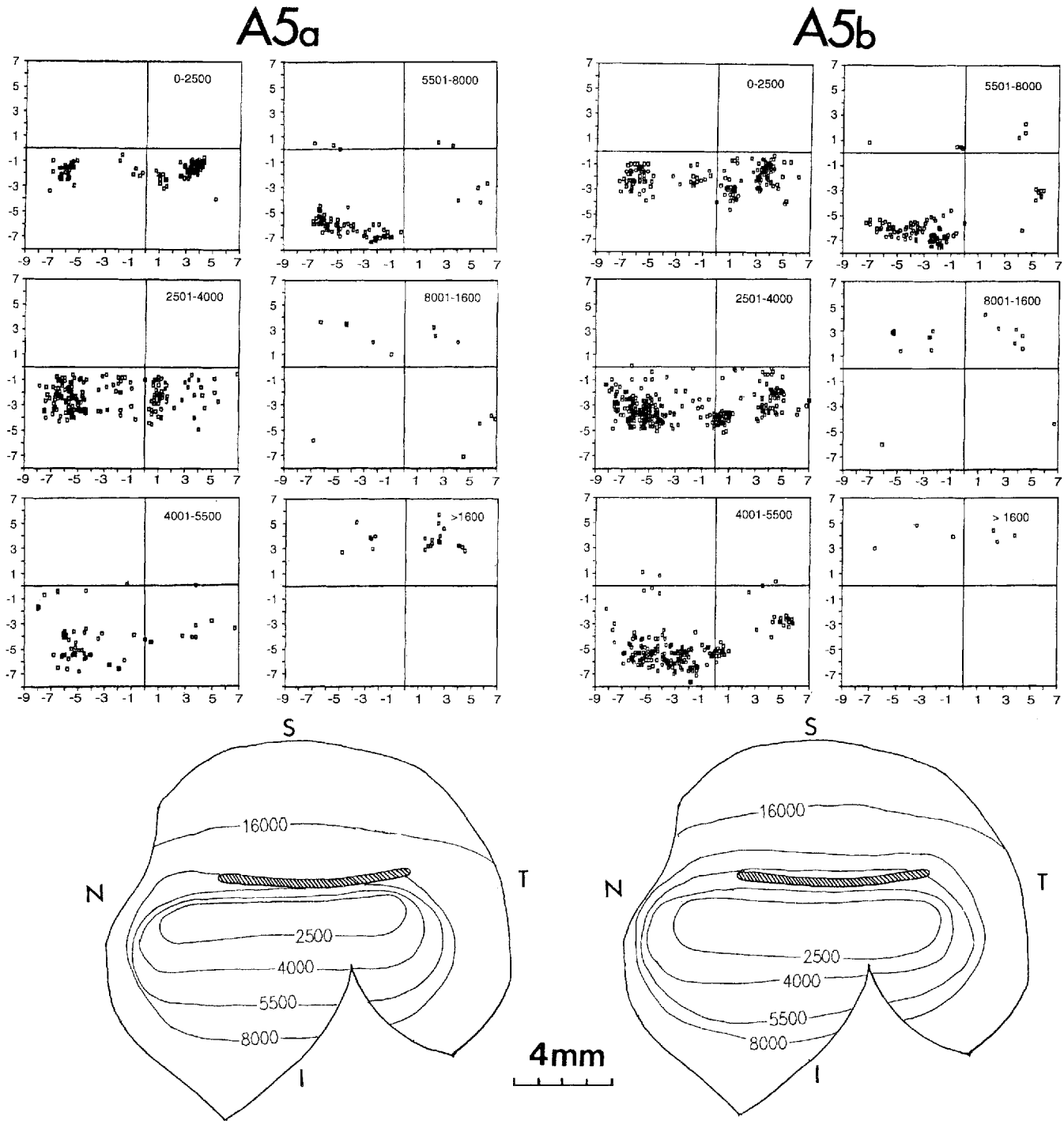

Fig. 12. Representation shows dendritic field area (in μm^2) versus retinal location for the A5a and A5b amacrines. The hatched area in each wholemount diagram represents the ONH. Note that the smallest cells cluster around the visual streak 2 mm inferior to the optic nerve head. The largest size classes mostly lie in the superior retina. Above the wholemount diagrams for each A5 subtype are graphs of the 6 size bins showing the locations of cells found in each. A total of 1,235 A5 cells are represented.

fill in space. Its dendritic tree is much larger, but far less dense, than that of the A3 type also stratifying to S3 and S4.

The A7 cell (Fig. 10) is a displaced amacrine cell whose soma thus lies in the GCL. A sturdy dendritic trunk rises just into the IPL where it gives rise to a large, loosely organized dendritic tree with branches confined to S5 (Fig. 21b). The tapering dendrites are beaded and bear both sessile and pedunculated spines.

The A8 cell (Figs. 10, 21i) has a large, ovoid cell body. Its fine, intertwining and tangled dendrites ramify somewhat broadly across S4 and S5. They bear varicosities and are tufted with many pedunculated and sessile spines as well as

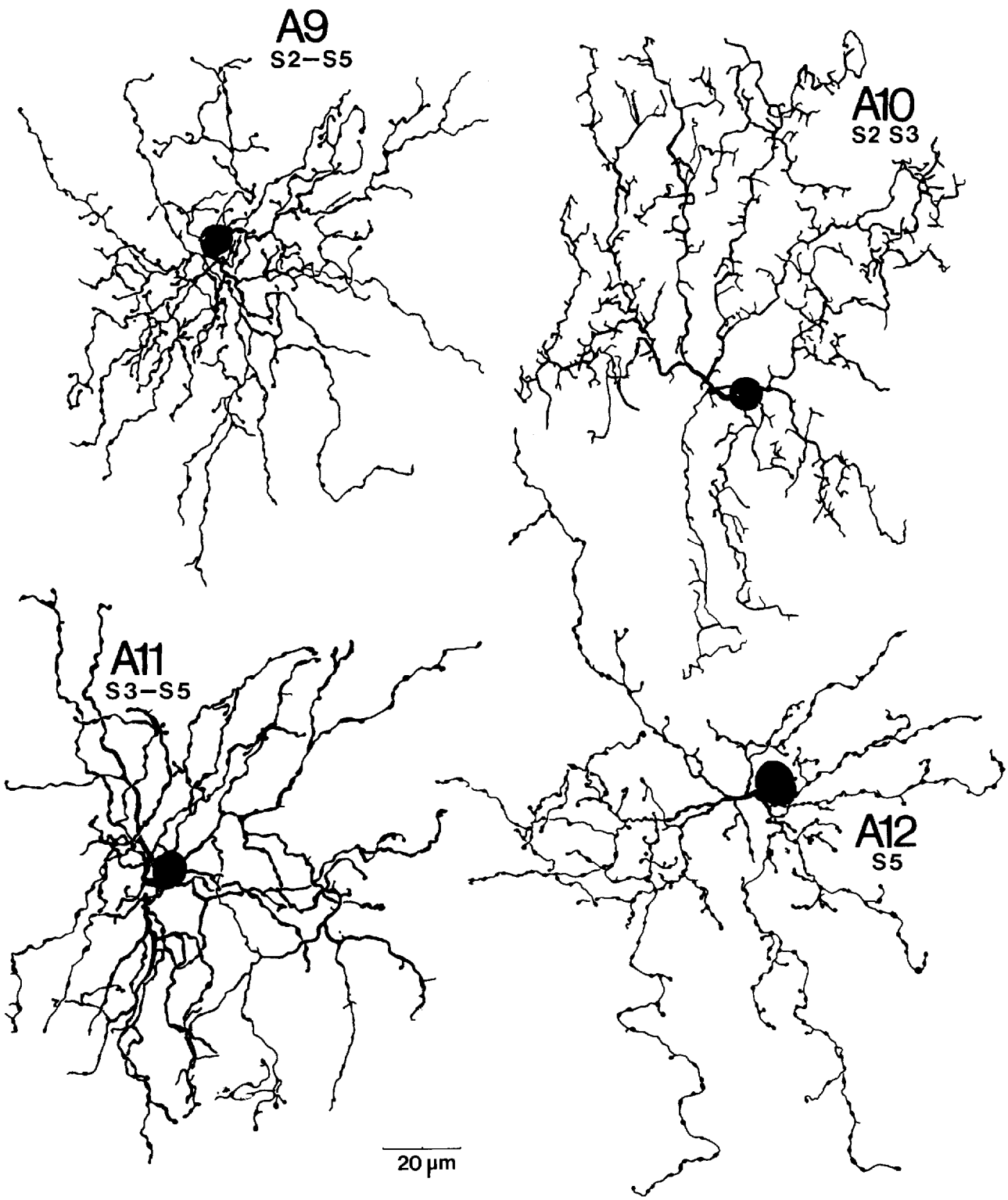

Fig. 13. The loosely intertwined A9 cell dendrites ramify broadly. The stout primary dendrite of the A10 cell arborizes in S2 and S3. The thick, beaded, and jagged dendrites of the A11 cell ramify broadly across IPL sublamina b. The large cell body of the A12 cell gives rise to dendrites narrowly stratified to S5.

simple branchlets of varying lengths. The photographed example in the superior hemiretina (Fig. 21i) is much bigger than the example near the visual streak depicted in Figure 10. Although somewhat larger, this cell type may correspond to the "narrow-field unistratified diffuse" A3 amacrine cell described in *S. mexicanus* (West, 1976).

The A9 cell (Fig. 13) has a small cell body that gives rise to a loose array of fine and curly dendrites ramifying diffusely across layers S2–S5 of the IPL. The dendrites are adorned with small beads and pedunculated spines. When collapsed onto a single plane, the dendrites appear to form a denser array than when viewed in the microscope, where they meander across all but IPL stratum S1.

The A10 cell perikaryon issues a single, stout dendritic trunk that descends into the IPL and gives rise to shaggy secondary dendrites that ramify broadly across S2 and S3. These jagged dendrites are distinctively decorated with mostly sessile spines and relatively short branchlets (Fig. 13). A10 dendrites seldom overlap.

The A11 cell (Fig. 13) has tangled, relatively thick dendrites that arborize across IPL sublamina b (S3–S5). They bear numerous beads, tuberous varicosities, and occasional sessile and pedunculated spines. In one specimen, where several A9 and A11 cells were stained side by side, the differences between these 2 broadly ramifying cell types were apparent. In comparison with the loose array of curly, fine, and overlapping A9 dendrites, those of A11 are thick, jagged, and angulated.

The A12 cell (Fig. 13) has a large cell body (12 × 10 μm) in the INL that sends forth a single thick dendritic trunk across the IPL to S5, where it gives rise to a narrowly stratified yet loosely organized array of fine, beaded, and wavy dendrites. These sometimes overlapping dendrites vary in length and bear pedunculated spines and multilobed appendages.

The elongate A13 amacrine cell occurs as 2 subtypes that form mirror pairs across the IPL. A13a has its cell body in the amacrine layer of the INL and its dendrites spreading in S2 (Figs. 14, 15), whereas A13b has its cell body in the GCL and its dendrites running in S4 (Fig. 14). Both subtypes have dendritic fields consisting centrally of thick, relatively straight, and tapering dendrites that seldom branch and bear only a few pedunculated spines. The examples in Figure 14 could well be understained. More completely impregnated examples may have much larger dendritic fields when their finest processes stain (Fig. 15). Note that these finest processes are beaded distally (see Fig. 14, double arrows).

The A14 cell body lies in the GCL. Three thick dendritic trunks branch to create a loosely organized and lobular dendritic tree narrowly confined to S5 (Fig. 14). These primary dendrites gradually thin after branching points. The frequently overlapping, delicate outer branches are beaded, somewhat crinkled, and sometimes retroflexive. We did not find an equivalent cell with its perikaryon in the INL.

The A15 cell body lies in the GCL and issues several thick primary dendrites that rise into the IPL before branching into wavy secondary and tertiary dendrites that taper and radiate widely but remain narrowly stratified to S4 (Fig. 15). Distally, the dendrites rarely overlap and are beaded and unbranching.

The displaced A16 amacrine cell (Fig. 15) is a very unusual type; the cell shown here was the sole example that we observed. Its perikaryon in the GCL gives rise to a single, thick dendritic trunk that rises obliquely into the IPL before radiating long, crinkly and beaded dendrites that, for the most part, gently rise through S4 into and across S3. These relatively straight dendrites seldom branch or cross one another. A number of them, however, abruptly change into frenzied, squiggly processes winding around on themselves and each other. Some meander across the same 2 strata as the straighter dendrites; most rise up and then down across the entire IPL without any apparent pattern. These twisting and retroflexive segments seem more heavily invested with beads, short branchlets, and sessile spines than the rest of the dendritic field. Taken together, the A16 cell dendrites occur in all IPL strata, and as such the resultant dendritic tree has diffuse characteristics, although its main stratification lies in S3 and S4. It is an open question whether this cell is purely anomalous or whether its squiggly processes, being more refractory to Golgi impregnation, are usually absent, leaving the central and planar A16 dendrites looking like understained versions of the A17b type (see below). In many respects, the A16 type morphologically resembles the interplexiform cell in human retina (Kolb et al., 1992) except that we did not observe any processes ascending to the OPL.

The A17 amacrine cell mirror-pair (Fig. 16) has two subtypes with round cell bodies that are central to circular dendritic fields comprised of a profusion of narrowly stratified, overlapping, and wavy dendrites. These fine, crinkly dendrites bear few beads or spines. The A17a cell body lies in the INL; its dendrites spread in S2. The A17b cell body lies in the GCL and its more densely organized and broadly stratified dendritic tree ramifies across both S3 and S4. On morphological grounds alone, this subtype seems similar in size and stratification to the single cell observed in *S. mexicanus* that, although no axon stained, West (1976) classified as his G15 ganglion cell. We have not observed any ganglion cell type in *S. beecheyi* that could be the equivalent of West's G15, although we certainly cannot rule out the possibility that such a cell might simply have failed to impregnate.

The characteristic morphology of the A18 cell (Fig. 16) is a dense arbor of fine, overlapping dendrites in the central 100 μm of its dendritic field, beyond which a few unbranching dendrites extend for varying distances. Its crinkly dendrites stratify to S3 and are heavily invested with fine beads, a fact all but lost at low magnification. The A18 I type in Figure 16 has its cell body in the INL, and that of the A18 II type lies in the GCL (Figs. 16, 21c). We saw roughly an equal number of both types. It was our impression that the displaced A18 II cells ramify somewhat more broadly across S3 and even into S4 than the normally placed examples. Although the two displaced examples shown here lie about a millimeter apart on either side of the visual streak, the example in Figure 16 is much larger.

The A19 amacrine cell has two subtypes: A19a, with its nucleus in the INL, and A19b, whose soma lies in the GCL (Fig. 16). The semicircular dendritic field of both subtypes is most apparent when noting that the cell body lies in the periphery of its respective dendritic field, more or less centered along the diametric edge. The radial, nonbranching, and wavy dendrites of the A19 cell are studded with large beads obviously larger than those on the A18 dendrites. A19a has a single, thick dendritic stalk that descends through the outer IPL to branch profusely and widely in S3 and the outer one-half of S4. The dendritic trunk of A19b rises from its cell body to ramify in S2 and S3, *above* the dendrites of A19a.

The A20 amacrine cell drawn in Figure 17 and photographed in Figure 21k and 21l is locally bistratified, arborizing centrally in S5 (Fig. 21k) and more widely in S1 (Fig. 21l), where several processes extend beyond the central dendritic mass, a few well beyond. The crinkly dendrites narrowly stratified at both levels bear occasional pedunculated spines. The dendrites in S5 are much more heavily

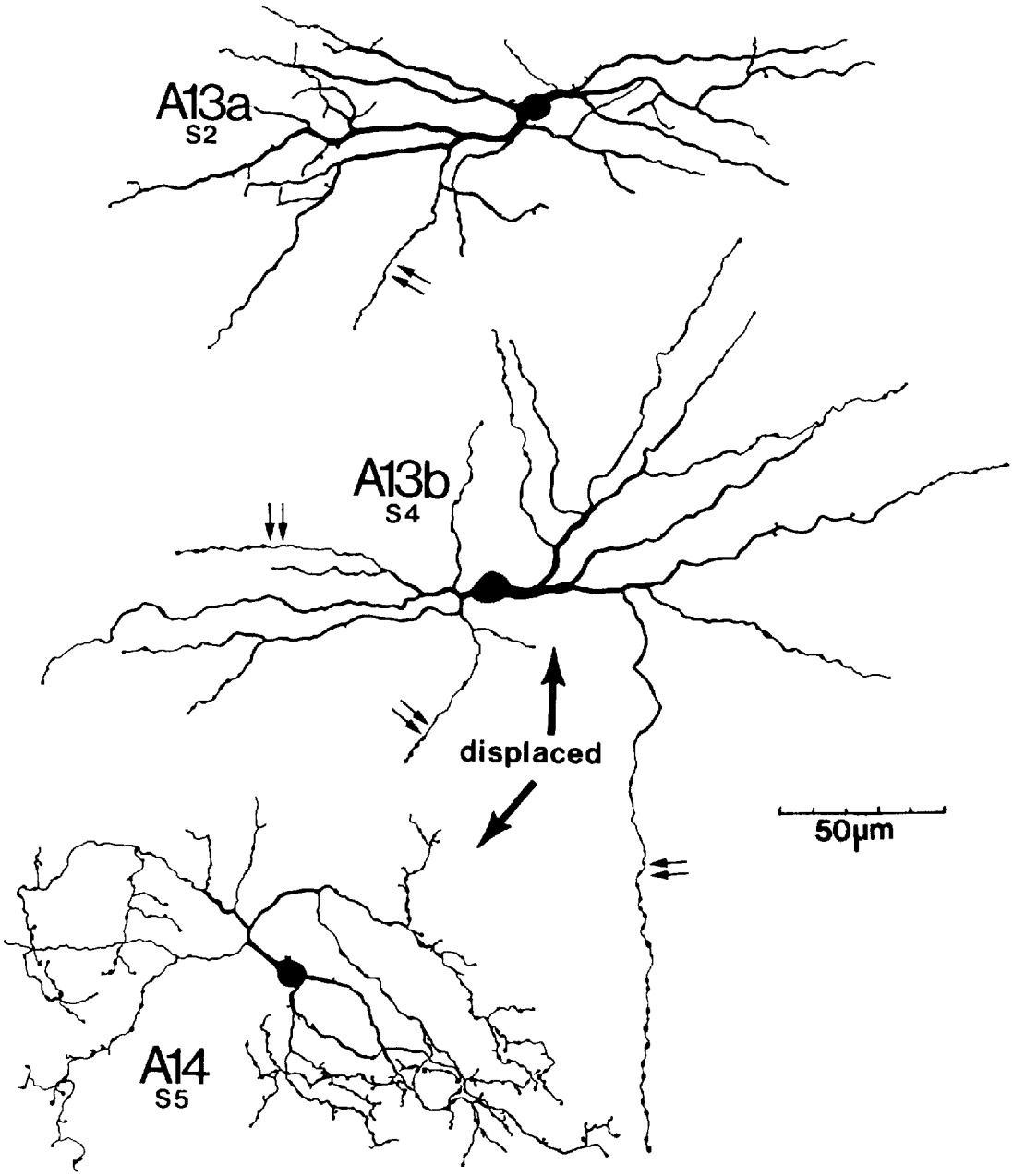

Fig. 14. The A13a cell has straight and tapering dendrites narrowly stratified to S2. Its displaced counterpart, A13b, has dendrites running in S4. Their finest processes are beaded distally (double arrows). The displaced amacrine cell, A14, has fine, beaded dendrites restricted to S5.

invested with beads than those in S1, a fact best appreciated in Figure 21k.

The A21 amacrine cell (Fig. 17) is tristratified with dendritic tiers spreading in S1, S3, and S5. It has an overall dendritic field of 220 × 170 µm. D_{max} values for each of the three layers are 220, 115, and 95 µm, respectively. The curved and loosely organized dendrites in all 3 strata bear uniformly large beads.

The A22 cell (Fig. 17) is regionally bistratified and has simple and beaded dendrites that are sparsely organized in both layers. Most of A22's processes spread across sublamina a (S1 and S2); the shorter, simpler processes that course through outer sublamina b (S3 and S4) arise from primary and secondary dendrites rather than the cell body. These latter dendrites have few branches and even fewer spines.

Another locally bistratified cell, A23, has a tangle of overlapping dendrites that bear beads, varicosities, and occasional spines (Fig. 17). The dendrites in S1 and S2 are relatively thick, whereas those in S4 and S5 are thin, crinkly, and, in some cases, much longer than the rest.

Largest of all the amacrine cells, the A24 cell (Fig. 18) has a few long, straight, and simple dendrites radiating in S1. These dendrites branch from the 2 dendritic trunks arising

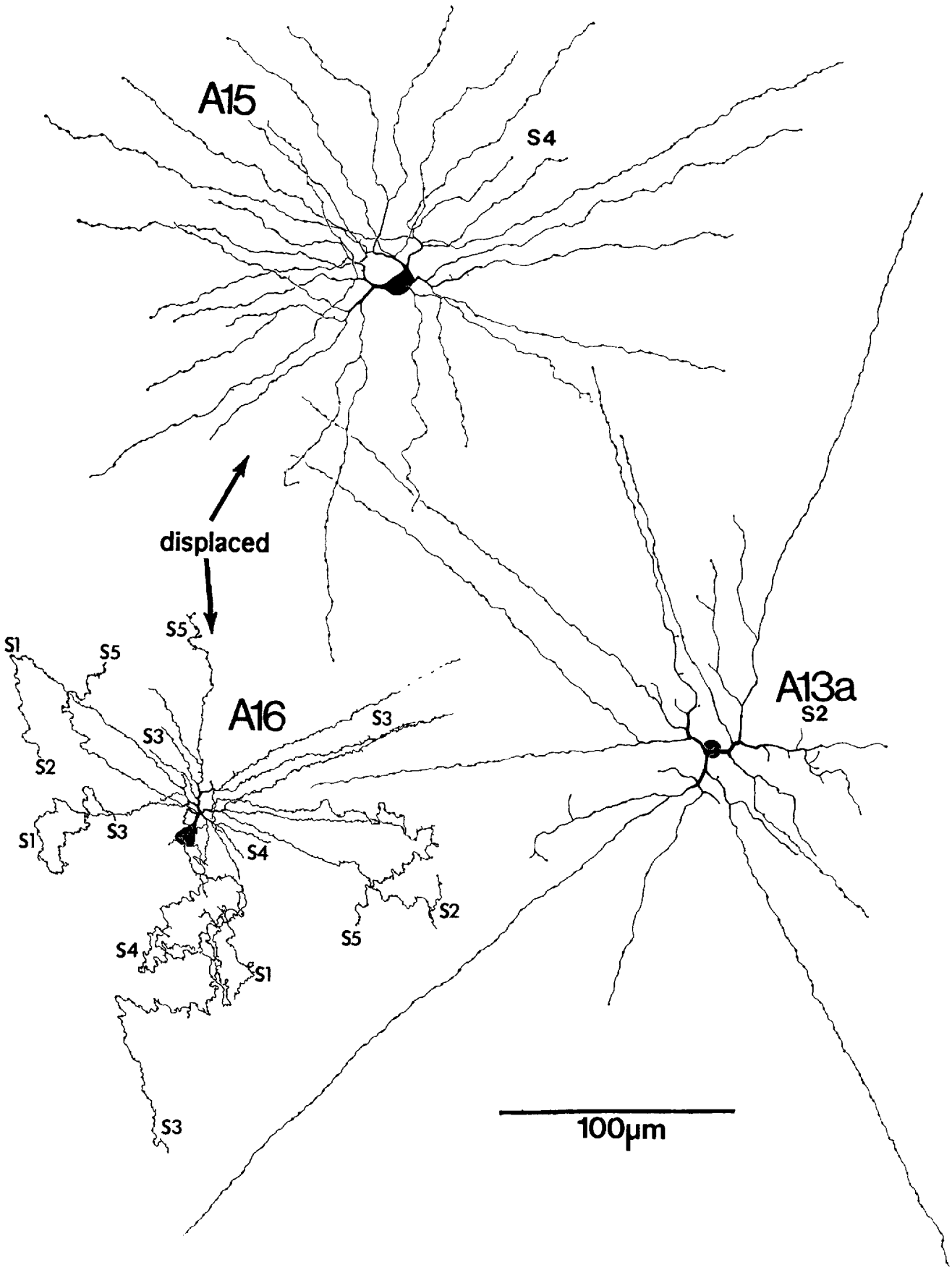

Fig. 15. The large A13a cell shown here is proposed as a more completely impregnated example of the OFF subtype of the A13 amacrine pair shown in Figure 14. Note the thick, tapering dendritic trunks and the thin, beaded distal dendrites. The displaced A15 cell has simple, seldom-branching dendrites radiating narrowly in S4. Its wavy dendrites are beaded distally. The unique A16 cell is displaced and radiates several wavy, beaded, and unbranching dendrites in S4 and S3. Some suddenly wriggle and twist as they run up and down and back and forth in the IPL.

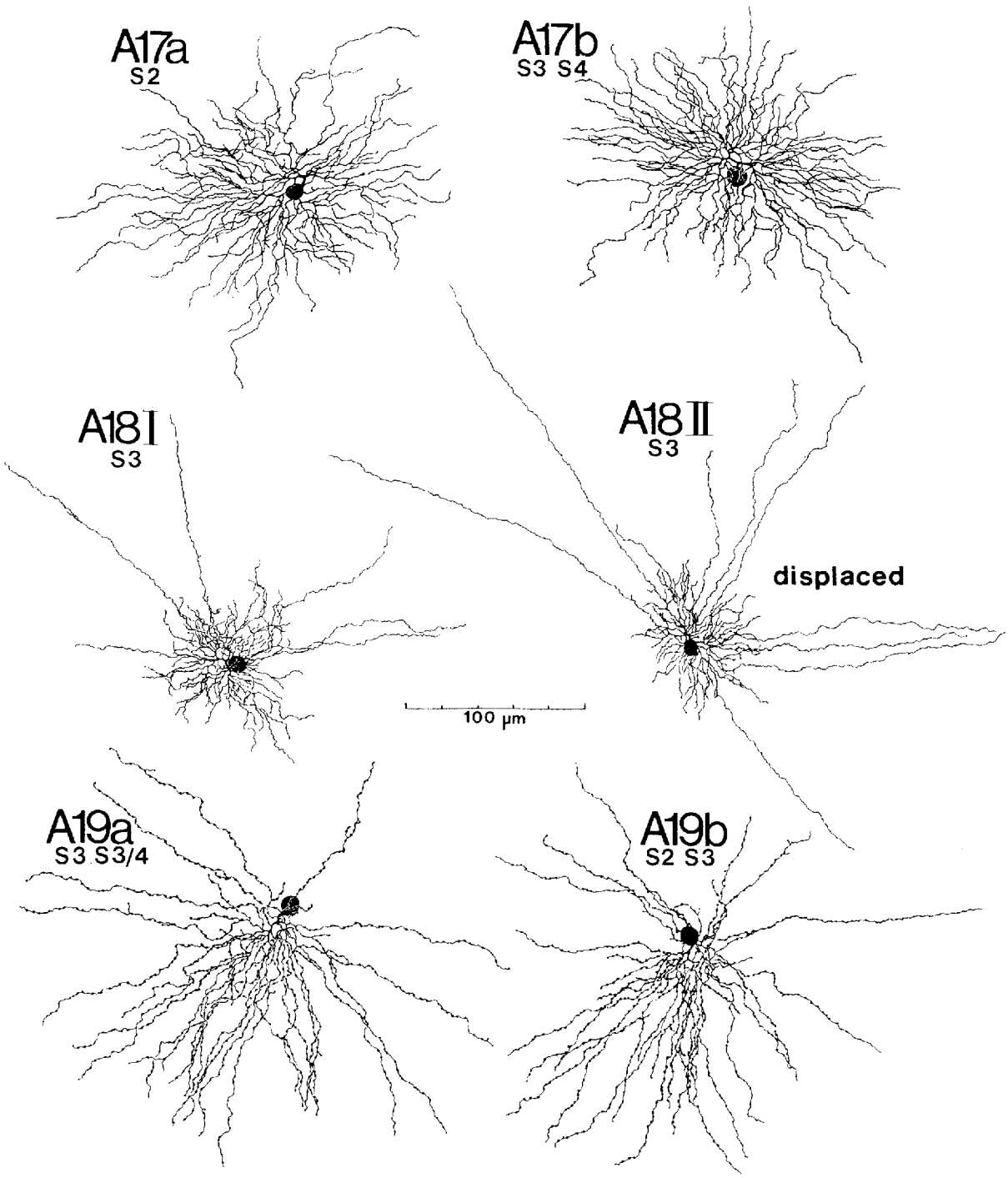

Fig. 16. The A17a cell has a round cell body, with a profusion of radial and overlapping dendrites in S2. Its displaced counterpart, A17b, has its dendrites more broadly stratified to S3 and S4. The A18 I cell has a few straight dendrites extending beyond its dense central field. Its displaced counterpart is A18 II. The dendrites of both stratify to S3. The A19a cell has a single, thick dendritic trunk that branches profusely in S3 and S4. Its displaced partner, A19b, has dendrites that run in S2 and S3, *above* those of A19a. The cell body in both subtypes lies to one side of its dendritic field.

on either side of the round cell body (Figs. 20, 21j). These nonoverlapping dendrites bear neither spines nor beads and, except close to the cell body, never branch. This cell may be the equivalent of the "broad-field unistratified" A5 in *S. mexicanus* (West, 1976).

The A25 amacrine cell (Fig. 18) has two subtypes: A25a, whose perikaryon lies in the INL, and A25b, whose perikaryon is "displaced" to the GCL. Both have large cell bodies whose dendritic trunks give rise to simple, straight, and symmetrically radiating dendrites that rarely cross or

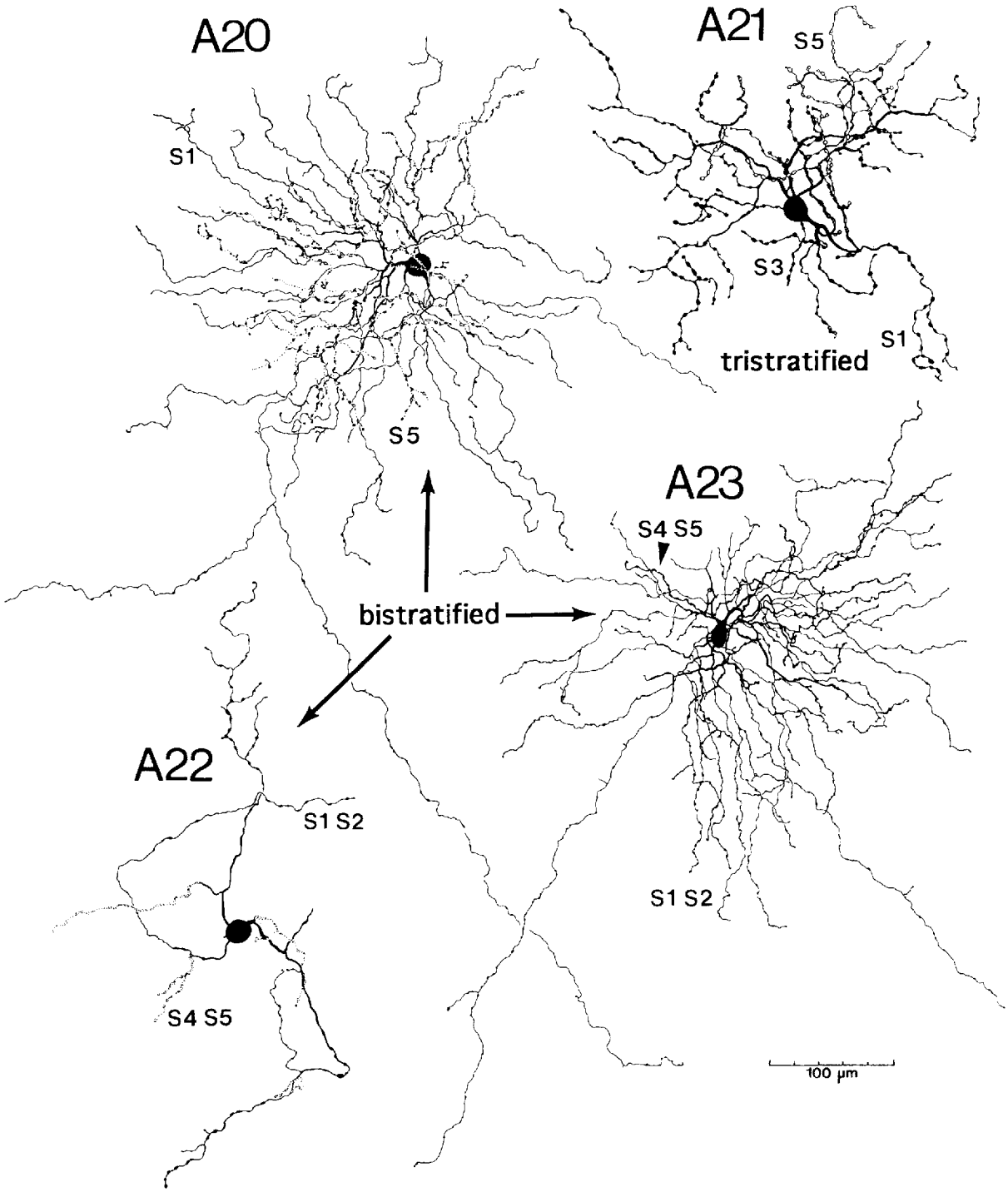

Fig. 17. A20 is a bistratified cell arborizing in S5 (dotted lines) and S1. Photographs of the 2 dendritic tiers of this same cell are shown in Figure 21k,l. A21 is tristratified to S1, S3, and S5. A22 has sparse, beaded dendrites that ramify loosely in both S4 and S5 (dotted lines) and in S1 and S2. A23 is bistratified with thick, shorter dendrites arborizing in S4 and S5 and thinner, longer processes running in S1 and S2, a few of which extend well beyond the central region.

branch; some run almost in parallel. At higher magnification, both A25 subtypes appear to have finely crinkled dendrites that are very sparsely adorned with beads and sessile spines (Fig. 20). Those of A25a are narrowly stratified to S2 (Fig. 21e). This subtype may correspond to the broad-field unistratified A2 amacrine cell of *S. mexicanus* (West, 1976). The dendrites of A25b spread in S4. This subtype may be equivalent to G13 in *S. mexicanus* (West, 1976) insofar as none of the 3 examples West studied had an axon. Moreover, the size and overall morphology of West's

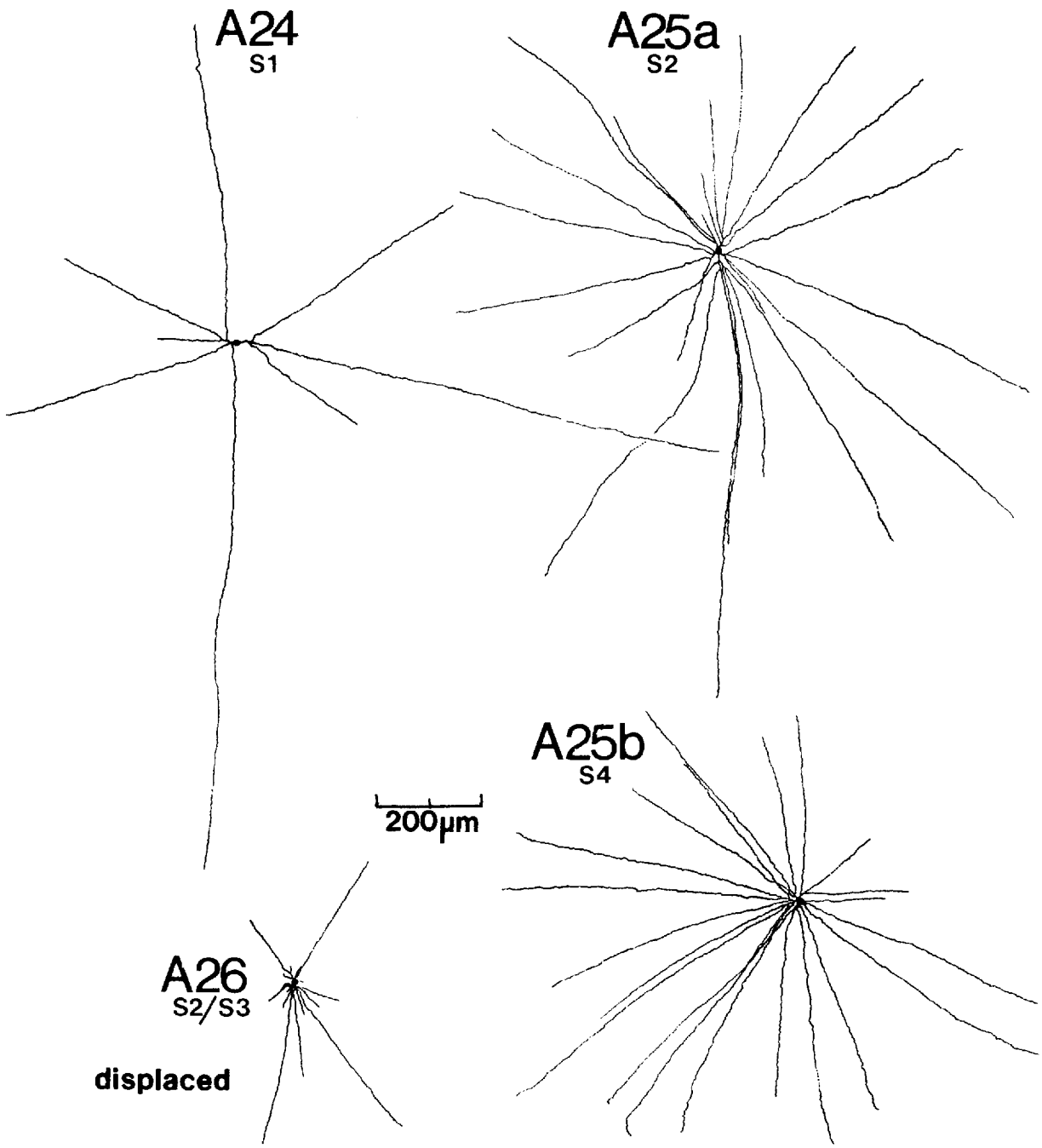

Fig. 18. A24 has the largest dendritic field of all amacrine cells, with straight and simple dendrites radiating in S1. The A25a cell has straight but crinkled dendrites narrowly stratified to S2 that are greater in number and finer in caliber than those of A24. The displaced A25b branches in S4. The displaced A26 cell has straight, fine, and simple dendrites stratified along the border of S2 and S3.

A2 and G13 seem similar, and, as was the case for A17b, we found no candidate ganglion cell in *S. beecheyi* with such a shape and dendritic stratification.

The displaced A26 amacrine cell (Fig. 18) has straight, simple, nonbranching, and nonoverlapping dendrites, yet its dendrites are much finer in caliber than those of other wide-field cells. A dendritic stalk rises from the cell body to issue branches that spread narrowly on the border of S2 and S3. The fineness of these processes can best be appreciated in Figures 20 and 21m, where they can be compared with the dendrites of other wide-field cells, all of which are shown to scale. As in the case of A14, we did not find any equivalent cell in the amacrine cell layer.

The large cell body of the A27a cell (Fig. 19) gives rise to 3 dendritic trunks that branch and spread widely in S1. The displaced cell, A27b, also has a large perikaryon that gives rise to 4 branched but simple dendrites stratified to S5. In addition to their larger dendrites, both A27 subtypes have

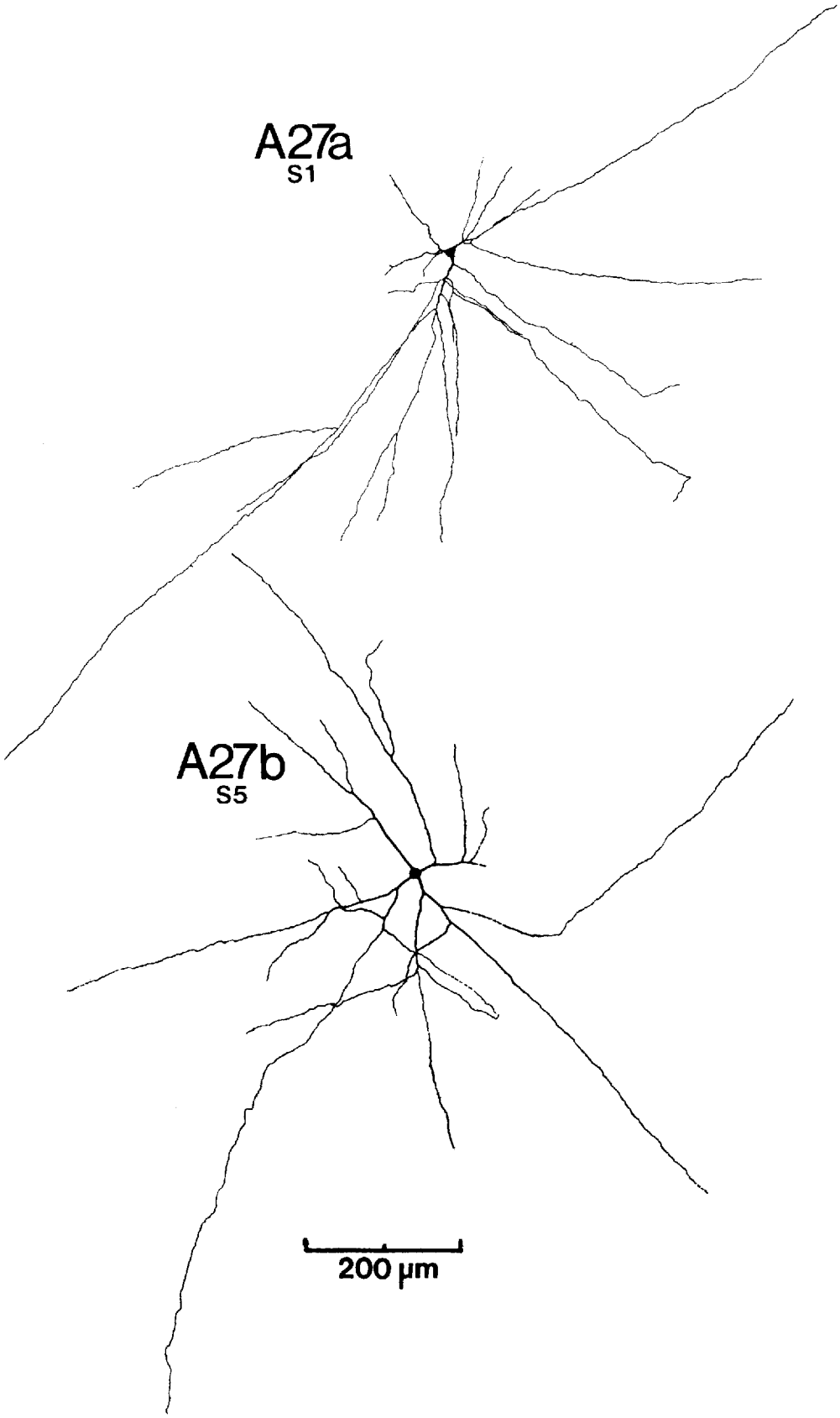

Fig. 19. The large cell body of A27a gives rise to straight and simple dendrites of varying lengths that spread out widely in S1. A27b has a displaced cell body that gives rise to similar, although thicker, dendrites stratified to S5.

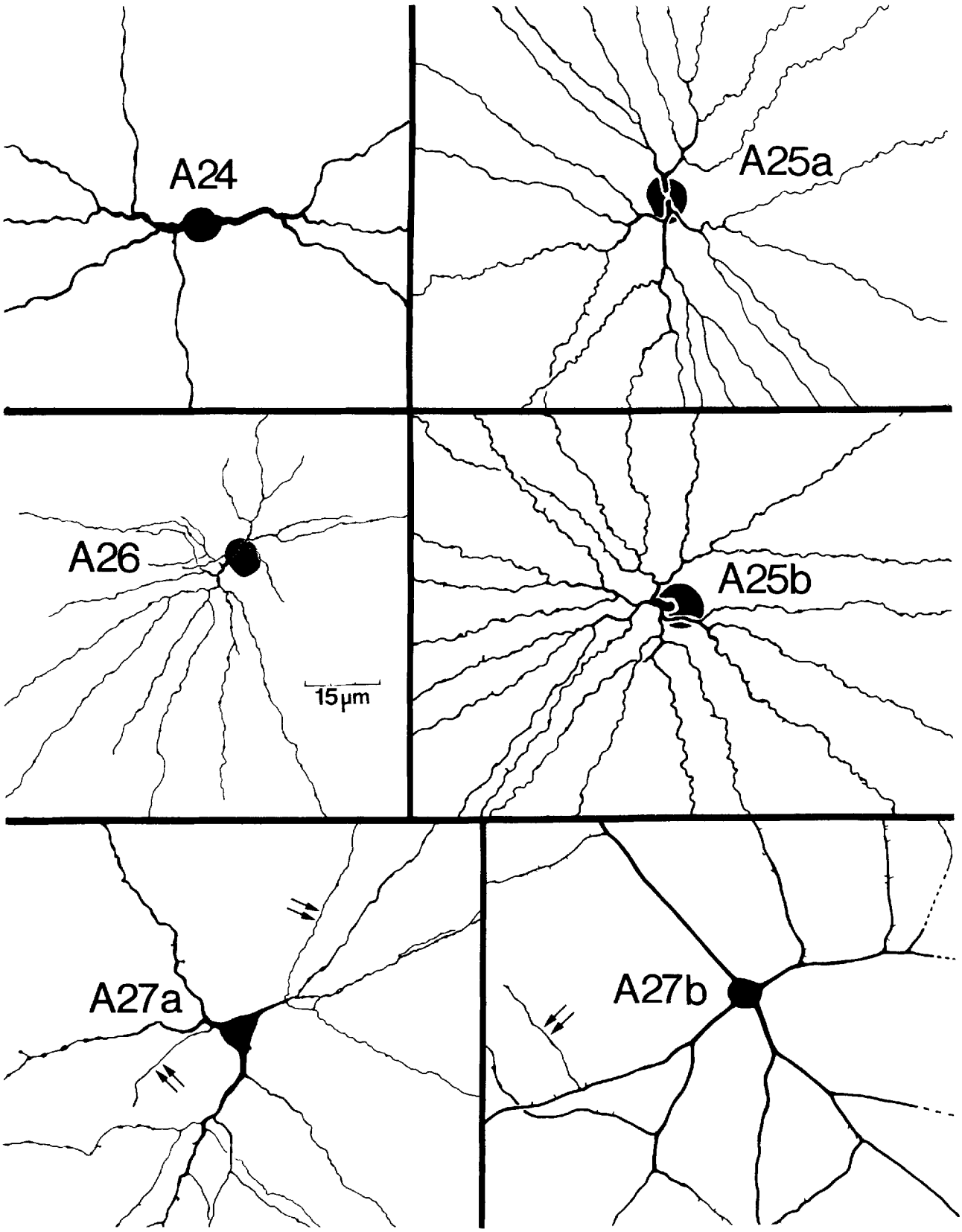

Fig. 20. The cell bodies and primary dendrites of the same amacrine cells shown in Figures 18 and 19 at higher magnification. Arrows point to fine, "axonlike" processes seen in both A27 cell subtypes.

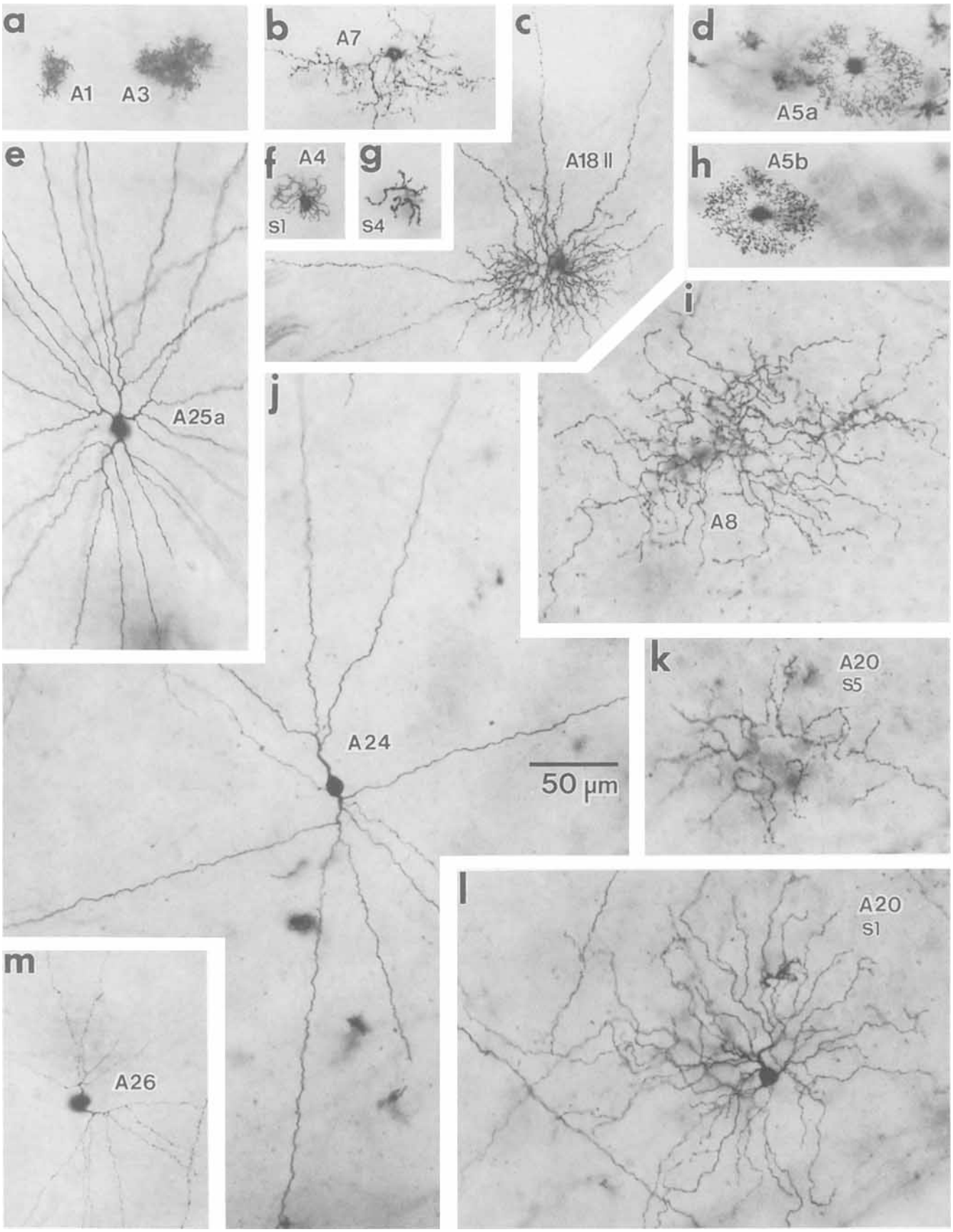
a
A1
A3
b
A7
c
A18 II
d
A5a
e
A25a
f
A4
S1
g
S4
h
A5b
i
A8
j
A24
50 µm
k
A20
S5
l
A20
S1
m
A26

Figure 21

TABLE 2. Amacrine Cells of *Spermophilus beecheyi*

Cell type	Stratification in IPL S1	S2	S3	S4	S5	Sample size	Some size (μm)	Soma layer	Dendritic field size (μm)	Displacement (mm) from ONH midpoint* (*x*, *y*)	Probable equivalent in *S. mexicanus*[1]	Possible equivalent in rabbit	Possible equivalent in human[10]
A1						many	7 × 6	A	20 × 14	−2.2, −4.1	A1		small diffuse
A2						many	8 × 7	A	44 × 26	−4.0, −4.6			A2
A3						many	8 × 7	A	27 × 15	−3.8, −4.5			A3
A4						many	7 × 7	A	41 × 29	−1.5, −4.6	A4		A8
A5a						many	10 × 9	A	74 × 65	−1.1, −2.8		starburst, [2,3]Ca[4]	ACh
A5b						many	12 × 9	G	68 × 53	−1.1, −2.8	G12	starburst, [2,3]Cb[4]	ACh
A6						several	9 × 8	A	59 × 47	−1.0, −6.0			A4
A7						several	10 × 8	G	100 × 59	−4.5, −4.2			
A8						several	11 × 7	A	130 × 120	−4.1, −1.6	A3		A5
A9						several	8 × 8	A	140 × 140	−2.9, +1.0			wooly diffuse
A10						few	9 × 9	A	170 × 110	−3.2, +2.0			
A11						several	11 × 9	A	160 × 150	−3.3, +2.2			A14?
A12						few	12 × 9	A	220 × 150	−2.0, +2.5		substance P-IR[5]	A12
A13a I						many	10 × 9	A	240 × 110	+0.2, +3.6			thorny 1
A13a II						many	8 × 8	A	540 × 460	+2.3, −5.2			thorny 1
A13b						many	12 × 9	G	320 × 240	−0.3, +4.4		polyaxonal 1[6]	thorny 2
A14						several	10 × 9	G	210 × 150	+3.7, +4.3			
A15						several	12 × 9	G	360 × 310	+2.1, +4.5			
A16						one	9 × 9	G	230 × 215	+1.8, +1.2			
A17a						several	11 × 10	A	230 × 180	+1.2, −2.4			A13?
A17b						several	12 × 12	G	230 × 220	+5.9, −0.8	G15		A13?
A18 I						many	10 × 10	A	290 × 150	−1.0, −2.0			spiny
A18 II						many	9 × 8	G	410 × 230	−0.8, −1.6			spiny
A19a						several	12 × 10	A	290 × 250	+1.2, −1.8			spiny varicose
A19b						several	11 × 9	G	250 × 230	−0.2, −2.0			spiny varicose
A20						few	10 × 9	A	270 × 220	−2.5, +1.8			
A21						few	11 × 9	A	220 × 170	+0.9, +4.6		DAPI-3[6]	tristratified
A22						few	10 × 9	A	250 × 140	−3.4, +2.8		polyaxonal 2[7]	A14?
A23						several	11 × 6	A	350 × 280	−3.0, +1.0		serotonin 2[8]	A17?
A24						many	11 × 9	A	1700 × 1400	−2.6, +1.7	A5	CA1[9]	semilunar 1
A25a						several	13 × 9	A	1300 × 1200	+2.5, +2.6	A2		stellate varicose
A25b						several	12 × 12	G	1100 × 1200	+1.5, +2.0	G13		stellate wavy
A26						few	11 × 10	G	600 × 500	+1.5, −4.0			wiry type 2
A27a						several	15 × 14	A	1600 × 600	−5.5, −5.5		polyaxonal 4[7]	
A27b						several	15 × 14	G	1300 × 1100	+4.5, +2.3		polyaxonal 3[7]	semilunar 3

*SN = +, +; ST = −, +; IN = +, −; IT = −, −.
[1]West, 1976.
[2]Famiglietti, 1983a.
[3]Tauchi and Masland, 1984.
[4]Vaney, 1984.
[5]Vaney, 1990.
[6]Famiglietti, 1992b.
[7]Famiglietti, 1992c.
[8]Sandell and Masland, 1986.
[9]Masland, 1988.
[10]Kolb et al., 1992.

fine processes that appear only partially impregnated (Fig. 20). These may be similar to the "axonlike" processes of certain amacrine cells described in monkeys (Dacey, 1989; Mariani, 1990), rabbits (Famiglietti, 1992b,c), and humans (Kolb et al., 1992).

Fig. 21. Light micrographs of various amacrine cell types are all shown at the same scale. Table 4 lists the dimensions and retinal locations for the cells shown here. **a:** Located 2.4 mm above the ONH, an A1 cell and nearby A3 cell are photographed at IPL stratum S3. **b:** A "displaced" A7 cell lies 4 mm below the ONH and is photographed at the S4/S5 border. **c:** Photographed at the inner edge of S3, an A18 II cell, 2.6 mm below the ONH, has many radiating dendrites, a few of which extend beyond the rest. **d:** Located 2.8 mm below the ONH, a starburst amacrine cell, A5a, is photographed at S1. The shadow of a nearby A5b cell (shown in h) can be seen to the left. Drawings of both cells are shown in Figure 10. **e:** At 2.6 mm above the ONH, the central region of the same A25a cell shown in Figure 18 is photographed at IPL level S2. **f:** The outer dendritic tier of a bistratified A4 cell, lying 5 mm below the ONH, is shown at S1. The shadow of its soma in the INL can be seen. **g:** The more varicose inner dendritic tier of this same A4 cell is shown at S4. **h:** The A5b starburst amacrine cell that appears as a shadow in d is shown at IPL layer S5. Here the A5a cell appears as a shadow to the right. **i:** An A8 cell, lying 1.8 mm above the ONH, is photographed at S4. **j:** The largest amacrine cell, A24, lies 1.7 mm above the ONH and has long unbranching dendrites shown here at S1. **k:** The inner dendritic tier of a bistratified A20 cell is shown at S5. This cell lies 1.8 mm above the ONH, close to the A24 cell shown in j. **l:** The large outer dendritic tier of this same A20 cell is shown at S1. Its soma can be seen. **m:** Only the centralmost portion of an A26 cell's dendritic field is shown at the S1/S2 border. Just beneath the visual streak, its displaced soma lies out of the plane of focus.

Ganglion cells (Figs. 22–28; Tables 3, 4)

Nineteen morphologically distinct types of ganglion cell have been identified in wholemounted California ground squirrel retina. Only the G18 ganglion cell has the very large perikaryon (27 × 18 μm) reminiscent of the large-bodied ganglion cells of cat (Kolb et al., 1981) or primate (Rodieck, 1988; Kolb et al., 1992; Dacey, 1993) retina. The cell body size of the remaining types forms a continuum, ranging from 10 to 20 μm. West (1976) described 15 ganglion cells in the retina of *S. mexicanus*. We have proposed above that 3 of his ganglion cell types (G12, G15, G13) were in fact displaced amacrine cells similar to those found in *S. beecheyi* (A5b, A15b, A23b, respectively). All but 2 of the remaining 12 types reported for *S. mexicanus* appear to have correlates in *S. beecheyi*. We did not observe any narrow-field ganglion cell types that West (1976, G2, G3) documented in his Figure 2, although his G4 type has the same levels of stratification as our G11 (see below).

Table 3 presents data on those cells used as examples of the 19 types of ganglion cell that we found in *S. beecheyi* retina. Each cell's position relative to the ONH midpoint is given as well as its somal and dendritic dimensions and its dendritic stratification in the IPL. Table 4 gives the size and

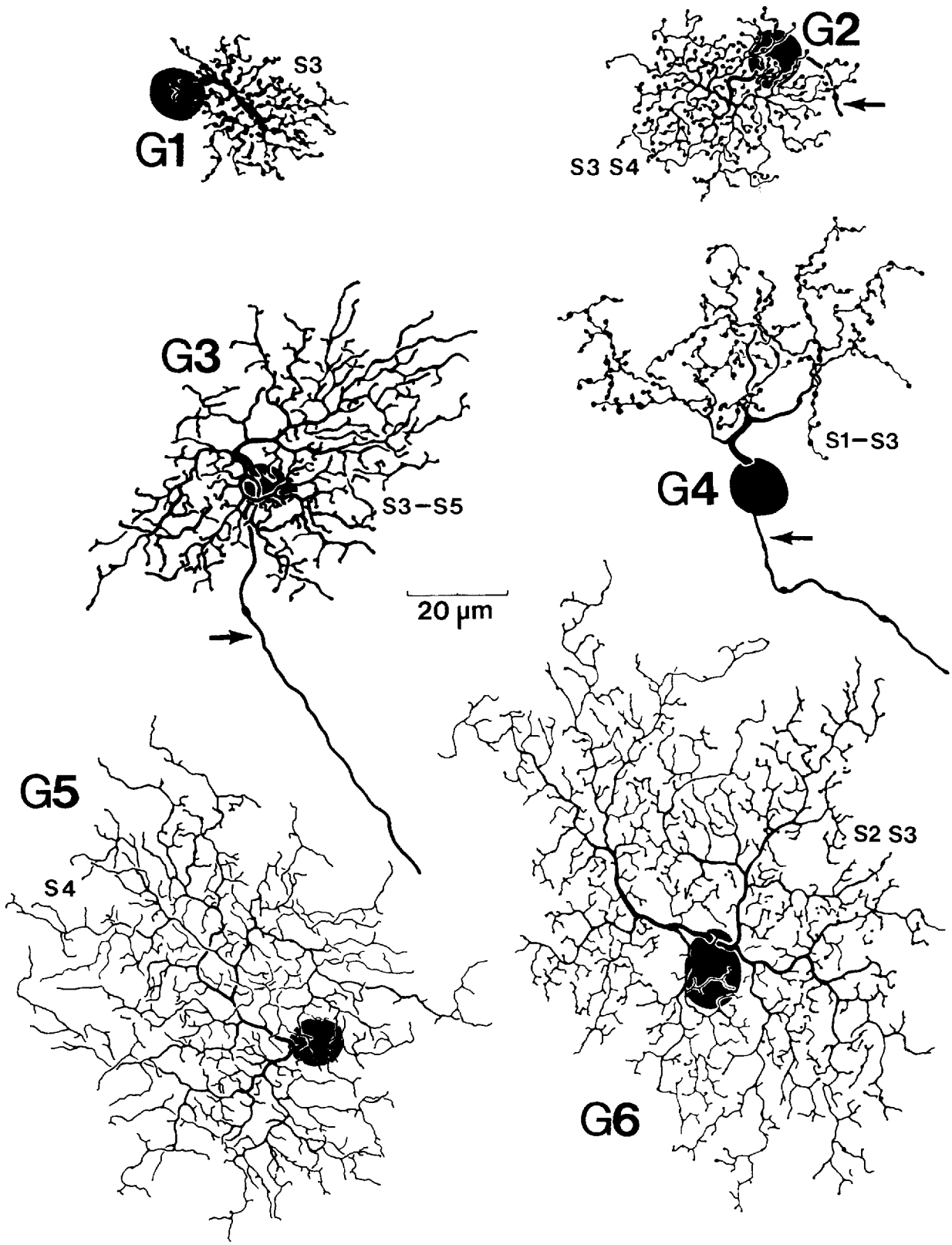

Fig. 22. The G1 cell arborizes in S3 and has the smallest dendritic field of all 19 types. G2 has a larger field than G1 and branches across S3 and S4. G3 has a large, elliptical field broadly stratified across sublamina b (S3, S4, S5). G4, with its somewhat larger soma, has a thick ascending dendrite arborizing in S1, S2, and S3. G5 has a highly branched dendritic tree narrowly stratified to S4. G6 has a large soma and profusely branching dendrites ramifying across both S2 and S3. Arrows point to axons.

retinal location of ganglion cells whose photographs comprise Figure 28.

The G1 cell (Figs. 22, 28c–d) has a sturdy dendritic stalk that ascends into the IPL and gives rise to the smallest dendritic field of all 19 ganglion cell types. It consists of tufted branches in S3 bearing small to medium-sized varicosities. G1 cells in the periphery have a somewhat larger and more loosely organized dendritic tree than those examples lying in the visual streak, but their small size still readily differentiates them from larger ganglion cell types at those eccentricities (data not shown). In terms of dendritic morphology and stratification, this cell closely resembles the G9 ganglion cell of *S. mexicanus* (West, 1976).

The G2 cell (Figs. 22, 28e) differs from G1 by virtue of its larger dendritic field diameter, the less varicose nature of its highly branched dendrites, the uniformity of size of its dendritic beads, and, most fundamentally, by its ramifying more broadly across both IPL substrata S3 and S4. The example shown in Figure 28e lies deep in the inferior periphery and is nearly twice the size of the G2 cell lying at the edge of the visual streak (Fig. 22). This cell type may be the counterpart of the G1a cell in *S. mexicanus* (West and Dowling, 1972; Fig. 2b), as we did not observe any small processes rising into sublamina a as was illustrated for the G1b type (West and Dowling, 1972; Fig. 2a).

The G3 cell (Figs. 22, 28f) has yet a larger, slightly elongated dendritic field broadly stratified across S3, S4, and S5 (sublamina b). Its many branches, appendages, and spines are all rather thick; its varicosities and beads are small. G3 may be the equivalent of G10 in *S. mexicanus* (West, 1976) as it also has loosely tangled dendrites meandering diffusely across sublamina b and is of equivalent size.

The G4 cell (Fig. 22) has a fairly large soma. Its thick ascending dendrite branches as it rises in the IPL to arborize across the outer strata, S1, S2, and S3. The G4 dendritic field is looser in organization than the denser dendritic fields of G1, G2, or G3. Its undulating branches that bear both beads and appendages rarely overlap. The G4 cell may be the same as the G5 cell of *S. mexicanus* because the single example observed and drawn by West (1976) has the same loosely organized dendrites spread across these same three strata of the IPL.

The G5 cell (Fig. 22) has a highly branched dendritic tree narrowly stratified to S4. Its delicate, overlapping branches bear mostly sessile spines but no beads or varicosities. The G5 cell may correspond to the medium-field G8 of *S. mexicanus* (West, 1976).

The G6 cell (Figs. 22,28g) has a large soma and its profusely branching dendrites, arising from several primary dendrites off the cell body, spread broadly across S2 and S3. The dendrites rarely cross one another, appearing to fill in space. They bear uniformly fine beads, simple pedunculated spines, and branched appendages. This cell type appears similar to the large-bodied G7 of *S. mexicanus* (West, 1976), although its dendritic tree seems to be more narrowly stratified to S2.

The G7 cell (Fig. 23) has a small, round cell body with 2 primary dendrites that rise to traverse most of the IPL before ramifying narrowly in S1. The loosely organized dendrites bear many uniformly large beads but few spines or appendages. This cell type may correspond to G6 of *S. mexicanus* (West, 1976) although the latter's dendritic field is roughly one-half of that seen in *S. beecheyi*.

The G8 cell (Fig. 23) has a large cell body that gives rise to sturdy primary dendrites that arborize narrowly in S3. Its dense and tufted dendritic tree consists of retroflexive branches, many of which overlap distally. They bear some irregularly thick varicosities, pedunculated spines, and multilobed appendages. This cell may be the equivalent of G11 in *S. mexicanus* (West, 1976).

The G9 cell (Figs. 23, 28i) has a small soma and its single primary dendrite bifurcates twice before the resultant branches abruptly taper and continue to arborize profusely but narrowly in S3, the level at which this same cell was photographed (Fig. 28i). These very fine, rarely overlapping processes lack both beads and varicosities and bear many sessile spines and simple branchlets that appear to fill in space. This cell type has not been described before in squirrel retina.

The G10 ganglion cell (Fig. 24) has an elongated dendritic field, narrowly stratified to S4, that arises from repeated branches off its sole dendritic trunk. This cell bears many uniformly large beads, pedunculated and sessile spines, and multilobed appendages; its fine dendrites rarely overlap and instead appear to fill in space.

The G11 ganglion cell (Fig. 24) is bistratified with branches narrowly stratified in both S2 and S4. Two primary dendrites sprout from the large cell body and each branches in both layers. The network of branches in S4 are typically thick, sometimes retroflexive, and bear a few spines. Those of S2 (Fig. 24, dotted lines) are of similar appearance, although finer. The dendrites in sublamina b of this example spread somewhat wider than those in a. Typically, the 2 dendritic tiers are assymetric and show local rather than global bistratification (see Amthor et al., 1983). Although its dendritic diameter is more than twice as large, the G11 cell of *S. beecheyi* branches in the same IPL strata as the G4 cell of *S. mexicanus* (West, 1976). This cell seems similar to the ON–OFF directionally selective ganglion cell described in rabbit retina by Amthor et al. (1984;1989b), Famiglietti (1992a), Oyster et al. (1993), and Vaney (1994).

The G12 cell (Fig. 25) has an ovoid cell body from which arise 4 primary dendrites. These in turn yield wavy secondary dendrites that have beads and a few simple appendages. The cell's dendritic tree is elongate and broadly stratified across S1, S2, and S3. An equivalent of G12 was not described in *S. mexicanus* (West, 1976).

The G13 ganglion cell (Figs. 25, 28a–b,j) is a more globally bistratified type than the G11 cell. It has a large soma giving rise to 4 primary dendrites, 2 of which, in the example shown, branch in both S1 and S5. The dendrites in sublamina a are fine and bear occasional varicosities (Fig. 28j). They do not spread as widely as the more profuse and sturdier dendrites in sublamina b that bear occasional spines, varicosities, and appendages (Fig. 28a). The dendritic tier in S1 consists of 2–5 independent segments of varying size, each connected to the dendrites in S5 by vertical connectives arising from them. Because of its similar size and dendritic stratification pattern, the G13 type resembles the blue-ON yellow-OFF ganglion cell that Dacey and Lee (1994) described in human retina.

The G14 cell (Fig. 25) has a cell body that lies far off the center of its dendritic tree, which is narrowly stratified to S5. Its profuse array of fine, wavy, and overlapping dendrites bear a few sessile and pedunculated spines, especially in the proximal portions of the field. This and all subse-

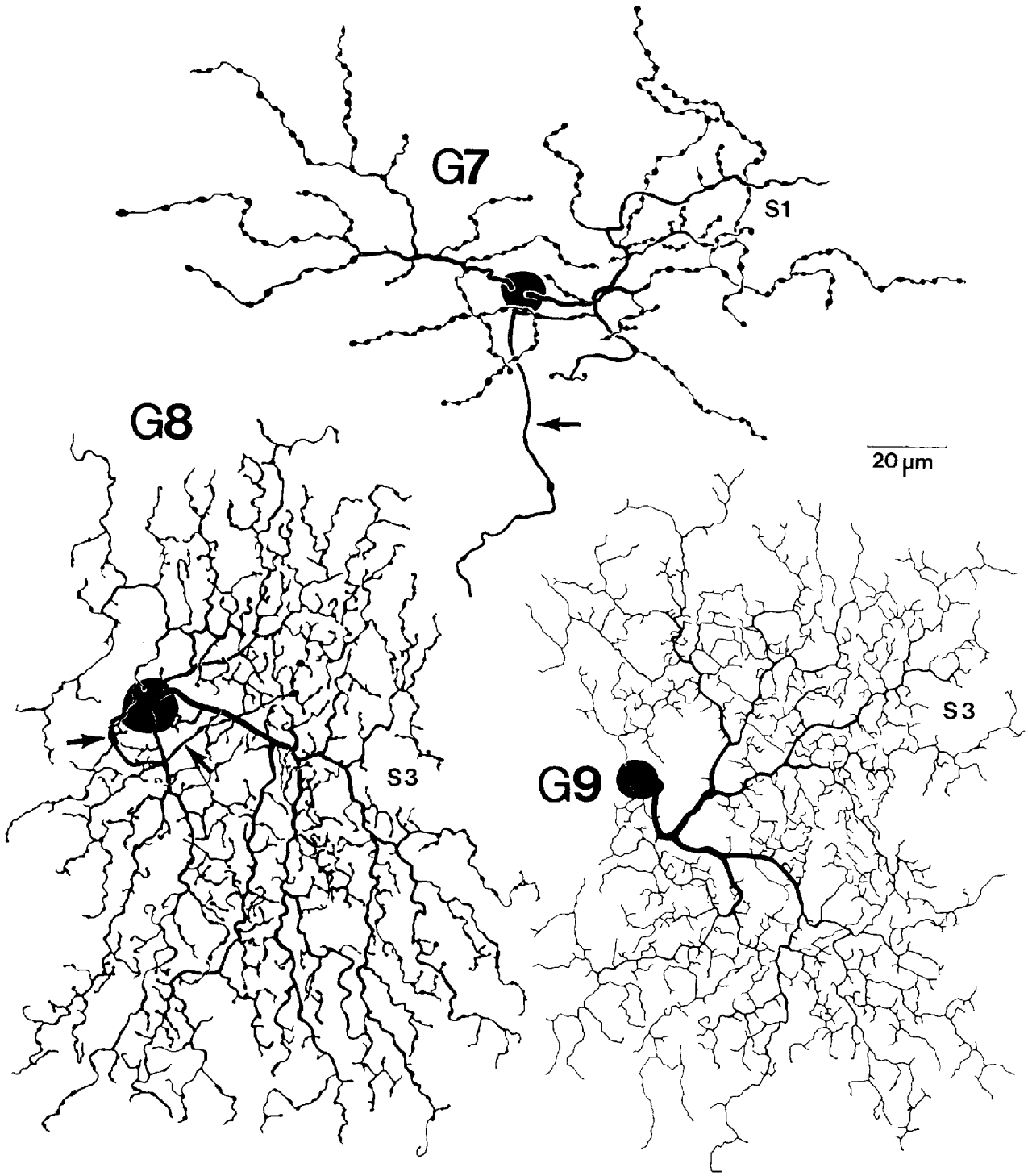

Fig. 23. G7 has a small round cell body. Two sturdy dendritic trunks rise through the IPL before branching in S1. G8 has a relatively large cell body, off of which arise several dendritic trunks that arborize profusely but narrowly in S3. The small G9 soma gives rise to a primary dendritic trunk that bifurcates twice before branching into a profuse array of fine, unadorned dendrites in S3. A photograph of this same cell is shown in Figure 28i. Arrows point to axons.

quent ganglion cell types, except perhaps G19 I, are described for the first time in squirrel retina.

The G15 ganglion cell (Fig. 26) has a very thick axon and an elongated dendritic field narrowly stratified to S2. Its sturdy and tapering dendritic branches, beaded distally, seldom overlap and run parallel to the ONH.

Despite its large dendritic field, G16 (Fig. 26) has one of the smallest perikarya of all ganglion cell types. By lying to

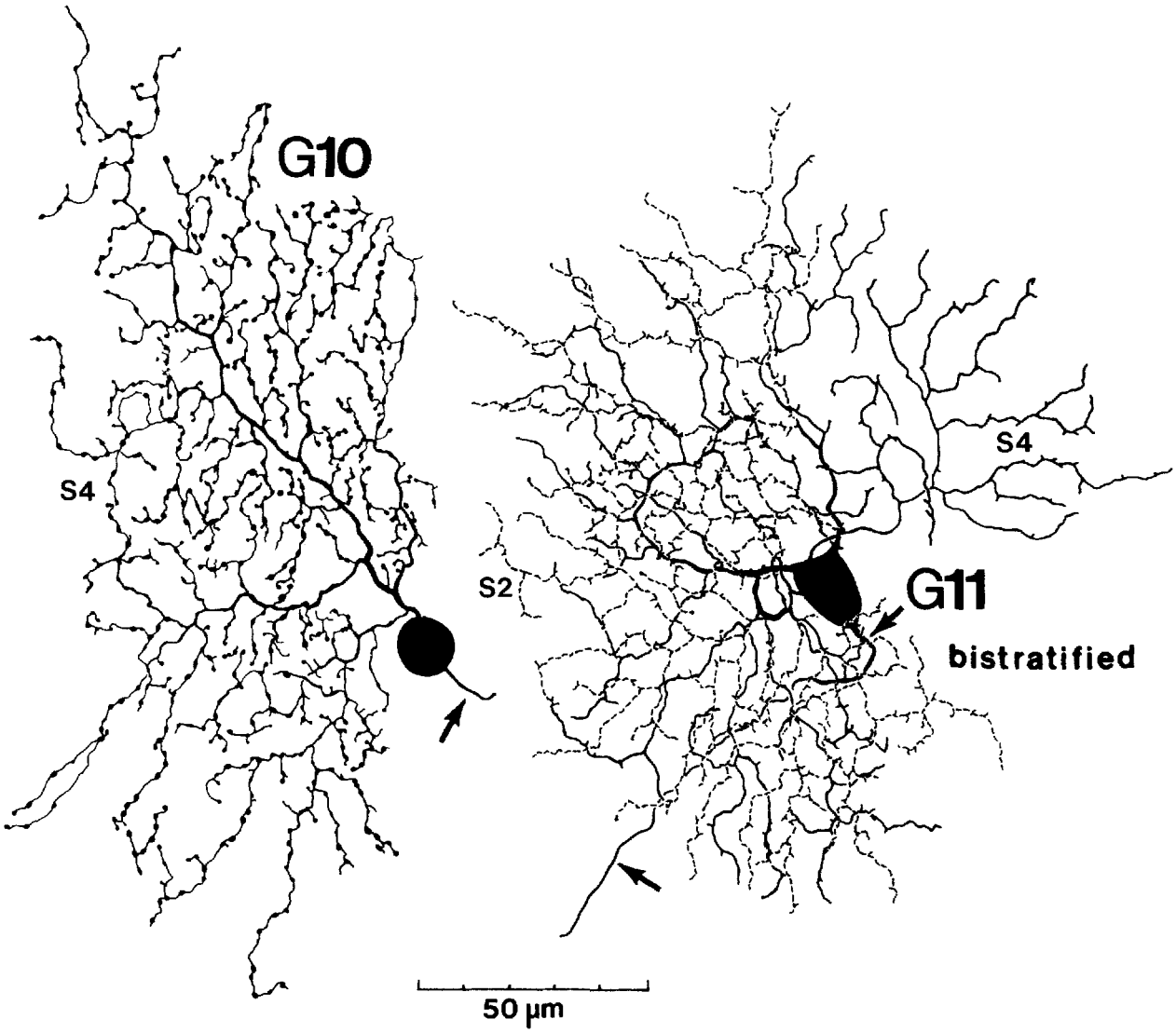

Fig. 24. G10 has an elongated field of beaded dendrites narrowly stratified to S4. G11 is a bistratified cell ramifying less widely in S2 (dotted lines) than in S4 (solid lines). Arrows point to axons.

one side of its otherwise radial dendritic tree, the soma creates an assymetry. Stout dendritic trunks ascend into the IPL before giving rise to crinkly, beaded dendrites that branch once or twice in the inner portion of the field, but are unbranching distally. They spread narrowly in S4. The dendrites on the side of the nucleus closest to the edge of the dendritic field are shorter than those radiating on the opposite side. These dendrites occasionally cross each other and are sparsely decorated with both pedunculated and sessile spines.

The G17 ganglion cell (Fig. 26) has a large cell body and an elongated dendritic tree. Several primary dendrites rise in the IPL to S3 before giving off wavy secondary branches that ramify narrowly along the border of S1 and S2. These relatively unadorned dendrites branch occasionally, sometimes overlap, and bear small beads and only a few spines. This cell may correspond to the OFF-alpha ganglion cell described in the retinas of cat (Boycott and Wässle, 1974; Kolb et al., 1981) and many other species (Peichl et al., 1987; Peichl, 1991).

The G18 cell (Fig. 26) has the largest cell body (27 × 18 μm) of all ganglion cell types. The soma generally lies off center with respect to the dendritic mass. Its sturdy primary and secondary dendrites branch often, taper, and spread widely although confined to the border of S4 and S5. The resulting dendritic tree bears beads, varicosities, and a small number of spines in varying numbers, sizes, and combinations. The G18 cell could be the ground squirrel's equivalent of an ON-alpha ganglion cell.

The G19 ganglion cell (Fig. 27) occurs in 2 forms: G19 I, whose large cell body resides in the GCL, and G19 II, whose perikaryon is displaced to the amacrine cell layer of the INL (Fig. 28h). Both subtypes have axons, are regionally bistratified, and have large, long, unbranching, and nonoverlapping dendrites that bear few, if any, spines. Both types ramify the widest in S1 (Fig. 28h) and to a far less extent in

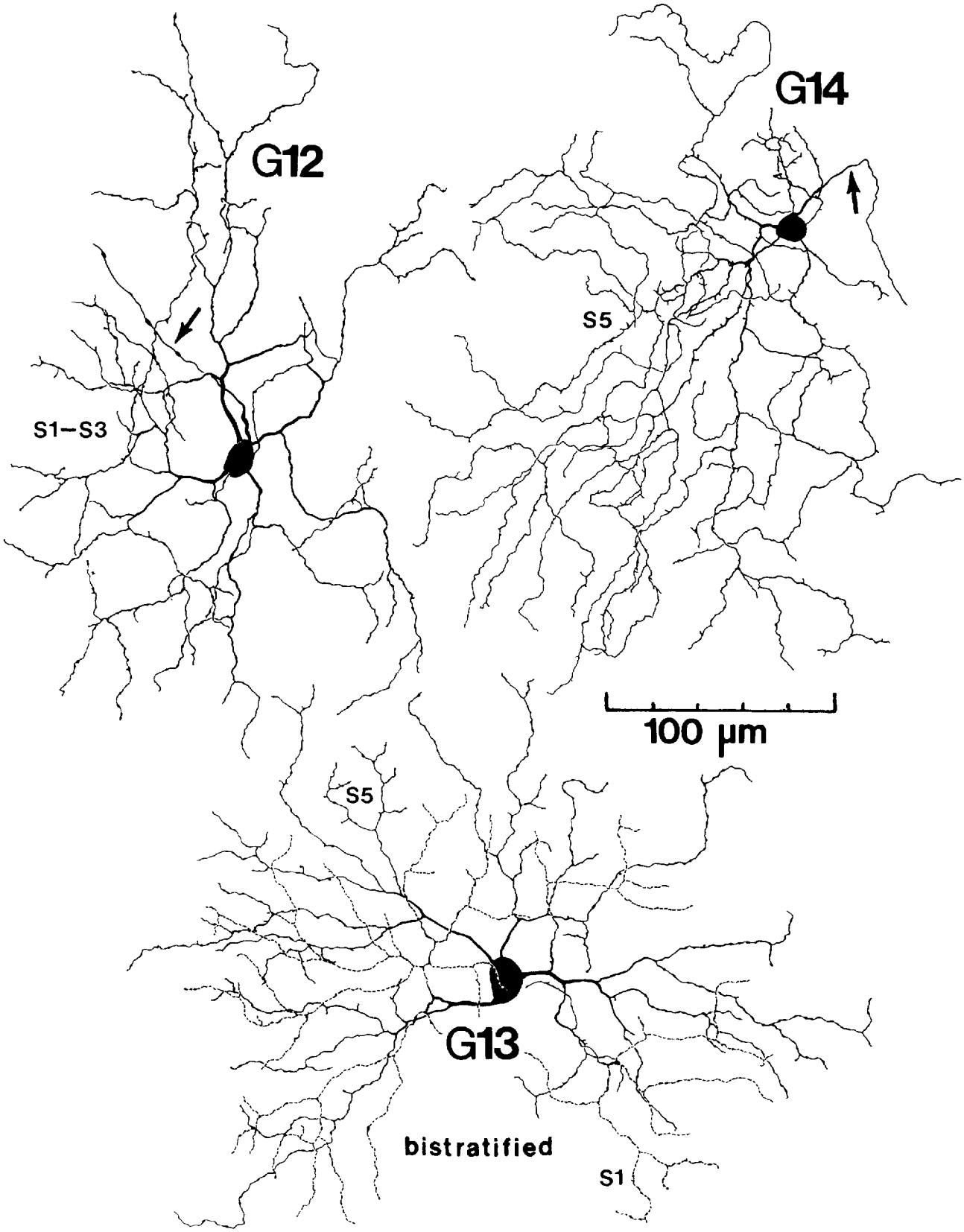

Fig. 25. G12 has an ovoid cell body and an elongate but loosely organized dendritic tree broadly stratified across S1, S2, and S3. G13 is a bistratified cell with a relatively large cell body and dendritic tiers of similar width in S1 (dotted lines) and S5 (solid lines). The G14 cell body lies at the periphery of its dendritic field that narrowly stratifies to S5. Arrows point to axons.

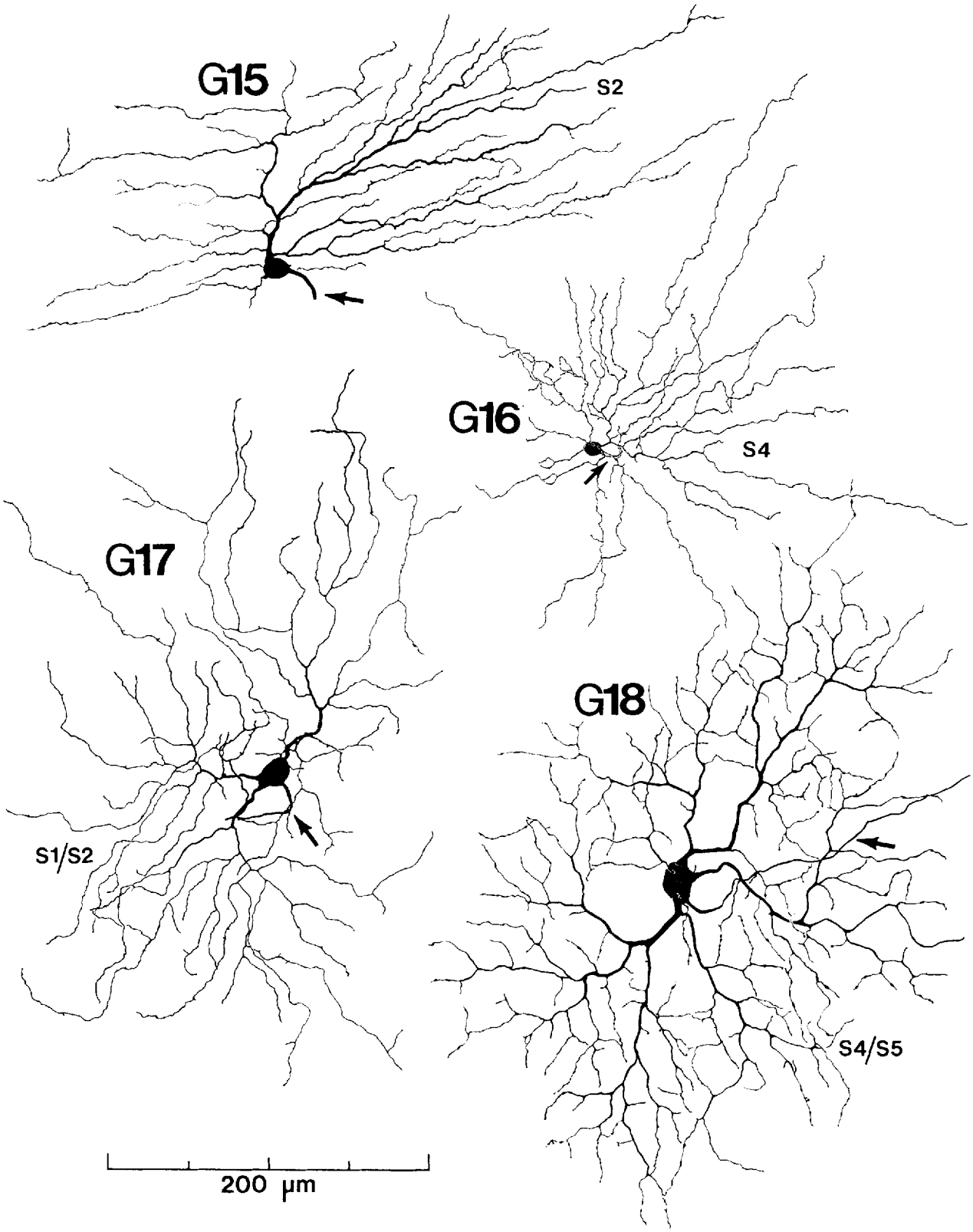

Fig. 26. G15 has a very thick axon and an elongated dendritic field, narrowly stratified to S2, that runs parallel to the visual streak. G16 has a very small cell body and primary dendrites giving rise to secondary and tertiary branches that radiate widely in S4 with little overlap. G17 has an elongated dendritic field that spreads along the border of S1 and S2. G18 has a very large cell body from which arise sturdy primary dendrites that branch often and ramify widely on the border of S4 and S5. Arrows point to axons.

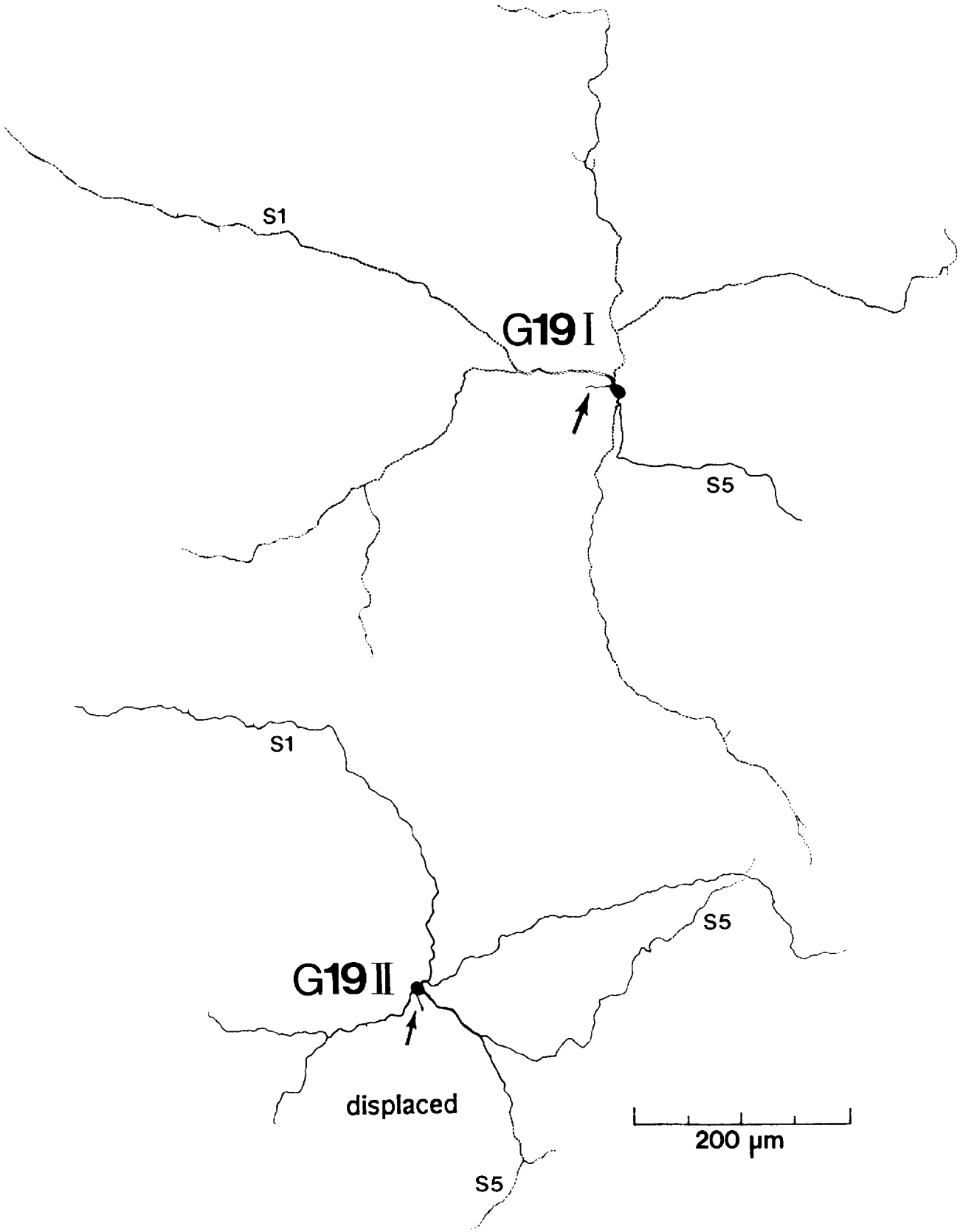

Fig. 27. The G19 ganglion cell has 2 types: the G19 I type, with its large cell body in the GCL, and the G19 II type, with its equally large cell body "displaced" to the amacrine cell layer of the INL. Both are bistratified, spreading the most in S1 and to a much lesser extent in S5. Arrows point to axons.

S5 (Fig. 28k). The G19 I type appears similar to the G14 cell described in *S. mexicanus* (West, 1976). Figure 28h shows that the displaced cell body of the G19 II type lies in the same focal plane as its outer tier of dendrites. Although we saw roughly the same number of each type, we observed too few impregnated examples to be able to conclude that both types independently tile the retina. As they both ramify in the same IPL substrata and in a similar fashion, we cannot deny the possibility that one type is simply a misplaced version of the other.

DISCUSSION

Not until the mid-1970s were rodlike photoreceptors proven to exist in squirrel retina (West and Dowling, 1975; Anderson and Fisher, 1976). The early impression that ground squirrels had all-cone rather than just cone-dominant retinas (see Dowling, 1964; Michael, 1968a–c) arose for several reasons. First, the number of rods in ground squirrel retina is very small: depending on the species, they number only 1 out of every 10–20 photoreceptors (Long and Fisher, 1983; Ahnelt, 1985; Szél and Röhlich, 1988; von Schantz et al., 1994). Second, the structural differences between cones and rods are sufficiently subtle at the light microscopic level to require the use of electron microscopy in documenting them (West and Dowling, 1975; Anderson and Fisher, 1976). Third, early optic nerve recordings from ground squirrels lacked electrophysiological evidence for the existance of rods (Michael, 1968c). Even after the scotopic component of ground squirrel vision had been detected and characterized (Jacobs et al., 1976), it was lacking in 1 out of every 3 animals in whose retinas rod photoreceptors could be confirmed ultrastructurally (Jacobs et al., 1980). More recent studies have further elucidated the distribution of rods in the retinas of several ground squirrel species (Long and Fisher, 1983; Ahnelt, 1985; Szél and Röhlich, 1988; von Schantz et al., 1994). Ground squirrels are now known to be dichromats, having mostly green-sensitive cones, a small population of blue-sensitive cones, and even fewer rods.

The existence of short-wavelength or "blue-sensitive" cones in ground squirrel retina was suspected quite early from both electrophysiological (Michael, 1968c) and behavioral (Anderson and Jacobs, 1972) studies. More intensive electrophysiological investigations on optic nerve fibers of *Spermophilus beecheyi* have implicated blue cones in the color opponency observed in 3 out of every 10 ganglion cells (Jacobs and Tootell, 1980, 1981; Jacobs et al., 1981, 1985). These observations suggest that somehow and to an uncertain extent, blue cone signals in this species are kept segregated as far as the ganglion cell level.

In this study, the use of retinal wholemounts has enabled us to not only describe many retinal neurons in *S. beecheyi* similar to those described by West (1976) in *S. mexicanus* but also introduce many new cell types to the atlas of ground squirrel retinal neurons. Here we confirm that *S. beecheyi* contains a second, axonless type of horizontal cell. In addition to describing 7 types of bipolar cell that are very similar to those shown in *S. mexicanus* (West, 1976), we introduce a large bistratified bipolar cell, B8. Inasmuch as West (1976) described only 5 types of amacrine cell and 15 types of ganglion cell, we have added many more types to both classes of retinal neurons, including reclassifying as amacrine cells in *S. beecheyi* several similar types identified as ganglion cells in *S. mexicanus*. These findings are appraised next.

Classes of retinal neurons in ground squirrel retina

Horizontal cells. As in many other studies of mammalian retina (see Gallego, 1986; Boycott, 1988; Kolb et al., 1992; Harman and Ferguson, 1994; Peichl and González-Soriano, 1994), the California ground squirrel has 2 very different types of horizontal cell. Both its axonless (H2) and axon-bearing (H1) types are morphologically most similar to those Mariani (1985) identified in the retina of the red tree squirrel *Tamiasciurus hudsonicus*. The structural dissimilarities between these 2 horizontal cell types in terms of shape, size, and dendritic cluster density seem certain to reflect their differing connections to the 2 spectral types of cone and perhaps the rods (see below). Most of what is currently known about horizontal cell connectivity in squirrel retinas stems from the studies of these cells in the Mexican ground squirrel (West and Dowling, 1975) and in the gray tree squirrel (West, 1978). By Golgi–electron microscopy, these investigators showed evidence that, in these species, both H1 dendrites and axon terminals contact cones only. West and Dowling (1975) did not observe an axonless horizontal cell in the retina of *S. mexicanus*. Moreover, it was concluded by Boycott and Hopkins (1981) that the axonless cell that West (1978) described in tree squirrel retina was in fact microglia, a type of non-neuronal cell also frequently impregnated in these wholemounts.

H1, the axon-bearing type. Axon-bearing horizontal cells occur in the retinas of most vertebrate species that have been studied to date. Gallego (1982, 1986) classified these "short-axoned horizontal cells" (SAHCs) into 2 morphologically distinct subtypes: SAHC-I and SAHC-II. The H1 cells of *S. beecheyi* described here along with those of *S. mexicanus* (West and Dowling, 1975) apparently belong to Gallego's SAHC-II category based on their less elaborate axon terminal arborizations and the presence of spines and branchlets along their respective axons. They thus differ from SAHC-I cells that have long, unbranched, and spine-free axons connecting to much more elaborate axon terminals. In all species studied to date, SAHC-II cells have been shown to innervate only cones. Leeper and Charlton (1985) demonstrated physiological evidence for such pure cone connectivity in sciurid horizontal cells in the gray tree squirrel *Sciurus carolinensis*. They produced horseradish peroxidase profiles of cells from which electrophysiological recordings had previously been made that clearly resemble the H1 cells described here. Other examples of SAHC-II cells include the type II horizontal cell in monkey (Kolb et al., 1980) and human (Kolb et al., 1992, 1994; Ahnelt and Kolb, 1994a,b), the H1 cell in the gray squirrel (West, 1978; Gallego, 1982), and perhaps the uniaxonal horizontal cell of the tree shrew (Mariani, 1985), although Müller and Peichl (1993) speculated that its sparsely branching axon terminal might innervate the few rods in that species.

We have shown that the H1 cells of *S. beecheyi* increase in dendritic field size with displacement from the central retina, a phenomenon first described in horizontal cells of monkey retina (Boycott and Kolb, 1973) and seen since in the retina of several other mammalian species. The reason why the horizontal cells lying above the visual streak should additionally increase in dimension at twice the rate for cells beneath it is unclear. Such a pattern might reflect changes in photoreceptor densities or even alterations in

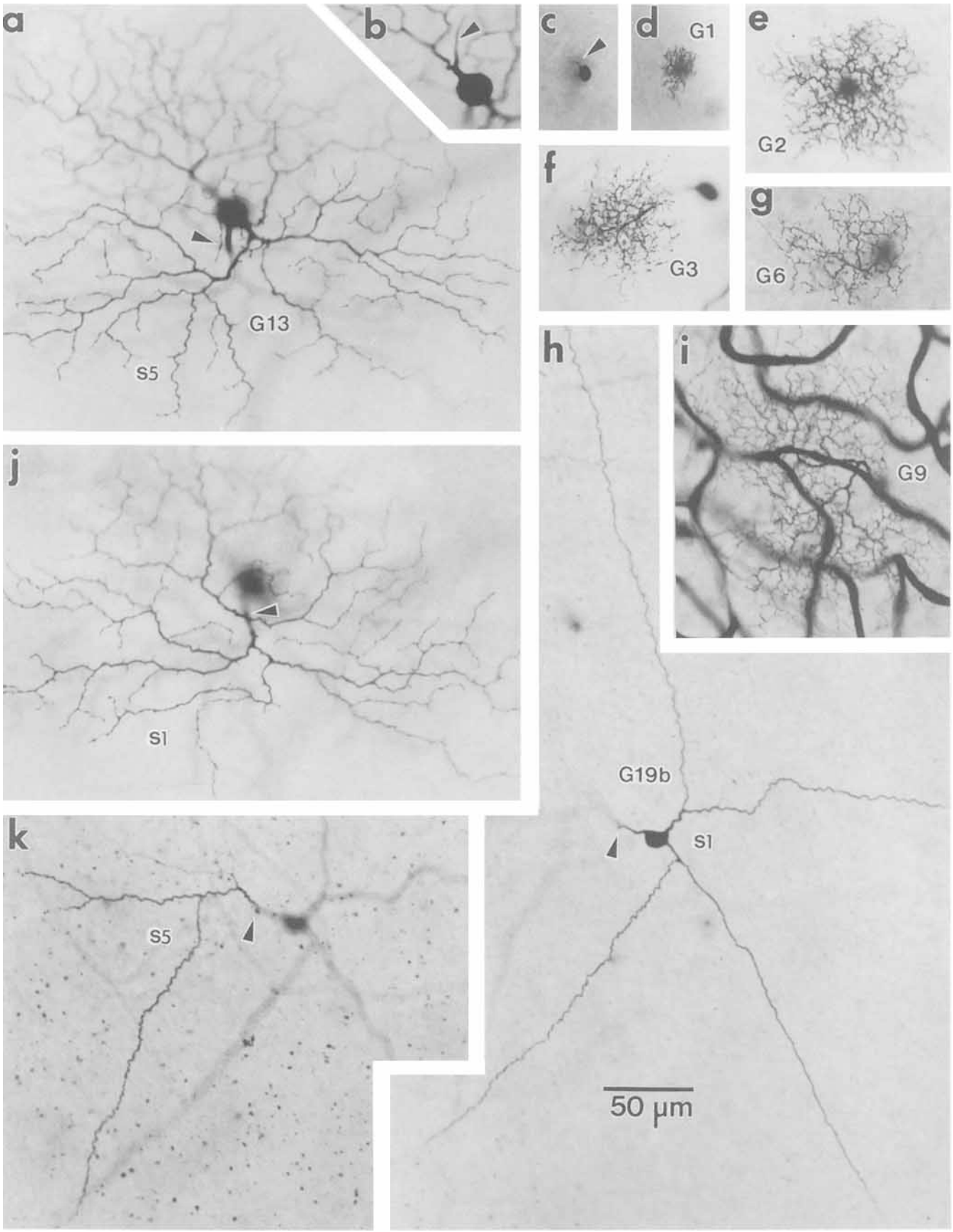

Figure 28

TABLE 3. Ganglion Cells of *Spermophilus beecheyi*

Cell type	Stratification in IPL S1	S2	S3	S4	S5	Sample size	Soma size (μm)	Soma layer	Dendritic field size (μm)	Displacement (mm) from ONH midpoint* (x, y)	Probable equivalent in *S. mexicanus*[1]	Possible equivalent in rabbit	Possible equivalent in human[5]
G1			■			many	11 × 10	G	30 × 25	−0.6, −2.3	G9		
G2			■	■		many	12 × 10	G	50 × 50	+0.4, −1.7	G1		P2b
G3			■	■	■	several	12 × 8	G	88 × 56	+4.0, −3.4	G10	brisk-sustained[2]	
G4	■	■	■			several	12 × 11	G	74 × 50	+1.5, −1.4	G5	vert. orient. selector[3]	G5
G5				■		several	11 × 9	G	97 × 85	−3.5, −4.9	G8	ON brisk-transient[2]	
G6		■	■			several	15 × 11	G	130 × 94	−4.9, −5.3	G7	LED[3]	
G7	■					several	11 × 11	G	210 × 160	+0.8, −1.3	G6	OFF sluggish[2]	
G8			■			several	14 × 14	G	200 × 190	−3.4, +2.7	G11		G8
G9			■			many	11 × 10	G	180 × 160	+0.1, +3.6		ON brisk-transient[2]	
G10				■		several	13 × 12	G	220 × 140	+0.7, +3.6		ON brisk-sustained[2]	
G11		■		■		many	16 × 12	G	150 × 140	−1.0, −6.1	G4	ON-OFF DS[3]	G7
G12	■	■	■			several	16 × 11	G	330 × 190	−2.9, +2.5		OFF sluggish[2]	G10
G13	■				■	many	19 × 14	G	320 × 240	−3.5, −4.7			G17
G14					■	few	13 × 11	G	270 × 270	−0.9, −3.4			G16
G15		■				few	16 × 14	G	460 × 140	0.0, +3.5			G22
G16				■		several	11 × 9	G	390 × 370	1.0, +1.8			
G17	■	■				many	19 × 14	G	450 × 290	0.0, −3.7		OFF-alpha[4]	
G18				■	■	many	27 × 18	G	480 × 320	−1.3, +2.8		ON-alpha[4]	
G19 I	■				■	several	17 × 11	G	890 × 760	+5.3, −6.2	G14		
G19 II	■				■	several	15 × 12	A	760 × 440	+4.3, −4.5			

*SN = +, +; ST = −, +; IN = +, −; IT = −, −.
[1]West, 1976.
[2]Amthor et al., 1989a.
[3]Amthor et al., 1989b.
[4]Peichl et al., 1987.
[5]Kolb et al., 1992.

their connections with the green and blue cones. This same phenomenon of an assymmetrical size increase for superior versus inferior SAHC dendritic trees has been described in tree shrew retina (Müller and Peichl, 1993).

We also noted other trends in H1 cell populations. There is an apparent decrease in density of H1 cell dendritic clusters with increasing distance from the visual streak (see Fig. 3), perhaps reflecting changes in the size and/or spacing of cone pedicles with changes in retinal location. We noted that, across the retina, neighboring H1 cell dendrites and axon terminals often extensively overlap, as seen in other species (Boycott et al., 1978; Dacheux and Raviola, 1982; Mariani, 1985; Gallego, 1986). Finally, the H1 cell axons of *S. beecheyi* cross each other at all angles rather than being oriented in some preferred angle to the linear visual streak or its overlying ONH, a phenomenon also noted in the retinas of monkey (Boycott and Kolb, 1973; Gallego and Sobrino, 1975), cat (Kolb, 1974; Boycott et al., 1978), rabbit (Kolb and Normann, 1982), and tree shrew (Mariani, 1985).

H2, the axonless type. The axonless H2 cell of *S. beecheyi* morphologically resembles the type A horizontal cells described in many subprimate mammals and various other vertebrates (Gallego, 1976, 1982, 1986). In some species such as cat and rabbit, these "axonless horizontal cells" (ALHCs) have dendritic fields that can vary in shape from circular to angular to elongated (Dacheux and Raviola, 1982; Kolb and Normann, 1982; Raviola and Dacheux, 1983). Such ALHC "pleomorphism," although evident, is much less extreme in *S. beecheyi*. In addition, H2 cells do not show any type of uniform change in size from central to peripheral retina. Thus, neighboring H2 cells not only can vary somewhat in shape, but also in size. We have shown that their dendritic fields can overlap peripherally. H2 cells in *S. beecheyi* are therefore not likely to form a "plexus" as has been shown for AHLCs in cat (Wässle et al., 1978), rabbit (Dacheux and Raviola, 1982; Mills and Massey, 1994), and tree shrew (Müller and Peichl, 1993) retinas.

Perhaps because so many of the sparse and loosely branched dendrites of H2 cells in *S. beecheyi* end singly, they make the others that converge to create clusters of dendritic tips stand out all the more. The fact that these distinctive clusters are spaced 15–40 μm apart raises the possibility that they might preferentially contact blue cones whose distance from the nearest neighbor is of a similar range (Long and Fisher, 1983). Such spectral selectivity has been proposed, for example, among the 3 types of horizontal cell in human retina (Kolb, 1991; Ahnelt and Kolb, 1994a,b)

Fig. 28. Light micrographs show various types of ganglion cell at the same scale. For purposes of comparison, this magnification is also the same as for the amacrine cell types shown in Figure 21. Table 4 presents the dimensions and retinal positions of the ganglion cells shown here. **a:** The inner dendritic tier of the bistratified G13 cell spreads in S5. The dendrites in the upper one-half of the micrograph appear out of focus due to this cell's location on the slope of a retinal fold. The arrowhead indicates the thick ascending process connecting the 2 dendritic tiers on this side of the cell's dendritic field. This cell is located 2.5 mm above the ONH. **b:** At a slightly more proximal level of focus, the very large soma of the G13 cell and its axon (arrowhead) can be seen. **c:** The small cell body and axon (arrowhead) of the tiny G1 cell are shown. This cell lies 2.2 mm below the ONH in a region bordering the visual streak. **d:** The G1 cell dendrites are seen at the border of S2 and S3. **e:** A G2 cell photographed at IPL substratum S3 is located at the inferior periphery, 8 mm below the ONH. This example is much larger than the G2 cell in Figure 22, which lies in the visual streak. **f:** A G3 cell lying 0.9 mm below the ONH is photographed at the border of S4 and S5. The shadow of its cell body lies to the right. **g:** The broadly stratified G6 cell, shown at IPL level S2, lies 2.2 mm above the ONH. **h:** A bistratified G19 II cell, its cell body displaced to the INL, has the largest dendritic field of all ganglion cell types. Located in the inferior periphery 6.5 mm below the ONH, it is photographed at S1 where most of its processes spread. The process descending to the inner tier is shown at the arrowhead. **i:** The intricate dendrites of the same G9 cell as shown in Figure 23 are photographed at S3 amid a tangle of Golgi impregnated blood vessels. This cell is located 3.5 mm above the ONH. **j:** Part of the outer dendritic tier of the G13 cell shown in a and b is photographed at S1. The dendritic connection to the lower tier is shown at the arrowhead. **k:** The inner and smaller dendritic tier of the G19 II cell shown in h is photographed at level S5. The arrowhead shows the connection between the 2 tiers.

TABLE 4. Retinal Cells of *Spermophilus beecheyi*

Figure	Cell type	Distance from ONH midpoint (in mm)* x	y	Dendritic (D) or axon terminal (A) field (μm)
		Horizontal cells		
1	H1	+3.4	−4.1	34 × 33 (D)
2a	H1	+3.1	−3.9	35 × 32 (D)
2b	H2	+1.2	−2.9	150 × 132 (D)
3a	H1	+1.4	−0.5	38 × 29 (D)
3b	H1	+0.3	−1.7	33 × 25 (D)
3c	H1	−2.5	−4.3	39 × 33 (D)
3d	H1	+4.3	−8.9	60 × 57 (D)
3e	H1	+1.7	+0.1	70 × 57 (D)
3f	H1	−2.3	+3.8	92 × 76 (D)
3g	H1	+2.3	+4.4	127 × 93 (D)
5a	H1	+4.5	−7.5	59 × 55 (D)
5b	H2	+1.2	−2.9	150 × 132 (D)
5c	H1at	+2.0	−0.5	188 × 85 (A)
5e,f	H1	+0.8	+2.5	—
5g	H2	+4.0	−3.7	—
		Microglial cells		
2c	μglia	+4.3	−4.7	103 × 75
5d	μglia	−3.8	+2.4	120 × 60
		Bipolar cells		
8a	B1	−4.9	−7.3	3 × 3 (D)
8b	B1	−0.5	+5.5	39 × 37 (D)
8c	B1	−0.5	+5.5	42 × 30 (A)
8d	B1	−2.3	+0.3	—
8e	B2	−4.9	−7.6	24 × 23 (D)
8e	B3	−4.9	−7.6	15 × 14 (D)
8e	B4	−4.9	−7.6	49 × 35 (D)
8e	B5	−4.9	−7.6	25 × 24 (D)
8e	B6	−4.9	−7.6	29 × 21 (D)
8f	B2	−4.9	−7.6	27 × 21 (A)
8f	B3	−4.9	−7.6	18 × 12 (A, upper)
8g	B3	−4.9	−7.6	20 × 12 (A, lower)
8g	B6	−4.9	−7.6	17 × 10 (A, upper)
8h	B4	−4.9	−7.6	35 × 34 (A)
8h	B5	−4.9	−7.6	23 × 15 (A)
8h	B6	−4.9	−7.6	23 × 15 (A, lower)
8i	B7	−0.5	+4.4	14 × 8 (D)
8j	B7	−0.5	+4.4	69 × 51 (A)
8k	B6	+3.5	−4.3	18 × 12 (D)
8k	B8	+3.5	−4.3	24 × 9 (D)
8l	B8	+3.5	−4.3	50 × 44 (A, upper)
8m	B6	+3.5	−4.3	9 × 8 (A, upper)
8n	B6	+3.5	−4.3	11 × 6 (A, lower)
8n	B8	+3.5	−4.3	66 × 41 (A, lower)
		Amacrine cells		
11a	A5a	+1.5	−0.5	93 × 63
11b	A5a	−1.4	−2.0	68 × 44
11c	A5a	+0.8	−3.9	110 × 73
11d	A5a	+1.4	−7.2	122 × 85
11e	A5a	−2.6	+0.5	136 × 82
11f	A5a	−2.8	+4.0	194 × 158
21a	A1	+2.3	+2.4	33 × 22
21a	A3	+2.3	+2.4	47 × 35
21b	A7	−4.5	−4.0	131 × 72
21c	A18 II	+1.0	−2.6	294 × 140
21d	A5a	−1.1	−2.8	74 × 65
21h	A5b	−1.1	−2.8	68 × 53
21e	A25a	+2.5	+2.6	—
21f	A4	−1.8	−4.2	34 × 28 (S1)
21g	A4	−1.8	−4.2	36 × 32 (S4)
21i	A8	−3.0	+1.8	274 × 192
21j	A24	−2.6	+1.7	—
21k	A20	−2.5	+1.8	170 × 108 (S5)
21l	A20	−2.5	+1.8	270 × 220 (S1)
21m	A26	−0.7	−2.4	—
		Ganglion cells		
28a,b	G13	−2.7	+2.5	304 × 232 (S5)
28j	G13	−2.7	+2.5	304 × 203 (S1)
28c,d	G1	−3.5	−2.2	36 × 22
28e	G2	+2.2	−8.0	111 × 95
28f	G3	+5.9	−0.9	87 × 75
28g	G6	+0.8	+2.2	90 × 65
28h	G19 II	−4.3	−6.5	513 × 353 (S1)
28k	G19 II	−4.3	−6.5	212 × 131 (S5)
28i	G9	+0.1	+3.6	180 × 160

*SN = +, +; ST = −, +; IN = +, −; IT = −, −.

and specifically for a type of wide-field horizontal cell recently described in rabbit retina postulated to innervate blue cones (Famiglietti, 1990).

All mammalian ALHCs studied to date are believed to be cone driven, as are SAHC-II cells. Lacking Golgi–electron microscopic data in *S. beecheyi* to confirm or counter either or both of these assertions leaves us in the perplexing position of having neither H1 nor H2 cells innervating the rods that here represent roughly 1 out of every 10 photoreceptors (Long and Fisher, 1983). Although West and Dowling (1975) presented data indicating that both the dendrites and axon terminals of H1 cells in *S. mexicanus* contact cones, they cautioned that their sample was too small to preclude the possibility that its axon terminals might also innervate rods. Bear in mind, however, West's later report (1978) that the H1 cells of *Sciurus carolinensis* contact cones only, as well as Leeper and Charlton's (1985) identification in this same species of a morphologically similar type of horizontal cell that is purely cone driven. Still, the H1 cells of *S. beecheyi* could be different and have both rod and cone input. Or more likely, the H2 cells described here might differ from AHLCs in other mammals by contacting both cones (perhaps blue cones) and rods. Although they did not describe its morphology, Leeper and Charlton (1985) recorded from a second type of horizontal cell in tree squirrel retina with mixed rod/cone responses. Ultimately of course, it is also possible that a third type of horizontal cell that innervates rods in this retina might simply have failed to stain by the Golgi technique.

Bipolar cells. With the exception of the infrequently impregnated B8 type, the remaining bipolar cell types of *S. beecheyi* retina are close analogs to the 7 types reported in *S. mexicanus* (West 1976, 1978). Moreover, all the bipolar cell types described here share features common to other mammalian bipolar cells (Famiglietti, 1981; Kolb et al., 1981, 1992; Boycott and Wässle, 1991). Apparently, the California ground squirrel retina has a single, although atypical, type of rod bipolar cell and 7 cone-related types differentiated in part by how their axon terminal spreads in IPL OFF-sublamina a and/or ON-sublamina b. Possible correlates to these 8 types in rabbit and human retina are provided in Table 1. In this study, we have noted that neighboring bipolar cells of the same type have axon terminals that do not overlap but instead fit together as pieces of a jigsaw puzzle. This "tiling" phenomenon has been reported for bipolar cell axon terminals in several mammalian species (Boycott and Wässle, 1991; Young and Vaney, 1991; Wässle et al., 1994).

Despite such similarities with other mammalian cone bipolar cells, the sciurid types are rather notorious for having morphological characteristics at odds with the accepted conventions of bipolar cell classification. For example, the narrow-field bistratified B6 cell described in the retinas of both *S. mexicanus* (West, 1976) and *Sciurus carolinensis* (West, 1978) violates one of these conventions by its dendrites making flat contacts on cone terminals while its axon terminal spreads in ON-sublamina b. This pattern of contact has only been documented for one other cell type: the cb6 bipolar cell of cat retina (Nelson and Kolb, 1983). In yet another example, B3, the narrow-field bistratified cell described by West (1976, 1978) that contributes 1 of its 2 axon terminal tiers to each IPL sublamina makes flat contacts with both rods and cones. Such mixed-rod/cone bipolars are themselves unusual, and flat contacts by bipolar cells onto rod spherules are otherwise unknown in mammalian retinas. Presumably, the dendrites of this particular cell type were partially reconstructed from thin sections by Jacobs et al. (1976) and shown to make sequen-

tial contacts with both cone and rod terminals (see their Figs. 16, 17). If the B2 and B5 types of bipolar cell in this retina can be considered "diffuse" on the basis of their innervating several adjacent cones, they differ from diffuse cone bipolars in most other mammals by having narrow rather than broad dendritic fields. Finally, the rod bipolar cell (B4) of the gray squirrel makes both flat and invaginating contacts with the multi-invaginated rod terminals (West, 1978). Without the benefit of such synaptic information here, the B4 cell type in *S. beecheyi* still displays 2 major differences from most other mammalian rod bipolar cells: the number of dendritic terminals per cell is unusually small (perhaps reflecting the low density of rods) and its dendritic and axon terminal fields are roughly equivalent in size. This latter phenomenon has also been reported in tree shrew retina by Müller and Peichl (1991) who postulated that such a low convergence between rods and rod bipolar cells "may reflect the need to maintain a certain scotopic resolving ability despite the low rod proportion."

B1 and B7, the sciurid "midget" bipolar cells. West and Dowling (1972, 1975) first showed 2 types of ground squirrel bipolar cell with dendritic fields so narrow and compact that they seemed incapable of contacting more than a single photoreceptor base. West (1976) pointed out that these cells "comprise a significant proportion of those bipolars that are Golgi-impregnated in this retina." Although termed "midget bipolar cells," they differ in important ways from their well-studied counterparts in primate retina (Kolb et al., 1969, 1992; Kolb and DeKorver, 1991). West (1978) did not observe either of these cell types in the gray squirrel retina (which with 40% rods is not nearly as cone dominant), nor have they been described in cat or rabbit retinas. In *S. mexicanus*, the B1 cell was found to be an invaginating bipolar when examined by Golgi–electron microscopy; the B7 cell was shown to be a flat bipolar (West, 1976). Neither type have terminals at all similar to primate midget bipolar cells, which are known to maintain a 1:1 relationship with their targeted midget ganglion cells (Kolb et al., 1969; Kolb and DeKorver, 1991). Instead, B1 and B7 axon terminals are easily broad enough to contact multiple postsynaptic cells.

Unlike flat midget bipolars in primate retina, the B7 cell in the retinas of *S. mexicanus* and *S. beecheyi* has a very thin, axonlike dendrite that rises to the OPL to make flat contacts with cones (West, 1976). It was our impression here, however, that although small, the B7 dendritic field is easily larger than a single photoreceptor base.

The B1 cell described here has several morphological characteristics that make it decidedly different in form from the primate type of invaginating midget bipolar. Its ascending dendrite is stout and nontapering, although many examples have 1 or 2 thinner dendrites branching off this primary dendritic trunk at varying distances between the perikaryon and dendritic tips. In the central retina, most B1 cells appear to innervate a single photoreceptor usually located off to one side of their respective somata. In the peripheral retina and especially in the superior hemiretina, B1 cell dendrites often appear to seek out more than 1 cone but cones that certainly are not adjacent. The distance between such dendritic "heads" reported here is similar to the separating blue cones reported by Long and Fisher (1983). As such, the B1 cells of *S. beecheyi* retina resemble the blue cone bipolars seen in many species (Mariani, 1984; Boycott and Wässle, 1991; Kolb et al., 1992; Kouyama and Marshak, 1992). Because their axon terminals lie deep in the IPL as do those of blue cone bipolar cells in other species, the B1 bipolar may carry blue cone signals as far as the inner IPL to reach targeted amacrine and/or ganglion cells having dendrites in S5.

The bistratified B8 bipolar cell. The B8 bistratified cell introduced here also has an unusual morphology. Like the B7 type, it has a thin ascending process ending in fine, loosely organized dendrites whose field, although certainly larger than that of the B7 cell, is nevertheless far tinier than its own widely ramifying, 2-tiered axon terminal. The dendritic tips end singly rather than in clusters and appear to contact any overlying photoreceptor terminals rather than reaching out to certain ones while eschewing others. The axon terminal of the B8 cell is very broad and is reminiscent of the axon terminals of the giant bistratified cells reported in monkey (Mariani, 1983) and human (Kolb et al., 1992). It is the disparity between its wide axon terminal and its narrow dendritic field that sets the B8 cell type apart from other known "giant" bipolar cells.

Amacrine cells. The California ground squirrel joins a growing number of mammalian species in which a multiplicity of amacrine cell types have been identified—more than 2 dozen—based on our results. Incredibly, there may be any number of additional types that failed to impregnate, a predicament quite common to Golgi studies (Vaney, 1990). Nevertheless, of all the classes of retinal neurons in *S. beecheyi*, amacrine cells display both the greatest diversity of form and the greatest range in size (see Fig. 21). Due to this large number of morphological cell types, coupled with their relatively inaccessible position on one or the other edge of the IPL, it will be a challenging task to finally unveil the physiology and function of each of them. Although a few types of amacrine cell identified in *S. beecheyi* seem similar to well-studied types common to many species, the vast majority are of unknown physiology or function. Possible correlates to identified amacrine cells in rabbit and human retinas are given in Table 2.

Displaced and mirror-image amacrine cells. The possibility that 6 types of amacrine cell form mirror-image pairs across the IPL is intriguing. Beyond underscoring the obvious fact that the thick IPL of the ground squirrel is the site of complex interneuronal intercommunication, the functional significance of these pairs of cells is unknown. It is clear from our study that the concept of mirror-image among these pairs varies greatly in degree: from the amazingly similar starburst subtypes to the A27 subtypes whose similarities in form are approximate at best. It is not clear, except in the case of the starburst amacrine cells (A5), that the subtypes of each of these pairs independently tile the retina. The subtypes of each pair have dendrites that ramify exclusively in different IPL sublaminae, typically in whichever sublamina borders the nuclear layer housing their respective cell bodies. Only the A19 subtypes send their respective dendrites to nonadjacent IPL sublaminae.

Also intriguing are the many types of displaced amacrine cells in *S. beecheyi*, although as Hughes (1985) and Vaney (1990) explained, such cells are probably not in any way misplaced to the GCL but develop there normally. Indeed, displaced amacrines comprise a significant proportion of cells in the GCL in the retinas of several species: 35% in rabbit retina (Vaney, 1980), 50% in rat retina (Perry, 1981), and as much as 80% in cat retina (Wong and Hughes, 1987; Wässle et al., 1987). Long and Fisher (1983) pointed out the very large number of small cell bodies in the ganglion cell

layer of *S. beecheyi* and speculated on whether some might be amacrine cells even while noting that ground squirrel ganglion cell perikarya were themselves quite small. Here we have confirmed that at least 12 types and subtypes of amacrine cell reside in the GCL.

Starburst amacrine cells. Certainly the best-characterized type of mirror-symmetric amacrine cell is the starburst amacrine (Famiglietti, 1983a), identified here as the A5 subtypes. Starburst amacrines are the most obvious and commonly stained type of amacrine cell in the retinal wholemounts of *S. beecheyi*. We measured the dendritic fields of hundreds of examples of both subtypes and carefully drew scores of these cells at differing retinal locations. Unlike the sparsely branched and unadorned starburst cells in cat (Pourcho and Osman, 1986) and primate (Rodieck, 1989; Kolb et al., 1992) retina, ground squirrel starburst amacrine cells are perhaps even more elaborate than their well-studied counterparts in rabbit (Famiglietti, 1983a; Vaney, 1984; Tauchi and Masland, 1984). As seen by these same investigators in rabbit retina, ground squirrel starburst amacrine cells also increase in dendritic field size from central to peripheral retina. We observed that this increase in size is nonuniform as cells lying above the visual streak increase in size at a much greater rate than those lying below, a pattern also described for H1 cells.

Starburst amacrines are believed to be involved in directional selectivity. In rabbit retina, starburst amacrine cell dendrites are postsynaptic across their entire field, whereas only the distal ring of beaded dendrites is presynaptic to bistratified, directionally selective ganglion cells and certain unidentified amacrine cell types (Famiglietti, 1983b, 1991, 1992a–c). Recently, the 2 starburst amacrine cell subtypes in *S. beecheyi* have been shown to be positive for choline acetyltransferase (H.J. Karten, personal communication) as is typical of these cholinergic neurons in other species (Tauchi and Masland, 1984; Vaney, 1984; Rodieck and Marshak, 1992).

Interplexiform cells. Interplexiform cells were not observed in the retina of any species of squirrel. This lack of data certainly does not preclude the existence of interplexiform cells in these mammals because as a class of retinal neuron they are known to be particularly refractory to Golgi impregnation (Boycott et al., 1975).

Ganglion cells. In recording from optic nerve fibers, Michael (1968a–c) showed that ground squirrel ganglion cells fell into 2 broad categories based on their physiological responses to various photic stimuli. Cells with "simple" tonic responses had large receptive fields (60–500 μm) compared with those with "complex" transient responses which had small fields (60–115 μm). The former group had receptive fields with concentric, antagonistic domains; the latter group did not.

West and Dowling (1972) characterized the relative input from bipolar and amacrine cell synapses onto their 15 different types of ganglion cell in *S. mexicanus*. They found that smaller ganglion cell types tended to have very high amacrine cell input and that larger ganglion cell types had relatively equal bipolar and amacrine cell input. These they speculated might correlate with Michael's complex and simple categories, respectively. Nine of the 15 types of ganglion cell described in *S. mexicanus* (West, 1976) have close counterparts in the retina of *S. beecheyi*, and 3 are most likely the amacrine cells discussed earlier. We have identified 3 broad-field bistratified cells not described in *S. mexicanus* but failed to see the 3 narrow-field bistratified types described in that species (West and Dowling, 1972; West, 1976). Like amacrine cell types, ganglion cells of *S. beecheyi* display a wide diversity of morphology and size (see Fig. 28).

Soma size proved unhelpful in sorting ganglion cells in this retina because, as in rabbit retina (Amthor et al., 1983), the ganglion cells form a continuous spectrum of soma size rather than falling into discrete classes (Long and Fisher, 1983). However, ganglion cell output in *S. beecheyi* has been well characterized electrophysiologically (Jacobs and Tootell, 1980, 1981; Jacobs et al., 1981, 1985; McCourt and Jacobs, 1984a,b) with optic nerve fibers falling into 3 broad, functional groups: contrast sensitive, directionally selective, and spectrally selective.

Just under 60% of all the fibers display contrast sensitivity, including those that gave sustained, X-cell-like responses and others that had transient, Y-cell-like responses (McCourt and Jacobs, 1984a). Each of these 2 types in turn came in ON- and OFF-center varieties, none of which showed spectral opponency, deriving most of their input from the green (520 nm) cones (Jacobs et al., 1981). Cells of this physiological type might be expected to have morphologies similar to the alpha and beta cells identified in many species (Boycott and Wässle, 1974; Kolb et al., 1981; Peichl et al., 1987; Peichl, 1991). The G17 and G18 cells described here might represent OFF- and ON-alpha ganglion cells in this species. Neither type was described in *S. mexicanus* (West, 1976).

About 10% of all units in *S. beecheyi* are directionally selective and fall into 2 groups differing in response characteristics (McCourt and Jacobs, 1984b) yet deriving their input only from green cones (Jacobs et al., 1981). Because California ground squirrel retina has such a highly differentiated system of starburst amacrine cells, directionally selective ganglion cells might be expected to be as prominent in this species as in rabbit retina (Amthor et al., 1989b), where a well-developed starburst amacrine cell system also exists. On the basis of its bistratified morphology, the G11 cell described here probably corresponds to the ON–OFF directionally selective ganglion cell described by Amthor et al. (1989b).

Just under 30% of the optic nerve units are spectrally selective, showing antagonistic signals from the green (520 nm) and blue (440 nm) cones (Jacobs and Tootell, 1981; Jacobs et al., 1981). Three subclasses have been described, with most units showing ON responses to short wavelength light as in primate ganglion cells (G.H. Jacobs, personal communication). The bistratified G13 type described here has 1 tier of its dendrites in IPL stratum S5, where they would have to be if they were to synapse with the terminals of B1 cells, the putative blue cone bipolars. The G13 cell in *S. beecheyi* is also similar in size and dendritic morphology to the blue-ON yellow-OFF bistratified ganglion cell described in monkey retina (Dacey and Lee, 1994).

In summary, despite a wealth of physiological data about the ganglion cell population in this species, we are essentially unable, based on comparisons with other species, to positively ascribe functional type to any of the various ganglion cells, with the possible exception of 2 types that may be contrast selective and a single directionally selective type. Thus, it appears that the ground squirrel retina has evolved ganglion cells that subserve similar physiological functions as those in other species but with different

morphologies. Table 3, however, presents possible morphological correlates in rabbit and human retinas to the ganglion cell types described here.

Anomalies of the rod pathway

Rods constitute only a small minority of the photoreceptors in the retina of *S. beecheyi*, making it appropriate to ask which retinal cell types participate in carrying rod signals to higher visual centers.

Jacobs et al. (1976, 1980) showed that, although rod photoreceptors are morphologically present in all individuals, about one-third of the squirrels tested lacked scotopic responses. They cautioned that "even at best, the scotopic system found in the ground squirrels is a feeble one, quite unlike that scotopic system one usually associates with duplex vision in other mammals." In a curious way, the Golgi data presented here reinforces this rather ambiguous situation.

Anomalies in the rod pathway begin at the photoreceptor level because ground squirrel rods have a number of conelike characteristics. These include a multi-invaginated synaptic terminal (West and Dowling, 1975; Fisher et al., 1976; Jacobs et al., 1976, 1980), conelike spectral traits (see Jacobs, 1990), conelike photopigments (Szél and Röhlich, 1988), and conelike components in their phototransduction cascade (von Schantz et al., 1994). We know that horizontal cell processes form lateral elements in rod synapses of *S. beecheyi* (see Fig. 12 in Jacobs et al., 1976), yet we cannot identify the cell type making such connections. The putative rod bipolar cell, B4, has an atypical morphology. This retina has a type of cone bipolar cell that also connects to rods (Jacobs et al., 1976; West 1976, 1978), which is unusual in itself. Whereas the B4 axon terminal spreads deep in the IPL as most mammalian rod bipolar terminals do, the 2-tiered terminal of the mixed-rod/cone B3 cell spreads in the middle of the IPL, contributing 1 tier to either side (in S2 and S3) of the boundary separating sublamina a from b. Presumably at this location, rod information carried by this cell could interact with components of cone-driven cells in both the ON and OFF sublaminae.

Perhaps the most striking rod-associated anomaly among the third-order neurons in the retina of *S. beecheyi* is the apparent lack of the AII amacrine cell, a key interneuron of the rod pathway in most mammalian species, serving as the only route by which rod bipolar cell signals reach ganglion cells (Kolb and Famiglietti, 1974; Famiglietti and Kolb, 1975; Kolb and Nelson, 1983; Dacheux and Raviola, 1986; Daw et al., 1990). We cannot rule out the possibility that the ground squirrel AII cell simply failed to stain, anymore than we can rule out the possibility that AIIs in *S. beecheyi* might have an appearance totally different than that in other mammals. The "rod reciprocal amacrine cell" (A17 in cat; S1, S2 in rabbit) is prominent in the rod pathway of cats (Holmgren-Taylor, 1982; Kolb and Nelson, 1983) and rabbits (Sandell and Masland, 1986; Vaney, 1986; Vaney et al., 1991). Along with AII processes, this wide-field diffuse amacrine cell is postsynaptic, in these two species, to rod bipolar dyads deep in the IPL. We have not observed any wide-field diffuse cells in *S. beecheyi*, although the A23 cell described here may correspond to this cell type. A wide-field dopaminergic amacrine cell (A18 in cat) is presynaptic to AII cells in the outermost IPL substratum (Pourcho, 1982; Voigt and Wässle, 1987; Kolb et al., 1991), where it is believed to have an inhibitory effect (Daw et al., 1990). In the retina of *S. beecheyi*, only the A24 and A27a types have widely ramifying dendrites restricted to S1. It is not known whether either might correspond to the dopaminergic cell type.

Proposed to play less-understood roles in the rod pathway are the A6, A8, and A13 cells that Kolb and Nelson (1983) described in cat retina. The narrow-field bistratified cell, A8, has a dendritic morphology considered the opposite of the AII amacrine (Kolb et al., 1981; Pourcho and Goebel, 1985) and is thought to be another "through-conducting" amacrine cell type (Masland, 1988). The A4 cell described here is the only narrow-field bistratified amacrine observed in California ground squirrel retina and as such is a likely homolog to the A8 call of cat. We did not identify clear counterparts to either the A6 or A13 cat amacrine cell types.

There is no electrophysiological evidence for rod-driven ganglion cells in ground squirrels (Jacobs and Tootell, 1981; Jacobs et al., 1981; Jacobs, 1990), indicating that as in other mammalian retinas rod signals ride piggyback on the cone pathways (Strettoi et al., 1992).

The blue cone pathway in ground squirrel retina

Evidence for the existance of blue cones in ground squirrel retina has been shown physiologically by Michael (1968c). Long and Fisher (1983) described in *S. beecheyi* the distribution of cones that they speculated to be blue sensitive. As discussed previously, it seems likely that the B1 bipolar ("invaginating midget bipolar cell," West, 1976) is an ON-center blue cone bipolar cell. This cell type stained frequently at all retinal locations. The 2 other bipolar types that might be involved in this pathway are the B7 ("flat-midget bipolar cell," West, 1976) and the newly described B8 bistratified bipolar cell. Based on its stratification in the IPL, the former cell could be a candidate for an OFF-center blue bipolar cell; the latter's involvement is suggested simply because 1 layer of its terminal stratifies deeply in S5 near the B1 axon terminals.

It was concluded earlier that the H2 horizontal cell is likely to be cone driven. Instead of contacting all overlying cones as H1 cell dendrites appear to do, it seems to reach out to certain overlying cone terminals spaced in a somewhat regular array. It may not contact blue cones exclusively, but may show a preponderance of such input. Confirmation of any spectral selectivity in its connections necessarily must await analysis by Golgi–electron microscopy.

The only clue we have as to which amacrine and ganglion cells might be involved in the blue cone pathway is from the obvious requirement that their dendrites should be pre- and/or postsynaptic in S5 where the putative blue cone bipolar terminals lie. Tables 2 and 3 list a variety of candidates from both classes of retinal neuron with processes in S5—too many to allow more than pure speculation. As outlined ealier, blue cone opponency has been recorded in 30% of the optic nerve fibers of this species, originating from an unknown number of as yet unidentified ganglion cell types. Based strictly on its morphology, the G13 cell was proposed above to be a blue-ON yellow-OFF type. Almost certainly, a number of amacrine cell types as well as other ganglion cells also participate in this pathway.

It is thought that amacrine cell diversity might underlie the complexity of ganglion cell responses in the retina of

many species (see Dowling 1987). Based on this premise, it is perhaps not surprising that, in ground squirrels and many other species, the use of retinal wholemounts has allowed the identification of many amacrine cell types and subtypes, in our case at least 6 times the number seen in the original studies on *S. mexicanus*. Thus, the number of possible interactions between the cell types of both classes of retinal neuron is vastly greater than previously thought. It is hoped that this expanded catalog and description of retinal neurons in a species valued because of its cone-dominant retina will allow for additional advances to be made in our understanding of retinal information processing.

ACKNOWLEDGMENTS

We thank Drs. Gerald Jacobs, Helga Kolb, and Peter Ahnelt for their most helpful comments on various drafts of the manuscript and Steve Bernstein and Maura Jess for help with computer-generated data. We are also indebted to Mr. Robert Fariss for his assistance in acquiring the squirrels and in preparing the tissue. This study was supported by NIH grant EY00888 to S.K.F.

LITERATURE CITED

Ahnelt, P.K. (1985) Characterization of the color related receptor mosaic in the ground squirrel retina. Vision Res. *25:*1557–1567.

Ahnelt, P., and H. Kolb (1994a) Horizontal cells and cone photoreceptors in primate retina: A Golgi-light microscopic study of spectral connectivity. J. Comp. Neurol. *343:*387–405.

Ahnelt, P., and H. Kolb (1994b) Horizontal cells and cone photoreceptors in primate retina: A Golgi-electron microscope study of spectral connectivity. J. Comp. Neurol. *343:*406–427.

Amthor, F.R., C.W. Oyster, and E.S. Takahashi (1983) Quantitative morphology of rabbit retinal ganglion cells. Proc. Roy. Soc. Lond. B *217:*341–355.

Amthor, F.R., C.W. Oyster, and E.S. Takahashi (1984) Morphology of on–off direction-selective ganglion cells in the rabbit retina. Brain Res. *298:*187–190.

Amthor, F.R., E.S. Takahashi, and C.W. Oyster (1989a) Morphologies of rabbit retinal ganglion cells with concentric receptive fields. J. Comp. Neurol. *280:*72–96.

Amthor, F.R., E.S. Takahashi, and C.W. Oyster (1989b) Morphologies of rabbit retinal ganglion cells with complex receptive fields. J. Comp. Neurol. *280:*97–121.

Anderson, D.H., and S.K. Fisher (1976) The photoreceptors of diurnal squirrels: Outer segment structure, disc shedding, and protein renewal. J. Ultrastr. Res. *55:*119–141.

Anderson, D.H., and G.H. Jacobs (1972) Color vision and visual sensitivity in the California ground squirrel, *Citellus beecheyi*. Vision Res. *12:*1995–2004.

Bloomfield, S.A., and R.F. Miller (1982) A physiological and morphological study of the horizontal cell types of the rabbit retina. J. Comp. Neurol. *208:*288–303.

Boycott, B.B. (1988) Horizontal cells of mammalian retinae. Neurosci. Res. *8(Suppl.):*S97–S111.

Boycott, B.B., and J.M. Hopkins (1981) Microglia in the retina of monkey and other mammals; its distinction from other types of glia and horizontal cells. Neuroscience *6:*679–688.

Boycott, B.B., and H. Kolb (1973) The horizontal cells of the rhesus monkey retina. J. Comp. Neurol. *148:*115–140.

Boycott, B.B., and H. Wässle (1974) The morphological types of ganglion cells of the domestic cat's retina. J. Physiol. Lond. *240:*397–419.

Boycott, B.B., and H. Wässle (1991) Morphological classification of bipolar cells of the primate retina. Eur. J. Neurosci. *3:*1069–1088.

Boycott, B.B., J.E. Dowling, S.K. Fisher, H. Kolb, and A.M. Laties (1975) Interplexiform cells of the mammalian retina and their comparison with catecholamine-containing retinal cells. Proc. R. Soc. Lond. B. *191:*353–368.

Boycott, B.B., L. Peichl, and H. Wässle (1978) Morphological types of horizontal cell in the retina of the domestic cat. Proc. R. Soc. Lond. B. *203:*229–245.

Cameron, W.E., D.B. Averill, and A.J. Berger (1983) Morphology of cat phrenic motorneurons as revealed by intracellular injection of horseradish peroxidase. J. Comp. Neurol. *219:*70–80.

Dacey, D.M. (1989) Axon-bearing amacrine cells of the macaque monkey retina. J. Comp. Neurol. *284:*275–293.

Dacey, D.M. (1993) The mosaic of midget ganglion cells in the human retina. J. Neurosci. *13:*5334–5355.

Dacey, D.M., and B.B. Lee (1994) The "blue-on" opponent pathway in primate retina originates from a distinct bistratified ganglion cell type. Nature *367:*731–735.

Dacheux, R.F., and E. Raviola (1982) Horizontal cells in the retina of the rabbit. J. Neurosci. *2:*1486–1493.

Dacheux, R.F., and E. Raviola (1986) The rod pathway in the rabbit retina: A depolarizing bipolar and amacrine cell. J. Neurosci. *6:*331–345.

Daw, N.W., R.J. Jensen, and W.J. Brunken (1990) Rod pathways in mammalian retinae. Trends Neurosci. *13:*110–115.

Dowling, J.E. (1964) Structure and function in the all-cone retina of the ground squirrel. In: The Physiological Basis for Form Discrimination, a symposium sponsored by the Visual Sciences Study Section, NIH, at Brown University, Providence, RI, January 23–24, 1964, pp. 17–23.

Dowling, J.E. (1987) The Retina: An Approachable Part of the Brain. Cambridge, MA: Belknap Press, Harvard University Press.

Famiglietti, E.V. Jr. (1981) Functional architecture of cone bipolar cells in mammalian retina. Vision Res. *21:*1559–1563.

Famiglietti, E.V. Jr. (1983a) "Starburst" amacrine cells and cholinergic neurons: Mirror-symmetric ON and OFF amacrine cells of rabbit retina. Brain Res. *261:*138–144.

Famiglietti, E.V. Jr. (1983b) ON and OFF pathways through amacrine cells in mammalian retina: The synaptic connections of "starburst" amacrine cells. Vision Res. *23:*1265–1279.

Famiglietti, E.V. Jr. (1985) Starburst amacrine cells: Morphological constancy and systematic variation in the anisotropic field of rabbit retinal neurons. J. Neurosci. *5:*562–577.

Famiglietti, E.V. Jr. (1990) A new type of wide-field horizontal cell, presumably linked to blue cones, in rabbit retina. Brain Res. *535:*174–179.

Famiglietti, E.V. Jr. (1991) Synaptic organization of starburst amacrine cells in rabbit retina: Analysis of serial thin sections by electron microscopy and graphic reconstruction. J. Comp. Neurol. *309:*40–70.

Famiglietti, E.V. Jr. (1992a) Dendritic co-stratification of ON and ON–OFF directionally selective ganglion cells with starburst amacrine cells in rabbit retina. J. Comp. Neurol. *324:*322–335.

Famiglietti, E.V. Jr. (1992b) Polyaxonal amacrine cells of rabbit retina: Morphology and stratification of PA1 cells. J. Comp. Neurol. *316:*391–405.

Famiglietti, E.V. Jr. (1992c) Polyaxonal amacrine cells of rabbit retina: PA2, PA3, and PA4 cells. Light and electron microscopic studies with a functional interpretation. J. Comp. Neurol. *316:*422–446.

Famiglietti, E.V. Jr., and H. Kolb (1975) A bistratified amacrine cell and synaptic circuitry in the inner plexiform layer of the retina. Brain Res. *84:*293–300.

Famiglietti, E.V. Jr., and H. Kolb (1976) Structural basis for ON-and OFF-center responses in retinal ganglion cells. Science *194:*193–195.

Fisher, S.K., and B.B. Boycott (1974) Synaptic connexions made by horizontal cells within the outer plexiform layer of the retina of the cat and rabbit. Proc. R. Soc. Lond. B *186:*317–331.

Fisher, S.K., G.H. Jacobs, D.H. Anderson, and M.S. Silverman (1976) Rods in the antelope ground squirrel. Vision Res. *16:*875–877.

Gallego, A. (1971) Horizontal and amacrine cells in the mammal's retina. Vision Res. *3(Suppl.):*33–50.

Gallego, A. (1976) The horizontal cells of the terrestrial vertebrate retina: I. Mammals and birds. In E. Yamada and S. Mishima (eds): The Structure of the Eye. Tokyo: Japanese Journal of Ophthalmology, pp. 273–280.

Gallego, A. (1982) Organization of the outer plexiform layer of the tetrapoda retina: Horizontal cells of mammalian and avian retina. In J.G. Hollyfield (ed): Structure of the Eye. New York: Elsevier, pp. 151–164.

Gallego, A. (1986) Comparative studies on horizontal cells and a note on microglial cells. Prog. Ret. Res. *5:*165–206.

Gallego, A., and J.A. Sobrino (1975) Short-axon horizontal cells of the monkey's retina. Vision Res. *15:*747–748.

Green, D.G., and J.E. Dowling (1975) Electrophysiological evidence for

rod-like receptors in the gray squirrel, ground squirrel and prairie dog retinas. J. Comp. Neurol. *159:*461–472.

Harman, A.M., and J. Ferguson (1994) Morphology and birth dates of horizontal cells in the retina of a marsupial. J. Comp. Neurol. *340:*392–404.

Holmgren-Taylor, I. (1982) Electron microscopical observations on the indoleamine-accumulating neurons and their synaptic connections in the retina of the cat. J. Comp. Neurol. *208:*144–156.

Hughes, A. (1985) New perspectives in retinal organization. In N.N. Osborne and G. Chader (eds): Progress in Retinal Research, vol. 4. Oxford: Pergamon, pp. 243–313.

Jacobs, G.H. (1990) Duplicity theory and ground squirrels: Linkages between photoreceptors and visual function. Vis. Neurosci. *5:*311–318.

Jacobs, G.H., and R.B.H. Tootell (1980) Spectrally opponent responses in the ground squirrel optic nerve. Vision Res. *20:*9–13.

Jacobs, G.H., and R.B.H. Tootell (1981) Spectral response properties of the optic nerve fibers in the ground squirrel. J. Neurophysiol. *45:*891–902.

Jacobs, G.H., B. Blakeslee, and R.B.H. Tootell (1981) Color-discrimination tests on fibers in the ground squirrel optic nerve. J. Neurophysiol. *45:*903–914.

Jacobs, G.H., J. Neitz, and M. Crognale (1985) Spectral sensitivity of ground squirrel cones measured with ERG flicker photometry. J. Comp. Physiol. A *156:*503–509.

Jacobs, G.H., S.K. Fisher, D.H. Anderson, and M.S. Silverman (1976) Scotopic and photopic vision in the California ground squirrel: Physiological and anatomical evidence. J. Comp. Neurol. *165:*209–228.

Jacobs, G.H., R.B.H. Tootell, S.K. Fisher, and D.H. Anderson (1980) Rod photoreceptors and scotopic vision in ground squirrels. J. Comp. Neurol. *189:*113–125.

Kolb, H. (1974) The connections between horizontal cells and photoreceptors in the retina of the cat: Electron microscopy of Golgi preparations. J. Comp. Neurol. *155:*1–14.

Kolb, H. (1991) Anatomical pathways for color vision in the human retina. Vis. Neurosci. *7:*61–74.

Kolb, H., and L. DeKorver (1991) Midget ganglion cells of the parafovea of the human retina: A study by electron microscopy and serial section reconstructions. J. Comp. Neurol. *303:*617–636.

Kolb, H., and E.V. Famiglietti Jr. (1974) Rod and cone pathways in the inner plexiform layer of cat retina. Science *186:*47–49.

Kolb, H., and R. Nelson (1983) Rod pathways in the retina of the cat. Vision Res. *23:*301–312.

Kolb, H., and R.A. Normann (1982) A-type horizontal cells of the superior edge of the linear visual streak of the rabbit retina have oriented, elongated dendritic trees. Vision Res. *22:*906–916.

Kolb, H., B.B. Boycott, and J.E. Dowling (1969) A second type of midget bipolar cell in the primate retina (Appendix). Phil. Trans. R. Soc. B *255:*177–184.

Kolb, H., A. Mariani, and A. Gallego (1980) A second type of horizontal cell in the monkey retina. J. Comp. Neurol. *189:*31–39.

Kolb, H., R. Nelson, and A. Mariani (1981) Amacrine cells, bipolar cells and ganglion cells of the cat retina: a Golgi study. Vision Res. *21:*1081–1114.

Kolb, H., N. Cuenca, and L. DeKorver (1991) Postembedding immunocytochemistry for GABA and glycine reveals the synaptic relationships of the dopaminergic amacrine cell of the cat retina. J. Comp. Neurol. *310:*267–284.

Kolb, H., K.A. Linberg, and S.K. Fisher (1992) The neurons of the human retina: a Golgi study. J. Comp. Neurol. *318:*147–187.

Kolb, H., E. Fernandez, J. Schouten, P. Ahnelt, K.A. Linberg, and S.K. Fisher (1994) Are there three types of horizontal cell in the human retina? J. Comp. Neurol. *343:*370–386.

Kouyama, N., and D.W. Marshak (1992) Bipolar cells specific for blue cones in the macaque retina. J. Neurosci. *12:*1233–1252.

Leeper, H.F., and J.S. Charlton (1985) Response properties of horizontal cells and photoreceptor cells in the retina of the tree squirrel, *Sciurus carolinensis*. J. Neurophysiol. *54:*1157–1166.

Linberg, K.A., S. Suemune, R.N. Fariss, and S.K. Fisher (1988) A golgi study of the cone-dominant, California ground squirrel retina with special reference to starburst amacrine cells. Invest. Ophthalmol. Vis. Sci. *29(Suppl.):*204.

Long, K.O., and S.K. Fisher (1983) The distribution of photoreceptors and ganglion cells in the California ground squirrel, *Spermophilus beecheyi*. J. Comp. Neurol. *221:*329–340.

Mariani, A.P. (1983) Giant bistratified bipolar cells in monkey retina. Anat. Rec. *206:*215–220.

Mariani, A.P. (1984) Bipolar cells in monkey retina selective for the cones likely to be blue-sensitive. Nature (London) *308:*184–186.

Mariani, A.P. (1985) Multiaxonal horizontal cells in the retina of the tree shrew, *Tupaia glis*. J. Comp. Neurol. *233:*553–563.

Mariani, A.P. (1990) Amacrine cells of the rhesus monkey retina. J. Comp. Neurol. *301:*382–400.

Masland, R.H. (1988) Amacrine cells. Trends Neurosci. *11:*405–410.

McCourt, M.E., and G.H. Jacobs (1984a) Spatial filter characteristics of optic nerve fibers in California ground squirrel (*Spermophilus beecheyi*). J. Neurophysiol. *52:*1181–1199.

McCourt, M.E., and G.H. Jacobs (1984b) Directional filter characteristics of optic nerve fibers in California ground squirrel (*Spermophilus beecheyi*). J. Neurophysiol. *52:*1200–1212.

Michael, C.R. (1968a) Receptive fields of single optic nerve fibers in a mammal with an all-cone retina. I. Contrast-sensitive units. J. Neurophysiol. *31:*249–256.

Michael, C.R. (1968b) Receptive fields of single optic nerve fibers in a mammal with an all-cone retina. II. Directionally selective units. J. Neurophysiol. *31:*257–267.

Michael, C.R. (1968c) Receptive fields of single optic nerve fibers in a mammal with an all-cone retina. III. Opponent color units. J. Neurophysiol. *31:*268–282.

Mills, S.L., and S.C. Massey (1994) Distribution and coverage of A-and B-type horizontal cells stained with neurobiotin in the rabbit retina. Vis. Neurosci. *11:*549–560.

Müller, B., and L. Peichl (1991) Rod bipolar cells in the cone-dominated retina of the tree shrew *Tupaia belangeri*. Vis. Neurosci. *6:*629–639.

Müller, B., and L. Peichl (1993) Horizontal cells in the cone-dominated tree shrew retina: Morphology, photoreceptor contacts, and topographical distribution. J. Neurosci. *13:*3628–3646.

Nelson, R., and H. Kolb (1983) Synaptic patterns and response properties of bipolar and ganglion cells in the cat retina. Vision Res. *23:*1183–1195.

Oyster, C.W., F.R. Amthor, and E.S. Takahashi (1993) Dendritic architecture of ON–OFF direction-selective ganglion cells in the rabbit retina. Vision Res. *33:*579–608.

Peichl, L. (1991) Alpha ganglion cells in mammalian retinae: Common properties, spectral differences, and some comments on other ganglion cells. Vis. Neurosci. *7:*155–159.

Peichl, L., and J. González-Soriano (1994) Morphological types of horizontal cell in rodent retinae: A comparison of rat, mouse, gerbil, and guinea pig. Vis. Neurosci. *11:*501–517.

Peichl, L., E.H. Buhl, and B.B. Boycott (1987) Alpha ganglion cells in rabbit retina. J. Comp. Neurol. *263:*25–41.

Perry, V.H. (1981) Evidence for an amacrine cell system in the ganglion cell layer of the rat retina. Neuroscience *6:*931–944.

Pourcho, R.G. (1982) Dopaminergic amacrine cells in the cat retina. Brain Res. *252:*101–109.

Pourcho, R.G., and D.J. Goebel (1985) A combined golgi and autoradiographic study of (^{3}H)Glycine-accumulating amacrine cells in the cat retina. J. Comp. Neurol. *233:*473–480.

Pourcho, R.G., and K. Osman (1986) Cytochemical identification of cholinergic amacrine cells in the cat retina. J. Comp. Neurol. *247:*497–504.

Ramón y Cajal, S. (1893) La rétine des vertébrés. La Cellule *9:*17–257.

Raviola, E., and R.F. Dacheux (1983) Variations in structure and response properties of horizontal cells in the retina of the rabbit. Vision Res. *23:*1221–1227.

Rodieck, R.W. (1988) The primate retina. Comp. Primate Biol. *4:*203–278.

Rodieck, R.W. (1989) Starburst amacrine cells of the primate retina. J. Comp. Neurol. *285:*18–37.

Rodieck, R.W., and D.W. Marshak (1992) Spatial density and distribution of choline acetyltransferase immunoreactive cells in human, macaque and baboon retinas. J. Comp. Neurol. *321:*46–64.

Sandell, J.H., and R.H. Masland (1986) A system of indoleamine-accumulating neurons in the rabbit retina. J. Neurosci. *6:*3331–3347.

Strettoi, E., E. Raviola, and R.F. Dacheux (1992) Synaptic connections of the narrow-field, bistratified rod amacrine cell (AII) in the rabbit retina. J. Comp. Neurol. *325:*152–168.

Szél, Á., and P. Röhlich (1988) Four photoreceptor types in the ground squirrel retina as evidenced by immunocytochemistry. Vision Res. *28:*1297–1302.

Tauchi, M., and R.H. Masland (1984) The shape and arrangement of the cholinergic neurons in the rabbit retina. Proc. R. Soc. Lond. B *223:*101–119.

Vaney, D.I. (1980) A quantitative comparison between the ganglion cell populations and axonal outflows of the visual streak and periphery of the rabbit retina. J. Comp. Neurol. *189:*215–233.

Vaney, D.I. (1984) "Coronate" amacrine cells in the rabbit retina have the "starburst" dendritic morphology. Proc. R. Soc. Lond. B *220:*501–508.

Vaney, D.I. (1986) Morphological identification of serotonin-accumulating neurons in the living retina. Science *233:*444–446.

Vaney, D.I. (1990) The mosaic of amacrine cells in the mammalian retina. In N.N. Osborne and G. Chader (eds): Progress in Retinal Research, vol. 9. New York: Pergamon, pp. 49–100.

Vaney, D.I. (1994) Territorial organization of direction-selective ganglion cells in rabbit retina. J. Neurosci. *14:*6301–6316.

Vaney, D.I., H.M. Young, and I.C. Gynther (1991) The rod circuit in rabbit retina. Vis. Neurosci. *7:*141–154.

Voigt, T., and H. Wässle (1987) Dopaminergic innervation of AII amacrine cells in mammalian retina. J. Neurosci. *7:*4115–4128.

von Schantz, M., Á. Szél, T. van Veen, and D.B. Farber (1994) Expression of phototransduction cascade genes in the ground squirrel retina. Invest. Ophthalmol. Vis. Sci. *35:*2558–2566.

Wässle, H., and B.B. Boycott (1991) Functional architecture of the mammalian retina. Physiol. Rev. *71:*447–480.

Wässle, H., L. Peichl, and B.B. Boycott (1978) Topography of horizontal cells in the retina of the domestic cat. Proc. R. Soc. Lond. B *203:*269–291.

Wässle, H., M.H. Chun, and F. Müller (1987) Amacrine cells in the ganglion cell layer of the cat retina. J. Comp. Neurol. *265:*391–408.

Wässle, H., U. Grünert, P.R. Martin, and B.B. Boycott (1994) Immunocytochemical characterization and spatial distribution of midget bipolar cells in the macaque monkey retina. Vision Res. *34:*561–579.

West, R.W. (1976) Light and electron microscopy of the ground squirrel retina: Functional considerations. J. Comp. Neurol. *168:*355–378.

West, R.W. (1978) Bipolar and horizontal cells of the gray squirrel retina: Golgi morphology and receptor connections. Vision Res. *18:*129–136.

West, R.W., and J.E. Dowling (1972) Synapses onto different morphological types of retinal ganglion cells. Science *178:*510–512.

West, R.W., and J.E. Dowling (1975) Anatomical evidence for cone and rod-like receptors in the gray squirrel, ground squirrel and prairie dog retina. J. Comp. Neurol. *159:*439–460.

Wong, R.O.L., and A. Hughes (1987) The morphology, number and distribution of a large population of confirmed displaced amacrine cells in the adult cat retina. J. Comp. Neurol. *255:*159–177.

Young, H.M., and D.I. Vaney (1991) Rod-signal interneurons in the rabbit retina: 1. Rod bipolar cells. J. Comp. Neurol. *310:*139–153.